



Master Thesis

## The step-pool morphology of a steep mountain stream

**Author(s):**

Milzow, Christian

**Publication Date:**

2004

**Permanent Link:**

<https://doi.org/10.3929/ethz-a-005140049> →

**Rights / License:**

[In Copyright - Non-Commercial Use Permitted](#) →

This page was generated automatically upon download from the [ETH Zurich Research Collection](#). For more information please consult the [Terms of use](#).

**THE STEP-POOL MORPHOLOGY OF  
A STEEP MOUNTAIN STREAM**

March 2004

Diploma thesis of                      Christian Milzow

Supervisors:                              Dr. Peter Molnar, Prof. Paolo Burlando  
*Institut für Hydrologie und Wasserwirtschaft, ETH Zürich*

In collaboration with                  Dr. Brian McArdell  
*Abteilung Wasser-, Erd- und Felsbewegungen,  
Forschungsbereich Naturgefahren, WSL Birmensdorf*

## Abstract

Mountain streams with alluvial sediment often develop a fairly regular step-pool morphology. This finding has been based on observations of reach-averaged step heights and lengths of many mountain rivers, and has been argued to be a signature of self-organisation in the process of energy dissipation. The observations were generally conducted on stream reaches with average slopes of less than 0.2 m/m. Here, the step-pool morphology of a very steep mountain stream in the Alptal basin in Switzerland is analysed. Its average slope ranges between 0.10 and 0.35 m/m. In order to illustrate the large variability in channel geometry, bed sediment size and step-pool morphology along the stream profile, a continuous 1.5 km section of the stream was surveyed. This variability is due to bedrock control, lateral sediment input, and a highly variable sediment transporting capacity along the channel. The proposed hypothesis is that step-pool morphology of the stream should be treated as a system of superposed step-pool sequences, with step height as an independent variable. It was assumed that the average step height and length of each of these sequences was determined by streamflow required for incipient motion. The result was a strong linear relationship between the sequence-averaged step height and length of the superposed step-pool system. This geometric similarity found between steps of different sizes seems to suggest that even in very steep and variable mountain streams, regularity may be observed in some morphological features.

To examine the frequency of channel forming flow, a flood frequency analysis was conducted based on 18 years of runoff data. The results are comparable with results from a previous study based on the analysis of probable storm events and hydrologic response units. Channel top widths were simulated at 22 cross sections of the stream for different flood discharges, taking into account the variation of topography and roughness along the stream. The simulated widths correlate well with widths measured in the stream.

To control sediment movement and protect property, check dams are numerous in the Alptal basin. Check dams are the anthropogenic equivalent to step-pool sequences. A comparison of dimensions of natural step-pools and check dams is presented and general agreement is found.

---

## Zusammenfassung

Gebirgsbäche mit alluvialem Sediment bilden oft eine relativ regelmässige Stufen-Becken-Struktur. Die Beobachtung der Regelmässigkeit wird unterstützt durch Abschnittsmittelwerte von Stufenhöhen und -längen, die in vielen Gebirgsbächen gemacht wurden. Diese Regelmässigkeit wurde als Folge der Selbstorganisation im Energieumwandlungsprozess gedeutet. Die untersuchten Abschnitte wiesen im allgemeinen durchschnittliche Steigungen von weniger als 0.2 m/m auf. In dieser Studie wird die Stufen-Becken-Struktur eines sehr steilen Gebirgsbaches im Schweizerischen Alptal-Einzugsgebiet untersucht, dessen Steigung zwischen 0.10 und 0.35 m/m variiert. Ein 1.5 km langer durchgehender Abschnitt des Baches wird mit dem Ziel untersucht, die grosse Variabilität in Bachbettgeometrie, Sedimentgrösse, und Stufen-Becken-Morphologie entlang des Bachverlaufes zu erfassen. Diese Variabilität wird durch die Kontrolle des Untergrundgesteins, durch seitlichen Sedimentzufluss und durch mit dem Bachverlauf stark variierende Sedimenttransportkapazitäten hervorgerufen. Als Hypothese wird vorgeschlagen, die Stufen-Becken-Morphologie des Baches als überlagertes System mehrerer Stufen-Becken-Sequenzen zu behandeln und die Stufenhöhe als unabhängige Variable zu betrachten. Es wird angenommen, dass die mittlere Stufenhöhe und -länge jeder dieser Sequenzen durch dem Bewegungsanfang entsprechende Abflussverhältnisse bestimmt wurden. Das Ergebnis für ein System mit überlagerten Stufen-Becken-Sequenzen ist ein stark lineares Verhältnis zwischen sequenzgemittelter Stufenhöhe und -länge. Diese zwischen Stufen verschiedener Grössen gefundene geometrische Ähnlichkeit scheint zu zeigen, dass sogar in sehr steilen Gebirgsbächen mit abrupten Änderungen Regelmässigkeit in einigen morphologischen Merkmalen beobachtet werden kann.

Um die Jährlichkeit von bettbildendem Abfluss zu untersuchen, wird eine statistische Hochwasseruntersuchung mit 18 Jahren Abflussdaten durchgeführt. Die Resultate gleichen denen einer älteren Studie, die auf vermutlichem Starkregen und der Unterteilung in Hydrotope basiert. Bachbettoberkantenbreiten an 22 Querprofilen werden unter der Berücksichtigung der variablen Topographie und Rauigkeit entlang des Bachverlaufes für verschiedene Hochwasserabflüsse simuliert. Die simulierten Breiten korrelieren deutlich mit im Wildbach gemessenen Breiten.

Wildbachverbauungen kommen im Alptal häufig zum Einsatz, um den Sedimenttransport zu kontrollieren und Bewohnungen zu schützen. Wildbachverbauungen können als das anthropogene Äquivalent zur Stufen-Becken-Morphologie betrachtet werden. Es wird ein Vergleich der Dimensionen dieser Bauwerke mit denen der natürlichen Strukturen versucht und im Allgemeinen eine gute Übereinstimmung gefunden.

## Résumé

Des torrents ayant un lit composé de sédiments alluviaux développent souvent une structure assez régulière en escaliers appelée structure marche-bassin. Cette régularité observée a été vérifiée par des études basées sur les valeurs moyennes de longueurs et hauteurs de marche prises sur de courtes sections de nombreux torrents. La régularité a été interprétée comme découlant d'auto-structuration dans le processus de dissipation d'énergie. Les observations ont généralement été menées sur des sections de torrent de pentes moyennes n'excédant pas 0.2 m/m. La présente étude analyse la structure marche-bassin d'un torrent affluent de l'Alp (rivière de Suisse centrale) composé de pentes moyennes comprises entre 0.10 et 0.35 m/m. Des relevés sur une section continue de 1.5 km sont effectués avec pour but d'étudier la grande variabilité de la géométrie du lit, de la taille des sédiments et de la morphologie marche-bassin le long de cette section du torrent. Cette variabilité est due au contrôle par la roche mère, les entrées latérales de sédiments et une capacité de transport des sédiments variant fortement le long de la section. L'hypothèse est proposée que la morphologie marche-bassin du torrent devrait être traitée comme un système de différentes séquences marche-bassin superposées avec la hauteur des marches définie comme une variable indépendante. Il est supposé que la longueur et la hauteur moyenne des marches dans chacune de ces séquences sont déterminées par le débit du torrent lors de la formation de chacune des séquences. Le résultat pour un système de séquences marche-bassin superposées est une relation fortement linéaire entre la hauteur et la longueur moyenne des marches regroupées par séquence. Cette similarité géométrique présente entre marches de différentes tailles semble indiquer que même dans des torrents très escarpés et contenant de brusques changements de pente, une régularité est observable dans certaines caractéristiques morphologiques.

Pour étudier la fréquence d'écoulements actifs dans la formation du lit, une étude statistique de la fréquence des crues est menée avec 18 ans de mesures de débit. Les résultats sont proches de résultats obtenus dans une précédente étude basée sur l'analyse de précipitations maximales et d'hydrotopes. Les largeurs du lit sont simulées dans 22 profils du torrent pour différents débits de crues en tenant compte des variations de topographie et de résistance à l'écoulement le long du torrent. Les largeurs simulées corrèlent fortement avec les largeurs mesurées dans le torrent.

Des structures de stabilisation du lit sont nombreuses dans les affluents de l'Alp de manière à y assurer un contrôle du transport des sédiments et une protection des habitations. Ces structures artificielles implantées dans des torrents peuvent être considérées comme l'équivalent anthropogène des structures naturelles de marches et de bassins. Une comparaison des dimensions de ces structures artificielles avec les structures marche-bassin naturelles est effectuée et en général une bonne concordance est trouvée.

## Contents

<b>ABSTRACT .....</b>	<b>II</b>
<b>ZUSAMMENFASSUNG .....</b>	<b>III</b>
<b>RESUME.....</b>	<b>IV</b>
<b>1 INTRODUCTION.....</b>	<b>1</b>
1.1 MOTIVATIONS .....	1
1.2 CHANNEL CLASSIFICATION.....	1
1.3 STEP-POOL FORMATION.....	2
1.4 RESEARCH OUTLINE .....	4
<b>2 STEP-POOL DEVELOPMENT, LITERATURE REVIEW.....</b>	<b>5</b>
<b>3 STUDY AREA.....</b>	<b>9</b>
3.1 ALPTAL EXPERIMENTAL CATCHMENTS OF WSL.....	9
3.2 CHARACTERISTICS OF THE VOGELBACH.....	9
3.2.1 <i>Situation, geology and landuse</i> .....	9
3.2.2 <i>Channel type</i> .....	10
3.2.3 <i>Climate and hydrology</i> .....	10
3.2.4 <i>Description of study reach</i> .....	12
<b>4 FIELD INVESTIGATIONS.....</b>	<b>13</b>
4.1 LONGITUDINAL PROFILE.....	13
4.2 CROSS SECTIONS .....	14
4.3 CHANNEL WIDTH.....	14
4.4 BED SEDIMENT SIZE.....	14
<b>5 COMPUTATION OF PARAMETERS .....</b>	<b>15</b>
5.1 SLOPE.....	15
5.2 STEPS AND THEIR CLASSIFICATION .....	16
5.2.1 <i>Relative position of steps and pools</i> .....	18
5.2.2 <i>Step categories</i> .....	18
5.2.3 <i>Step height</i> .....	19
5.2.4 <i>Step length</i> .....	19
5.3 DRAINAGE AREA .....	20
5.4 PARTICLE-SIZE DISTRIBUTION .....	22
5.4.1 $D_m$ .....	22
5.4.2 $D_{84}$ .....	23

---

<b>6</b>	<b>ANALYSIS OF STEP-POOL PARAMETERS .....</b>	<b>25</b>
6.1	INFLUENCE OF SLOPE AND DISCHARGE .....	25
6.1.1	<i>Step height and length against longitudinal distance .....</i>	<i>25</i>
6.1.2	<i>Step height and length against slope.....</i>	<i>25</i>
6.2	VARIATION OF STEP LENGTH WITH STEP HEIGHT .....	29
6.3	STEEPNESS (H/L) .....	31
<b>7</b>	<b>STATISTICAL ANALYSIS OF STEP-POOL GEOMETRY.....</b>	<b>37</b>
7.1	STATISTICAL MOMENTS.....	37
7.2	DISTRIBUTION TYPE .....	37
7.3	CORRELATION COEFFICIENTS .....	39
7.4	AUTO-COVARIANCES.....	40
<b>8</b>	<b>FLOOD FREQUENCY ANALYSIS .....</b>	<b>42</b>
8.1	ANNUAL PEAK METHOD.....	43
8.2	PARTIAL DURATION METHOD .....	46
8.3	FLOOD ESTIMATION WITHOUT FLOW MEASUREMENTS.....	47
8.4	COMPARISONS.....	50
<b>9</b>	<b>CHANNEL WIDTH SIMULATION .....</b>	<b>51</b>
<b>10</b>	<b>COMPARISON WITH CHECK DAMS IN NEARBY STREAMS.....</b>	<b>55</b>
<b>11</b>	<b>CONCLUSIONS.....</b>	<b>59</b>
<b>12</b>	<b>ACKNOWLEDGMENTS .....</b>	<b>60</b>
<b>13</b>	<b>REFERENCES.....</b>	<b>61</b>
<b>14</b>	<b>APPENDIX .....</b>	<b>63</b>

# 1 Introduction

## 1.1 Motivations

The intensification of landuse in mountain basins in the past decades and the resulting impacts on headwater streams themselves and on downstream river networks has led to a growing interest in the processes occurring in mountain streams. Studies on headwaters have in the past been neglected in comparison with lowland rivers. The downstream impact of a change in headwater flow and sediment supply may create a wide spectrum of problems. Higher sediment supply to valley rivers can cause the aggradation of streambeds and generate flooding. Retaining sediment volumes in headwaters can create strong erosion around bridge pillars and on the outer side of river bends creating bank instabilities. Causes are various. The transformation of forest areas in pastures increases the direct runoff and therefore the sediment transport capacity of a stream. Badly designed flow regulation may retain sediment and release it only violently during low frequency high discharge events. Of course a change in the distribution of heavy rainfall events due to climate change or variability will also force river systems to adjust towards a new equilibrium state. A better understanding of processes occurring in headwater streams and an insightful management will help to minimise effects resulting from human and natural disturbances.

## 1.2 Channel classification

A classification of channels coupling reach processes with morphologies as done by Montgomery and Buffington (1997) is a first step in understanding and comparing different channel types. Bedrock and colluvial reach types were defined separately to 5 alluvial reach types. The morphological differences in the alluvial reaches are reflected in different ranges of slope, grain size, shear stress and roughness. In the order of increasing steepness, the classification comprises dune ripple, pool riffle, plane bed, step-pool and cascade types. The two last ones correspond to steep headwaters on which the present study focuses.

Montgomery and Buffington define *cascade channels* as streams in which energy dissipation is dominated by continuous tumbling and jet-and-wake flow over and around individual large clasts. Longitudinally and laterally disorganized bed material typically consisting of cobbles and boulders is characteristic.

In contrast to cascade channels, *step-pool channels* are characterized by longitudinal steps formed by large clasts which are organized into discrete channel-spanning accumulations that separate pools containing finer material (Montgomery and Buffington 1997). The repetitive sequence of steps and pools results in the typical staircase-like structure which can be seen as analogous to meanders in the vertical dimension. Step forming particles have large sizes in comparison with normal flow depth and are often tightly imbricated (Chin 1989). The typical visual appearance at low flow (Figure 3.2) results from low frequency high magnitude flood events (Whittaker 1982). Steps tend to be very stable structures at normal flow conditions. The staircase-like structure of the bed results in alternating critical to supercritical flow over steps and subcritical flow in pools. Roller eddies forming at the change to subcritical flow dissipate large amounts of kinetic energy that would otherwise be available for erosion and sediment transport. Scouring of the pools at the base of the steps increases the slope difference between steps and pools and adds form resistance (Chartrand and Whiting, 2000). Steps provide an important percentage of roughness and elevation drop in step-pool channels (Montgomery and Buffington 1997).



Two morphological dimensions can easily be determined for step-pool units. Step height as the vertical drop generated by a step and the step length or wavelength as the distance parallel to the slope separating steps (Figure 1.1).

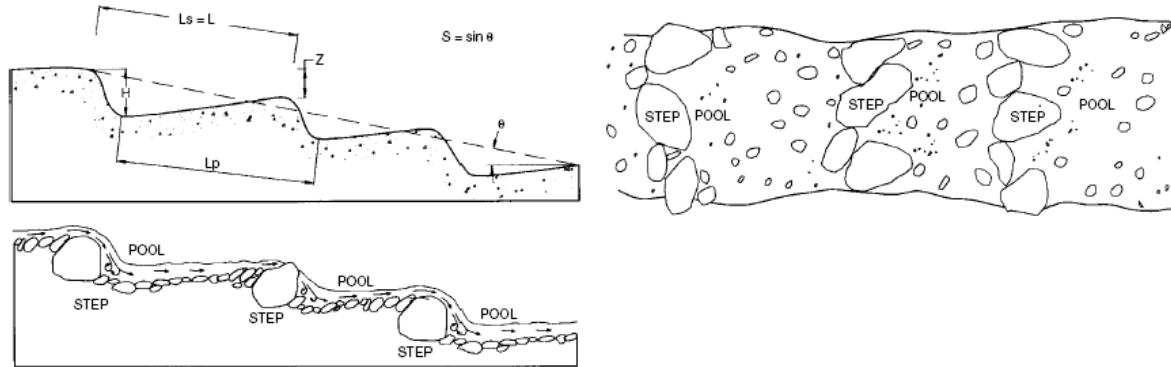


Figure 1.1: Sketch of idealized step-pool sequence, from Lenzi (2001).

### 1.3 Step-pool formation

Step-pool channels are associated with steep gradients, small width to depth ratios and pronounced confinement by valley walls (Montgomery and Buffington 1997). Step-pool channels add a much higher stability to a stream than it would have with the same sediment and constant slope, but the physical mechanisms responsible for step-pool formation are not so clearly defined. No clear rule exists to decide if a stepped morphology will develop in a stream knowing its topography, sediment and flow parameters. Much of our current knowledge comes from flume studies with inherent scale problems. Field observations and measurements are difficult and long but give precious new information on streams that are normally heterogeneous from reach to reach and allow comparison with the largely simplified situation of flume studies. Nonetheless, requirements have been found in various studies for step-pool development which are reviewed by Chartrand and Whiting (2000):

1. Steep gradients (Grant et al. 1990, Montgomery and Buffington 1997)
2. Heterogeneous sediment cover with the largest particles immobile except under step-forming flow conditions (Grant and Mizuyama 1991)
3. High magnitude low frequency flow events with return periods ranging from 20 to 50 years or more (Whittaker and Jaeggi 1982, Grant and Mizuyama 1991, Chin 1998)
4. Near-critical to supercritical flows (Grant and Mizuyama 1991)
5. A low sediment supply environment (Grant and Mizuyama 1991, Grant et al. 1990)

Different approaches were followed when trying to understand the formation of step-pool systems. Whittaker and Jaeggi (1982) report three different mechanisms for step-pool formation:

- **Antidune theory.** Steps are relicts of antidunes that were formed under standing waves where the waveform of the bed is in phase with the waveform of the water

surface. A Froude number range varying with flow depth and step spacing can be determined in which antidunes are likely.

- **Dispersion and sorting theory.** Over steps, where the local energy gradient is higher than average, there is a high rate of shearing of bed material. Coarse particles will move to the surface and increase the bed elevation. On flatter sections where sediments are smaller, large particles are preferentially exposed and will tend to move to the next step.
- **Velocity reversal theory.** With increasing discharge, a greater increase of velocities can be observed in pools than over the steps. By extrapolation one could expect the velocity in pools to exceed the one over steps during large floods. At high flows, unstable coarse grains will move quickly from one step through a pool to be deposited on the next step, thus, maintaining the step-pool features.

The two last theories were developed for riffle-pool systems and are only by analogy considered to apply to step-pool systems. Also, they do not explain the initial formation but only the conservation of steps. In addition to those presented above, Abrahams, Li and Atkinson (1995) develop a theory combining step-pool structure and flow resistance.

- **Maximum flow resistance model.** Step-pools develop in conditions where the largest floods are just capable of transporting the largest debris. Those will tend to form steps acting as keystones retaining smaller debris. Now, some arrangements of steps impart greater resistance to flow than others. Because greater resistance to flow means lower flow velocity and lower flow competence, those step arrangements that impart greater resistance might be expected to last longer than others, which tend to be destroyed and replaced with new step arrangements until the new arrangements have higher resistance to flow. Thus it is reasoned that step-pool streams evolve toward an arrangement of steps that maximizes resistance to flow.

In steep headwaters, with bedforms that are difficult to adjust where channels may be dominated by large roughness elements only rarely submerged, true antidunes may be impossible to achieve (Chin 1999). Whereas the maximum flow resistance model does not require the particles forming the steps to be submerged. Step-pools that maximize resistance to flow may thus develop at Froude numbers below the range at which step-pools may form as antidunes (Abrahams et al. 1995). The same observations were made in flume studies by Whittaker and Jaeggi 1982. They noticed that at higher slopes ( $> 0.075$ ) and relatively small flows, the coarser grains had a considerable effect on the bed deforming process. The flow first formed regular wavetrains over the initially plane bed, but with some degradation the flow pattern subsequently developed increasingly in response to the location of larger individual roughness elements. These elements anchored some of the waves, preventing migration.

Parallel to the alluvial self-adjusting structures, forced morphologies need to be considered in natural streams. In forested environment large woody debris are a natural input to streams. If logs are large enough they will anchor on the banks and form very stable steps on which other alluvial structures will be overlaid or will have to adapt. Reaches where the transport capacity exceeds the sediment supply may develop as bedrock channels. In that case, some alluvial

---

material may be stored temporarily in scour holes. The geomorphological structure of a stream depends on the local geology and lithology.

### **1.4 Research outline**

This research focuses on the step-pool morphology of a steep alluvial mountain stream. The hypothesis is proposed that the step-pool structure of a stream is composed of superposed step-pool sequences. Each sequence is created by streamflow of a given (and different) frequency of occurrence which corresponds to a critical threshold of motion of bed sediment particles with a given size. The average step height of each sequence is related to the sediment size at incipient motion. Thus it is proposed that large floods with a low frequency of occurrence will form a step-pool sequence with large steps and long pools (runs). Subsequent floods with a higher frequency of occurrence will form smaller and shorter steps which are superposed in a random manner onto the first step-pool sequence. As a result, the observed step-pool system in a stream is a function of streamflow (flood) history, and is dynamic in time.

This research attempts to identify signatures of such a system of superposed step-pool sequences by statistical analysis of data from a mountain stream in Central Switzerland. First a literature review is presented in chapter 2, in which results of earlier studies on step-pool morphology are briefly presented. Chapter 3 deals with the characteristics of the study stream and the catchment area which is an experimental catchment of the WSL instrumented since around 1970. The field investigations that consist of a precise topographic survey and of sediment count in summer and fall 2003 are described in chapter 4. Step dimensions, channel slope and sediment size distribution are derived from the recorded data in chapter 5. The classification of steps in height categories in order to separate step-pool sequences resulting of different flow events is emphasized. In chapter 6, the evolution of step dimensions with slope and the relation of step length to step height is analysed. Strong relations are found between category-averaged values but large variances are dominant and only weak trends are observed without averaging. A statistical analysis of those variances is presented in chapter 7. Correlations between step dimensions are also analysed and the distribution type of step lengths and heights is described. To examine the frequency of channel forming flow, a flood frequency analysis is conducted with 18 years of runoff data in chapter 8 and the results are compared with previous studies. In chapter 9, channel widths are simulated with roughness values changing along the stream. The discharge used for the simulation is calibrated so that simulated widths fit measured widths. Considering the results of the flood frequency analysis, the frequency of channel forming flow can be determined. Check dams are the anthropogenic equivalent to natural step-pool systems. Their purpose is to decrease the sediment transport during flood events. A good comprehension of step-pool systems can be useful to improve check dam functionality. A comparison between these artificial steps with natural steps is presented in chapter 10.

## 2 Step-pool development, literature review

**Kennedy (1961)** studies pool-rifles and defines an area in a  $F$ -( $d \cdot k$ )-diagram for possible antidune formation (Figure 2.1).  $F$  is the Froude number,  $d$  the flow depth and  $k$  the wave number of riffle spacing.

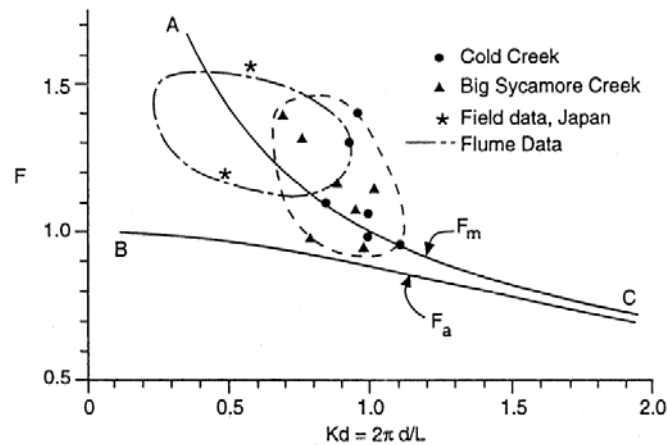


**Figure 2.1: Froude number vs. flow depth times wavenumber of step length. Upper ( $F_m$ ) and lower ( $F_a$ ) limits for antidune formation by Kennedy (1961). Diagram from Chin (1999) including her data.**

In 1982 **Whittaker and Jaeggi** undertake to clarify the origin of step-pool sequences and to assess their effect on the stability of the bed. They perform laboratory tests in a tilting 10 m channel. From an initially arranged plane bed they observe the formation of an irregular bed and a decrease in sediment transport for constant flow rates. They attribute this stabilization to an increase in form resistance and to armouring of the bed. Antidune formation is supported for relatively high discharges with lower slopes ( $< 0.075$ ) but not for higher slopes where the position of individual large grains is determinant.

**Whittaker (1987)** applies the inverse power law for step length and slope already proposed by Judd (1964). He relates step length,  $L$  to channel slope,  $S$  without influence of any other parameter and obtains a fairly good fit of the data (Figure 2.2). The overlap of slope ranges from the different reaches is however small. Chin (1998) tries to apply the same model to her data and finds an expression with different coefficients but a much less convincing fit (Figure 2.3).

$$L_{\text{Whittaker 87}} = \frac{0.3113}{S^{1.188}}, \quad L_{\text{Chin 98}} = \frac{2.67}{S^{0.206}} \quad (1) \text{ and } (2)$$

The conclusion from these studies is that average step length and channel slope are inversely (but weakly) related.

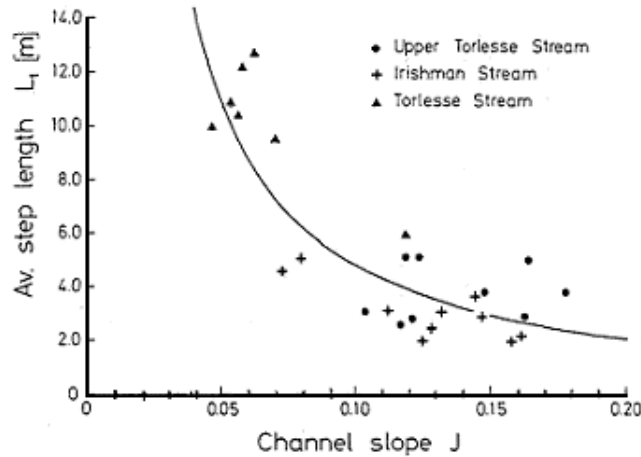


Figure 2.2: Plot of step length versus channel slope by Whittaker (1987).

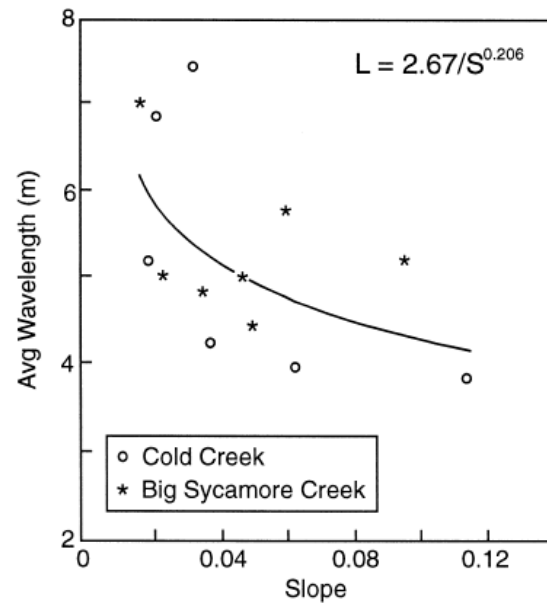


Figure 2.3: Relationship between step length and slope by Chin (1998).

A conceptual model for natural streams is developed in 1995 by **Abrahams, Li and Atkinson** stating that streams develop in a way that maximizes flow resistance. In addition to this “maximum flow resistance model” (explained in 1.3) they defend that steps are regularly spaced only if the step heights are uniform and that step height largely depends upon boulder size.

The reach average of steepness, relation of step height to step length,  $\langle H/L \rangle$  is found to exceed the slopes  $S$  of 18 tested natural reaches. All reaches give values of  $\langle H/L \rangle$  between  $S$  and  $2S$ . In flume experiments different step heights and lengths ratios are fixed for given slopes and maximum flow resistance found for regularly spaced steps with  $\langle H/L \rangle / S$  also between 1 and 2. The relation of  $\langle H/L \rangle = 1.5 S$  is found to fit data of the natural reaches as well as of the flume studies with maximal flow resistance pattern. The natural reaches should therefore have adjusted their form to maximize flow resistance. It is noteworthy that the natural reaches are very short (4 to 12 step-pool units) and were chosen to contain well developed step-pools without runs between them. The reaches are not necessarily representative of the overall stream.

The antidune theory is neither supported by data of natural reaches nor by flume step-pools features with maximal flow resistance. Froude numbers fall well below the ones usually associated with antidunes.

In a strongly field orientated study **Chin (1998)** analyses 13 reaches in two streams. The emphasis is set on variations of reach-average values between the reaches and especially on adjustment of parameters to slope. A strong positive correlation is found between step height and slope but it is also noticed that the control of slope on height may be secondary because changing slope downstream is commonly associated with changing particle size and discharge. Step height may vary because of changes either in discharge or particle size. Similarly, step length is thought to be correlated to slope only through discharge. Discharge increases downstream and usually slopes become gentler.

**Chartrand and Whiting (2000)** observe a systematic distribution of channel types with slope and propose to use slope as a first assessment to predict channel morphology. Because large overlap exists, field verifications remain necessary. It is interpreted that antidunes are the initial state for step-pool formation, giving rise to the regular spacing. Further erosion will modify structure dimensions such as step height. This may then maximise resistance to flow and explain why derived features no longer plot in the stability field of antidunes. Geometric relations are studied for step-pools and a strong positive correlation is found between step length and step height which is again strongly correlated to the median grain size measured on step risers. They find similar grain sizes for step risers of a same reach and suggest that similarity in step riser median grain sizes for reaches of a same stream indicates reaches built by same flow events. That step height depends upon the magnitude of the flood event by which it was created goes towards the hypothesis of superposed structures created by flow events of different magnitudes. Only very poor correlations are found for step height and length with slope, thus not verifying the inverse power law between step length and slope found by Whittaker (1987) and also Chin (1998).

**Chin (1999)** tests the antidune theory with data of her previous studies in the Santa-Monica Mountains. Analysis is done considering measured step lengths and hydraulic conditions associated with step formation. Flow depth and velocity representative for formative events are computed from sediment sizes on step risers. Although the results are in general in agreement with the antidune theory, they suggest that true antidunes may be difficult to achieve in steep headwaters (like those in this study) where channels may be dominated by large roughness elements. In gentle reaches where bedforms are more adjustable and easily submerged, antidunes are more likely.

Measurements during a median annual flood are done by **Zimmermann and Church (2001)**. They attempt to determine what forces act on the bed of a boulder-cascade channel during high flows. Calculations are based on channel gradient, pool gradients and flow velocities. Investigations on geometric relations of step-pools are a secondary objective. Differing from previous studies, attention is turned towards the variance of measured parameters more than to averages in order to determine correlations. The high variations found in step lengths, step heights and other parameters are considered to be indicative of the random nature of step location and structure along a reach. No convincing evidence is found by Zimmermann and Church that special conditions govern step formation. Histograms of step heights and lengths are appreciably positively skewed. The advanced explanation is not a distribution property but an artefact of the survey, inasmuch as small step-pool units were not systematically measured.

Neither the antidune theory nor the theory of maximum flow resistance is supported by the results. Froude numbers are found much too small for possible antidune formation. The steepness factor  $c = \langle H/L \rangle / S$  varies from 1.6 to 2.3 for the reach averages with of course much larger variations for individual step-pool units. Also, replotting data of number of previous studies it is shown that the ratio of  $\langle H/L \rangle / S$  becomes restricted to values below 2 for gradients above 0.075 and approaches  $c = 1$  asymptotically with increasing slope. (Figure 2.4).

The proposed mechanism of step formation begins with the random arrival of a large boulder in the river that flows cannot normally move acting as keystone. Smaller particles will get imbricated behind the keystone and eventually a step can form.

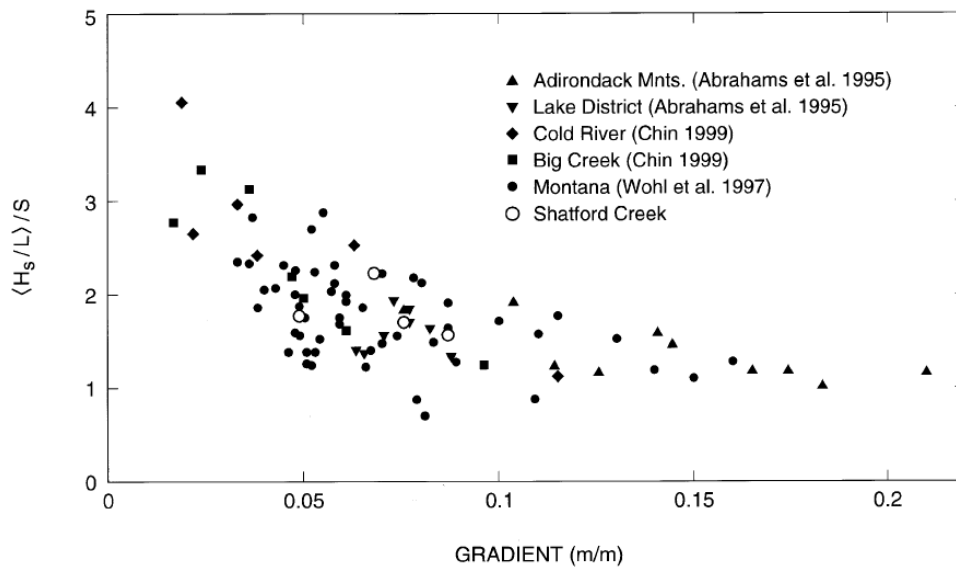


**Figure 2.4: Variation of  $\langle H/L \rangle / S$  with gradient from a number of studies as presented by Zimmermann and Church (2001) showing that there is no restriction of  $\langle H/L \rangle / S$  between 1 and 2.**

**Lenzi (2001)** studies a small mountain stream before and after a large flood with a return period between 30 and 50 years. Analysis is built on the principle that formative events, punctuated by periods of evolution, recovery or temporary periods of steady-state conditions, control the development of step-pool morphology. Lenzi emphasizes the importance of the temporal factor, the time since the last extraordinary flood and the succession of flood events of different magnitudes.

In the studied stream the extraordinary flood led to the breakdown of step-pool sequences, to a flattening and smoothing of the channel. The flow resistance diminished together with the steepness factor  $c$  which is usually less than 1. This is in disaccord with Abrahams et al. (1995). Four years later a flood with a return period of about five years led to the formation of new step-pool sequences. Ordinary events then scoured fine sediments from pools causing an increase of  $c$ . The steepness factor evolution measured all over the cycle demonstrates that maximum resistance conditions are gradually reached at the end of a cycle of ordinary flood events. Doubt is brought to equations which determine step length from only gradient (Whittaker, 1987; Chin, 1998) or gradient and step height like Abrahams' et al. fit of  $\langle H/L \rangle = 1.5 S$  because in the study stream temporal variations of  $L$  are observed without substantial change in hydraulic gradients and the ratio  $H/L$  largely changes during the flood. The fits apply to a particular "historic" moment in the stream, to equilibrium conditions. They do not take into account temporal evolution.

The antidune theory is not rejected by Lenzi. The structures formed by the extraordinary flood together with estimated flow conditions for that moment plot in the formation zone for antidunes in a plot like Figure 2.1. For the later and less extraordinary formative events the Froude numbers are too low for antidunes to be likely in association with dimensions of then existing dimensions of step-pools. This gives additional evidence that step-pools can originally be formed as antidunes and are then reshaped by later erosion during events of smaller magnitude.

In accordance with Lenzi (2001), this study also emphasizes the dynamic nature of the step-pool morphology, in that steps are rearranged under formative flows of different magnitudes.

## 3 Study area

### 3.1 *Alptal experimental catchments of WSL*

The Swiss Federal Institute for Forest, Snow and Landscape Research (WSL) carried out a large research project called EROSLOPE II (Rickenmann and Dupasquier 1995) within the framework of the EU “Environment Programme”. The aim of this project was a better understanding of dynamics of water and sediments in alpine catchments. The WSL has been studying runoff generation, sediment transport and erosion for a long time in forested mountain catchments in the prealpine region of northern Switzerland. The EROSLOPE II project evaluated new measurement techniques for sediment transport in steep streams studying single particle movement and changes in streambed morphology in relation with extreme flood events. Hydrophones recording the impact of sediments on a horizontal plate on the bottom of a gauge have shown a strong relation between number of impacts and volume of sediments deposited in the retention basin as well as with runoff. The effect of woody debris on step-pool formation and the step spacing was studied on a 530 m reach in the lower part of the Erlenbach. The Erlenbach is a tributary to the Alp close to the Vogelbach, which is studied here. These two streams are similar in many aspects. Characteristics of the Vogelbach are discussed in the following chapter 3.2.

Both streams were instrumented by the WSL around 1970. Discharge, water chemistry, precipitation and other meteorological parameters are measured since then. The catchments have been the focus of investigations on forest hydrology, water budget, water chemistry, rainfall-runoff modelling, erosion and sediment transport (Burch, 1994).

### 3.2 *Characteristics of the Vogelbach*

#### 3.2.1 *Situation, geology and landuse*

As one of the upstream tributaries of the Alp the Vogelbach lies way back in the Alptal (Kanton Schwyz). Its mouth to the Alp is at an elevation of 1000 m a.s.l. and the watershed divide rises up to 1500 m a.s.l. The geology is the Flysch formation, a tertiary sediment caused by alpine uplift. The composition of that formation in the Vogelbach is dominated mainly by calcareous sandstones as well as argillite and bentonite schist. With this kind of bedrock one can expect soils showing a large clay content, which generally means slow infiltration rates. A more complete description of the geology of the Alptal can be found in Stammbach, (1988). The stream is continuously cutting into the unstable slopes, carrying material during almost every intense storm. Due to the extreme steepness and a well developed dense drainage network, there is a very quick response of discharge to precipitation. The density and regularity of the drainage network observed in the field closely corresponds to the network of the map in Figure 3.1. The difference in aspect between the Vogelbach and the nearby Erlenbach is due to higher clay content and more schists in the Erlenbach leading to even less stable banks than in the Vogelbach. In the extreme, vegetation can hardly settle on them.

About 65 % of the basin surface is covered by forest. The most upper parts are covered by meadows but only infrequently used as pastures. The forest of the basin is exploited using small area treatment and single tree selection but because of the very deep incision of the Vogelbach no harvesting is done close to the stream itself. The amount of woody debris in the stream is therefore not influenced by harvesting. Woody debris forcing steps are not very numerous but appear throughout the investigated reach.



### 3.2.2 Channel type

With an average slope of 0.187 and reaches ranging from 0.1 to 0.4 the studied section of the Vogelbach representing about 70 % of the total main stream length is much steeper than reaches in other studies (e.g. Abrahams et al., 1995; Chin, 1999; Chartrand and Whiting, 2000; Zimmermann and Church, 2001).

Montgomery and Buffington 1997 find that alluvial reaches with slopes greater than 0.065 typically have cascade morphology. Even the flattest reaches of the Vogelbach have slopes well above this limit but morphologically a large part of the Vogelbach is to be considered as a step-pool stream. Chartrand and Whiting (2000) compare data from different studies and find largely overlapping slope ranges for the different morphologic forms. They reduce the limits of a possible appearance of a step-pool systems to a slope range between 0.05 and 0.134. Again, the Vogelbach lies well above this range but in its more gentle reaches, step-pools are not totally in disagreement with this classification. In its steepest alluvial reaches, the morphology is more irregular. Steps are not always nice features lying straight across the stream. An evolution towards cascade morphology becomes visible.

The streambed is mostly characterised by alluvial sediments. Bedrock reaches appear only in the steepest sections of the stream. The hillslope colluvial sediment supply is substantial but not regularly distributed along the stream. Mostly consisting of mass failure, it is neither spatially or temporally constant, depending on the steepness of the hillslopes that at some places can exceed 100 %.

### 3.2.3 Climate and hydrology

The amount of precipitation for the study region is about 2300 mm/year with a maximum in the summer months (Rickenmann and Dupasquier, 1995). This is distinctly higher than the average value for Switzerland of 1500 mm. About 30-40 % of the precipitation falls as snow. The start of the snowmelt season in spring is variable. It may be in early March or mid April and coincides with higher flows. Streamflow is typically perennial with low flows through the winter and higher flows during snowmelt. Flows due to high intensity rainfall events in the summer might reach very high magnitudes if they occur together with snowmelt.

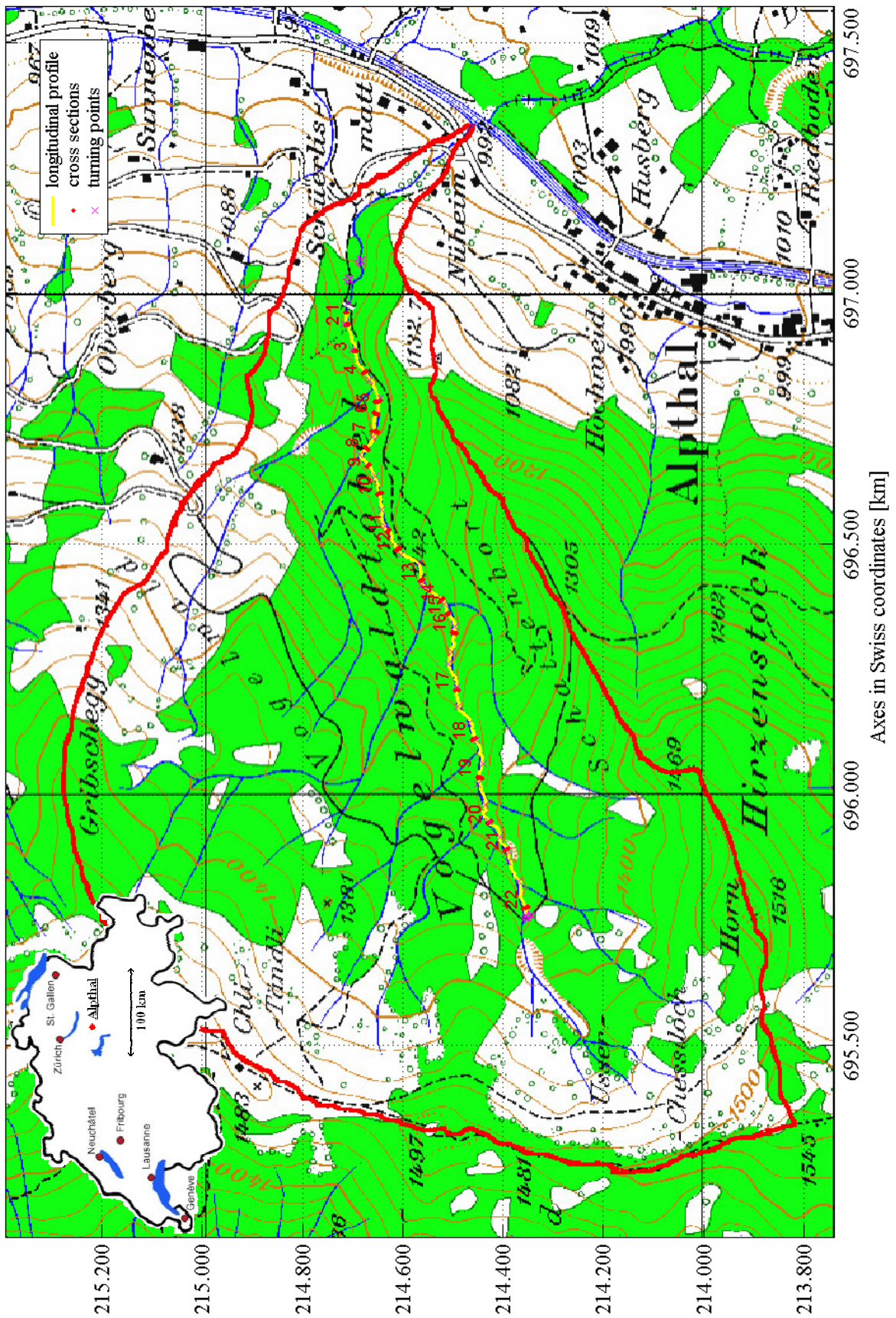


Figure 3.1: Situation map and map of the Vogelbach catchment (Swiss Topo). Also shown is the study reach with 22 cross section locations used in hydrological modelling.

### 3.2.4 Description of study reach

From its junction to the Alp the first 200 m of the stream bed are stabilized with about 20 check dams upstream of which the measurement cabin and gauge are situated. Measurements were started upstream of this gauge. The following 1.5 km are mostly alluvial with one steeper bedrock reach in the middle. This is the study section. Forced morphologies where alluvial patterns cannot develop independently appear where logs block the stream, in the bedrock reaches and where mass movements enter the stream with particles too large to be moved by floods.

Upstream of where measurements were stopped (this position corresponds to a road crossing the stream visible in Figure 3.1), the stream type is totally different. Due to a lack of fine sediment water is flowing underneath and between the rocks during normal discharges. It does not exhibit a step-pool system and a thalweg can hardly be determined. Boulders seem to be moved only very infrequently and are placed more by hillslope erosion and resulting incision of the bed than moved by floods.



Figure 3.2: Well developed step-pool sequence in the middle part of the Vogelbach.



Figure 3.3: Section of the Vogelbach dominated by large hillslope particles.

## 4 Field investigations

In this chapter a description of the recorded field investigations is provided. Measurements were carried out in the months of July to November 2003 during low flow conditions. In this time no flood capable of moving step forming boulders occurred.

Most of the measurements were made with two people. Table 4.1 shows a recapitulation of the needed time.

**Table 4.1: working time for measurements**

Measurement	Time [days · person]
general reconnaissance and learning of methods	7
longitudinal profile and cross sections	17
channel width and grain size distribution	4
total	28

### 4.1 Longitudinal profile

Rather than identifying and measuring individual steps and pools, a detailed and continuous survey of the longitudinal profile of the stream was conducted. Step-pool sequences were then objectively defined from the longitudinal profile.

Because of the steep topography, the dense vegetation and especially the deep incision of the Vogelbach in the topography surveying using GPS-technique was not possible. A Wild T1600 theodolite was used to survey the points of the longitudinal profile. The starting points for the investigation were taken from an older WSL field campaign in the lower part of the stream which was started using GPS outside of the forest. Except these first fixed points, the investigation was carried out independently starting at the gauge and ending at the road about 1.4 km upstream (Figure 3.1).

The thalweg or stream centreline was followed along the profile. The points were not chosen with a regular spacing but located at characteristic (horizontal and vertical) edges in the stream. Step crests, step bases and pool troughs were located visually and the reflector placed on them. With a profile of 1470m length and 1145 points the average distance between two measurement points is about 1.3 m but it is highly variable along the stream profile, depending on local morphology. For each measurement point note was taken whether it is situated on sediments, bedrock or woody debris.

Due to the dense vegetation, 29 fix turning points had to be chosen to place the theodolite. These points were generally placed on bedrock or very large boulders and marked with paint. Even with these measures, most of the fix points are not expected to have a long lifetime as even large boulders are moved in floods and bedrock is eroded quickly.

At the end of the profile two points were marked beside the road. At that spot the opening angle to the sky is much larger again and so a verification of these two points with GPS-technique is possible. For the purpose of this study, the absolute position of each point is not the important factor. Differences in position and elevation from one point to a few preceding and following ones is used to compute parameters like step height and length. Also all the points were plotted on a georeferenced map (Figure 3.1) from which no significant error could be detected. Checking the end position of the profile was done in case it will be used for other studies. The difference of about 1.5 m can seem large but has to be taken in the context of the difficult topography, the high number of turning points and the unstable ground.

## **4.2 Cross sections**

Points for 22 cross sections were measured together with the longitudinal profile. Attention was given to a more or less equal spacing of the cross sections and that the cross sections are representative for the stream section they are in. In regard to the sediment analysis the locations were chosen not to be situated on bedrock. The cross sections were always measured from the left to the right border including points much higher than the estimated water level during large floods. About 10 points were measured per cross section. Every cross section was marked in the field by a flag for later additional measures at each cross section.

## **4.3 Channel width**

At each cross section the active channel width was measured with a tape. Well established vegetation and break points in the bank slope were used to define the active channel width.

It was also attempted to define channel width from aerial pictures. However the vegetation comes too close to the stream and very precise pictures would be necessary, which are not available.

## **4.4 Bed sediment size**

Particle size samples were taken at chosen cross sections along the stream in order to compute the median diameter ( $D_m$ ). Sample areas should best be uniformly distributed along the stream. Unfortunately this could not be done in the steepest section of the stream. Sampling there would have been too difficult and dangerous. Changing the sampling technique would not have made sense in order to perform comparisons.

In the sampling, 100 stones were randomly picked and recorded in different classes at 12 locations out of the 22 cross sections in a way similar to the Wolman method. Randomly walking is not possible in the Vogelbach as the boulders are too large to allow not choosing where to step. A 1m stick was flipped around and each stone coming to lie under its ends measured. The stream was crossed in that way enough times to collect 60 particles, then another 20 and again 20 for a final total of 100 particles. So the sampling is not punctual but extends over a stream length of about 15 to 50 m. On some locations where the cross sections are close together the sampling is representative for two cross sections. The measured axis of the grains is always the b-axis. Classes were taken as 8 to 11, larger than 11, 16, 22, 32, 45, 64, 90, 128, 180, 256, 360, 512 and 720 to 1024 mm. Grains smaller than 8 or larger than 1024 mm were recorded but not counted for the total of 100 and not used for the sediment size distribution calculation.

In addition to this, the five largest (step building) boulders were measured at each cross section. The mean of this is often used (see for instance Chin 1997) as a value for  $D_{84}$ . This measure was intended to allow comparison with previous studies.

## 5 Computation of parameters

Starting with the sediment counts, the measured points of the longitudinal profile and the cross sections, derived parameters like median grain size, slope, step length and height can be determined. These parameters were computed with short Matlab codes.

### 5.1 Slope

The idea is to keep the stream as a continuously evolving element and not to divide it into reaches. Slope is defined as a function along the stream. To compute slope for each measurement point as the slope from the downstream point to the point itself of course gives - and this especially due to the step-pool character studied here - high fluctuations and no information on channel slope representative for individual step location. A larger distance than just two points has to be considered and best, a regression made. Several techniques were tried and compared:

- i. Representative slope for point  $i$  computed as the slope from point  $i$ -interval to the point  $i$ +interval (“interval” represents a certain number of points).
- ii. Representative slope for point  $i$  computed as the slope from a point  $j$  at a defined distance downstream of point  $i$  to a point  $k$  at the same distance upstream. As the points are not regularly spaced, an elevation grid was interpolated for the longitudinal distance with one point every 5 cm and the longitudinal position of point  $i$  rounded to the nearest 5 cm point.
- iii. As for the first technique, a certain number of points back and forward are used to define the interval but the slope is not computed between two points but as the slope of a first order regression curve through all points of the interval.
- iv. As for the second technique, a certain distance up- and downstream is used to define the interval but the slope is not computed between two points but as the slope of a first order regression curve through all points of the interval. This technique gives the best result and is used for further calculations. See appendix A.4 for Matlab code.
- v. A fifth and different approach is to fit the elevation data for the longitudinal profile with a polynomial curve and to derive this curve. This method does not give good results as it is difficult to obtain a good fit through a long and complex profile such as the Vogelbach one.

For the first four possibilities, it was not possible to compute the slope for the points lying within the interval from the beginning or the end of the stream. A constant slope was taken from the first/last point where slope was computable to the beginning/end of the stream. This is coherent with observations in the field.

The five techniques for determining mean channel slope give very different results. The choice of the interval length for the finally chosen fourth technique has a large influence on fluctuations of the slope along the stream. The influence is decreasing only slowly with the length of the intervals (Figure 5.1).

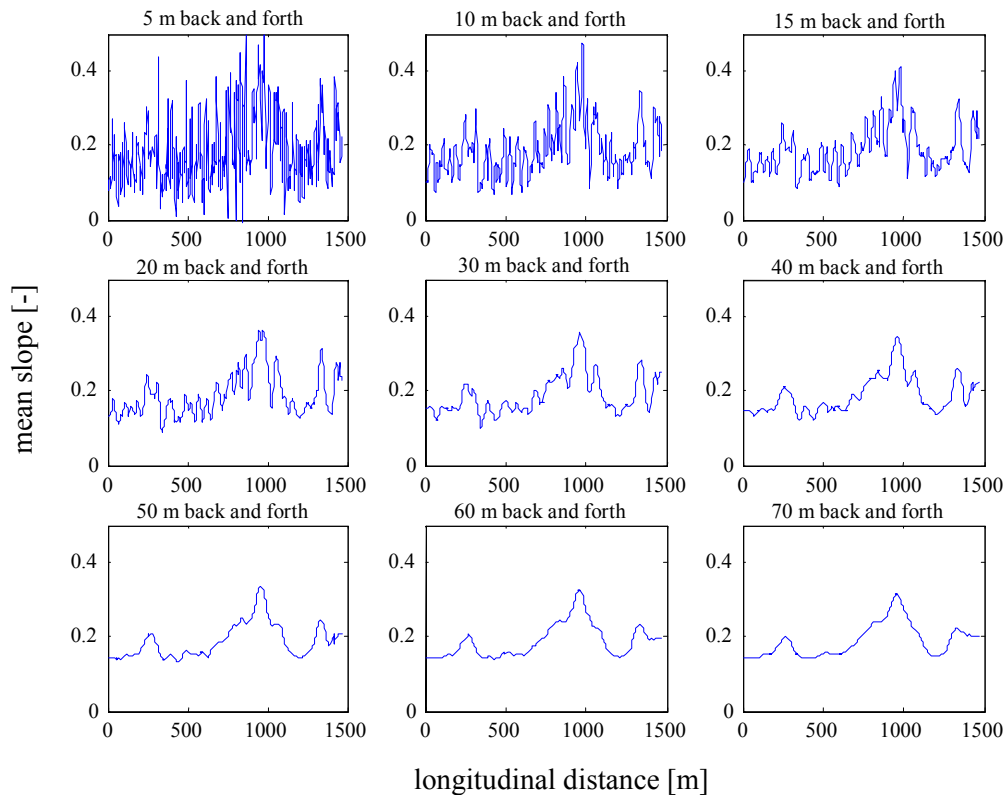


**Figure 5.1: Mean slope as a function of longitudinal distance showing different results when computed with different moving window sizes.**

A large moving window renders a regular evolution of the mean slope along the stream. But this is not the case in the Vogelbach. Slope changes occur over very short distances so a small moving window has to be taken. The choice of a window of 30 m (15 m back and forth, further mentioned as  $w = 15$ ) is discussed in chapter 6.1.2.

## 5.2 Steps and their classification

During measurement of the longitudinal profile, points situated on step crests were carefully recorded, but no notice was taken that those points are situated on crests. The idea is to define steps automatically and objectively out of the data. This was done using the slope between two successive points as the relevant parameter. A critical slope has to be defined for this purpose. If it is exceeded the upper point is considered as a step crest. If the slope between such a defined crest and the next upstream point exceeds again the critical slope, then the heights are merged to form one larger step, and so on till a slope is found that does not exceed anymore the critical slope. An exception is made to this rule if the directly following crests are not of the same type (alluvial sediment, bedrock, woody debris). In that case a new step is defined at each change in type (see appendix A.1 for the Matlab code). The critical slope must be chosen above the highest mean slope for any part of the stream which is about 0.4 in the Vogelbach.

Figure 5.2 shows the number of computed steps as function of the critical slope. For small critical slopes, the number of steps increases with increasing slope because of the above explained merging. But generally, the number of steps decreases with increasing critical slope. Too steep a critical slope will cause many steps to be lost.

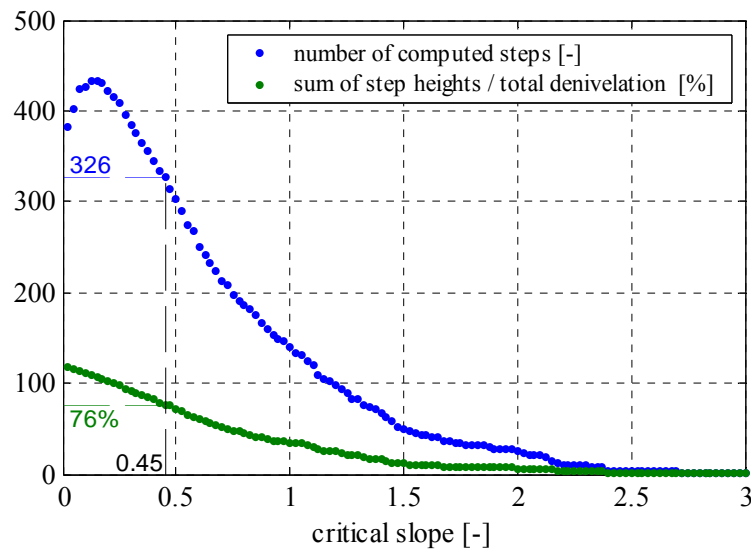


**Figure 5.2:** Number of steps as a function of critical slope and the percentage of stream elevation loss generated by steps.

The slope of 0.16 leading to the maximum number of steps is slightly under the overall mean slope of the stream (0.187). This representation does not show any characteristic slope that could mark the beginning of steps. The sum of heights of all computed steps divided by the total elevation loss of the stream gives the percentage of height generated by steps. For a very low critical slope this value exceeds 100 % because of reverse slopes in pools. Nearly all points are considered as steps and the elevation differences between pool bottom and upstream step base is recounted even if it was already counted just downstream of the pool.

A histogram of all slopes (Figure 5.3a) seems to show a very regular and skewed distribution. A distribution in more classes and a restriction to the centre of the distribution points out a secondary peak just above 0.5. (Figure 5.3b) This is due to a larger number of steps with slopes around 0.5.

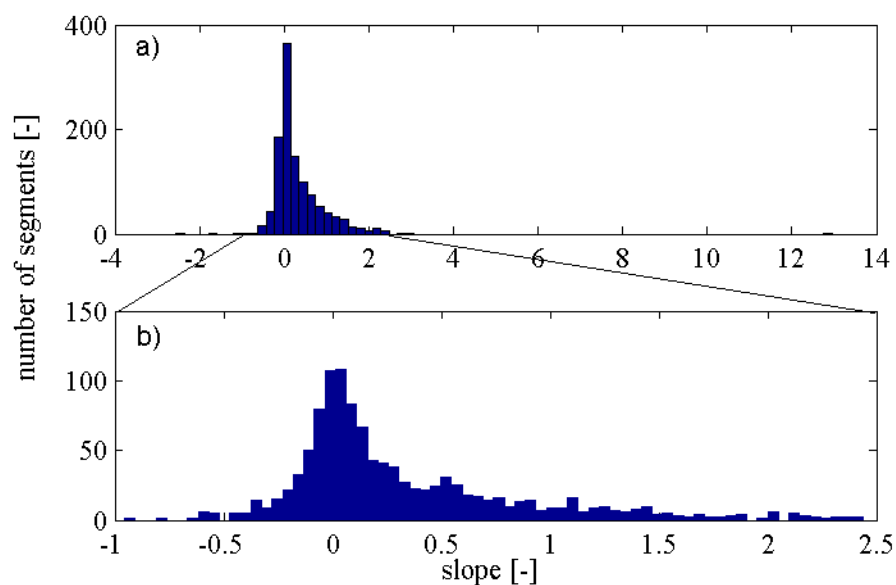


**Figure 5.3:** a) Histogram of all slopes between adjacent points. b) Zoom and refinement of classes showing secondary peak around 0.5.



A critical slope for step identification was chosen in regard to observed step slopes in the field and the secondary peak in Figure 5.3b. For all the further calculations 0.45 is used as the critical slope for step identification. This leads to 326 steps (246 alluvial sediment steps, 49 bedrock steps, 31 woody debris steps) in the studied section of the Vogelbach.

### 5.2.1 Relative position of steps and pools

The formation of a step on a regular slope can be seen as the immobilization of a boulder when the transport capacity decreases with discharge. The space upstream of the boulder will be filled up with smaller sediments leading to a decrease in slope above the step. Downstream of the step the bed will be eroded more efficiently due to the higher velocity of the water and the formation of roller eddies. A pool can be formed and the slope downstream of the step decreases too.

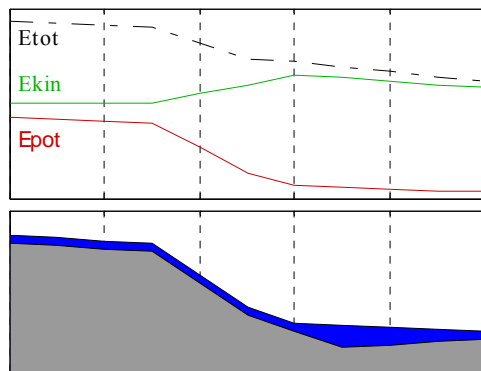


**Figure 5.4:** Schematic illustration of the change of the hydraulic head during flow over a step. The total energy ( $E_{tot}$ ) equals the potential energy ( $E_{pot}$ ) plus the kinetic energy ( $E_{kin}$ ).

Total hydraulic potential along the stream is composed of potential and kinetic energy of the water. The pressure term that normally enters the equation too can be neglected if only the water surface is considered. The potential energy is proportional to the elevation of the water surface. The kinetic energy increases over a step but decreases again afterwards due to the hydraulic jump and friction losses. The total hydraulic potential is always decreasing downstream (Figure 5.4).

Regarding the above explained mechanisms, a step has an up- and downstream influence on the stream bed topography. A nice definition for the length of a step is the one from Chin (1998) who measured step length from preceding to following pool bottom. This definition cannot be used for this study as a continuous suite of steps and pools is not present. The Vogelbach is on the edge between step-pool and cascade type. Because of the large grain size, pools do not occur between all steps.

In the Vogelbach case, step length is taken from one crest to another. It has to be decided whether the length is measured upstream or downstream of a crest. In other words: Is it the upstream or the downstream pool to a step that is more related to this last? The obtained lengths are not be influenced by this choice but the connection between step heights and lengths is. As the Vogelbach is a very steep stream, the downstream influence is considered more important than the upstream one. The backward effect on top of a step is considered less important than the eroding effect and incipient motion conditions below a step. Therefore the length corresponding to a certain crest is defined as the distance to the next crest downstream measured along the channel (thalweg).

### 5.2.2 Step categories

In previous studies, step length and height were often taken as averages over defined reaches. This study is based on a precise longitudinal profile over a single long reach and the subjective division into subreaches with average properties is avoided. The variability of step-related parameters has to be considered as much as the mean values. Additional attention was therefore paid to how the individual step dimensions are defined. A classification of the steps

into categories of height is the base of the definition of step dimensions here (see appendix A.2 for the Matlab code).

The working hypothesis in this study is that step-forming floods of a certain magnitude have the capacity to move sediment of a given calibre at (or close to) incipient motion. Sediment of this size forms the steps. Obviously, larger boulders need larger shear stresses corresponding to larger floods to start moving. As step height has been identified in earlier literature to be correlated to the sediment size making the step (Chin 1998), the larger steps will form only during less frequent larger flood events. During a major flood, small steps will be removed and new large ones created or moved. During the descending limb of that flood, or during following smaller ones, smaller steps will be superposed on the larger structures of previous steps. A stream presenting step-pool morphology can thus be seen as the result of flood events spread over a wide time period and of different magnitudes creating superposed sequences with steps of decreasing size when moving to the more recent sequences. For the computation of step lengths these superposed structures have to be separated.

### 5.2.3 Step height

The step height was computed similar to Chartrand and Whiting (2000) as being the elevation difference from a step crest to the point immediately downstream of the step and not to the deepest point in the pool below the step. Because of the very coarse material in the Vogelbach, pools do not occur downstream of every step. It would be difficult to decide for each step if a downstream depression is the corresponding pool or not related to that step. For the conditions found in the Vogelbach this way of computing height is consistent. Rickenmann and Dupasquier (1995) described the fact that well developed pools have greatest depths close to the upstream laying step. This was observable in the Vogelbach as well. The slope of the segment between pool bottom and step base is therefore generally steep enough to exceed the critical slope and will be automatically merged to the step.

### 5.2.4 Step length

The step length computed from the crest of a large step should expand to the crest of the next large step in the same step-pool sequence and not a smaller step created at a later time. Working with step length as the distance from each step crest to the next crest downstream regardless of size is not physically meaningful as the upper and lower step could have been formed during flow events of totally different intensity. This traditional length measure (further denominated length1) was however also computed in this study in order to allow comparisons with previous works.

Obviously there is no simple way to differentiate between large and small steps. The step length for a certain step  $i$  was therefore computed as the distance from the crest of  $i$  to the crest of the next downstream step with a height of at least the same order of magnitude. All the steps are for this purpose divided into height categories and step length taken as the distance to the next step of the same or larger category. That means the steps are superposed and the sum of all step lengths will exceed the stream length. The category limits are defined such that each category contains the same number of alluvial sediment steps. Woody debris and bedrock steps are not taken into account for the setting of the height limits, the total number of steps in each class is therefore not constant. But woody debris and bedrock steps are attributed to a category later on and used as possible ends for alluvial sediment steps (Figure 5.5).

The way in which categories are defined has a large impact on the resulting step lengths. Creating for instance many categories for small heights will increase the step length for small steps. That is why the limits are computed for the categories to contain an equal number of steps. The number of categories was chosen to be 5. As no arguments exist for a certain number of categories different numbers were tried during the analysis but no significant differences in the results were obtained.

With the above considerations there still remain different methods to compute step length. The question is whether to take the length as a horizontal projection or parallel to channel slope. The further denominated length2 is the distance following the horizontal projection of all points along the thalweg between two crests making out the step. To measure length parallel to channel slope is better from a hydraulic point of view as it is the loss of head per unit channel length. In this case length is computed as the straight distance in space linking two crests making out the step. This is chosen to be the standard length measure for this study (when compared to other length measures it is sometimes named length3). See appendix A.3 for the Matlab code.

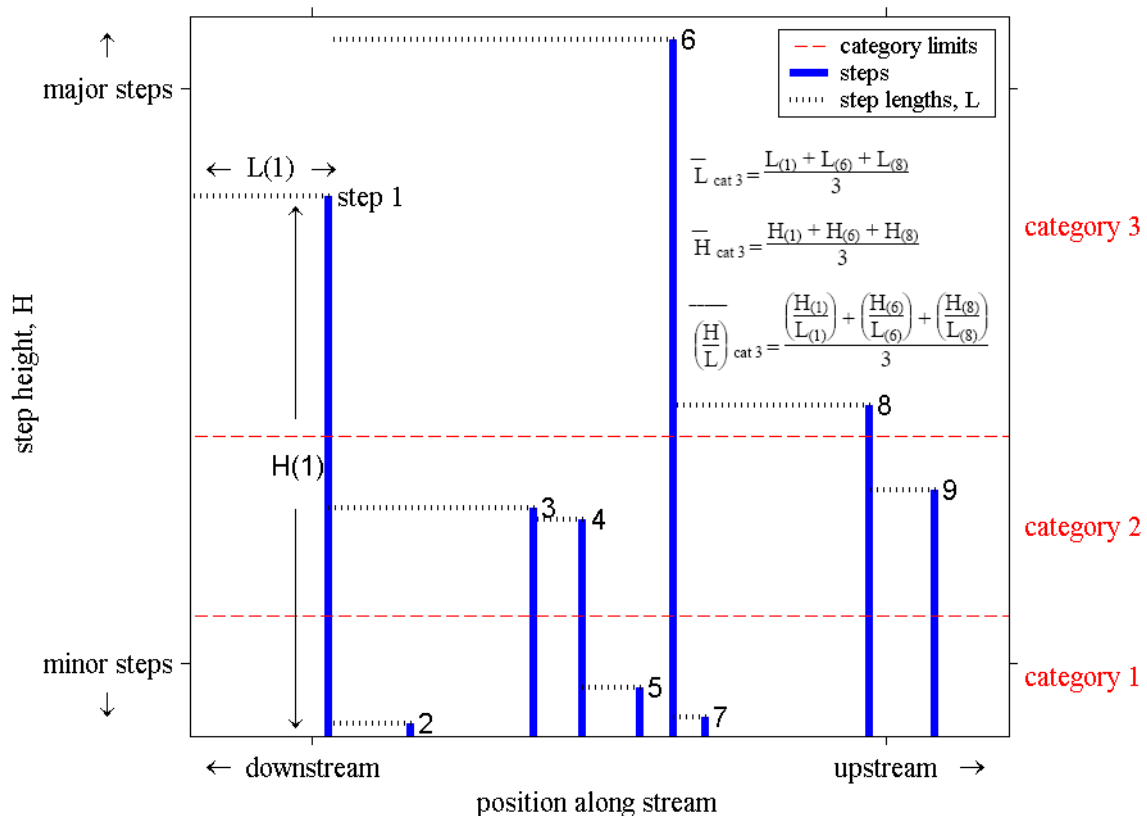


Figure 5.5: Illustration of step length computation: Equal number of steps in each category. Step length as distance to the next downstream step of equal or higher category.

### 5.3 Drainage area

Drainage area needed for the hydraulic calculations in chapter 9 was computed for the main stream positions corresponding to the 22 cross sections. The 25-meter digital elevation model (DEM) of the Vogelbach basin is used as input data (Geostat).

The first step in processing the DEM is to fill sinks - points with all surrounding points higher. This is very important as even a small sink would induce a loss of all the overlying points' accumulated flow. Second, the flow direction from every cell is defined as the one to

the neighbour cell leading to the steepest downward slope (8 neighbour cells are considered here and the greater distance between diagonal-connected cells are taken into account). The last step is to sum for each cell  $i$  the values of surrounding cells with flow direction to cell  $i$  and to assign this sum as new value to the cell  $i$ . This has to be done by an iterative process. Initially every cell has a value of one (they only drain themselves). After the first run, cells with peaks (cells with no higher neighbours) are identified. After the second run, cells  $i$  with higher neighbours composed of only cells identified in the preceding run or which got definitive values in the same run but are checked before the cell  $i$  get definitive values. This process is repeated until there is no more change in the value of any cell. The value of each cell  $i$  now corresponds to the number of cells from which water will flow towards cell  $i$ , this is the drainage area of cell  $i$ .

The above operations were done with Matlab (by a code created in this study) as well as with ArcView GIS for comparison. The differences in the flow accumulation matrix are very small and concentrate outside the Vogelbach basin. The differences are mostly due to a different approach for model borders. The m-file adds a “-99” margin around the DEM inducing the loss of all virtual precipitation to the outer most columns and rows. In ArcView GIS the borders are treated more consequently. This difference is of no importance for the Vogelbach basin because its edges never touch the model borders.

The channel network that results from the representation of the flow accumulation matrix (Figure 5.6) is very close to the one drawn in the map of the Federal Institute of Topography (Figure 3.1). The measured profile matches well the line of highest drainage areas. But because of the 25 m resolution of the input digital elevation model, working with drainage areas along the stream at intervals closer than at each cross section would not make sense.

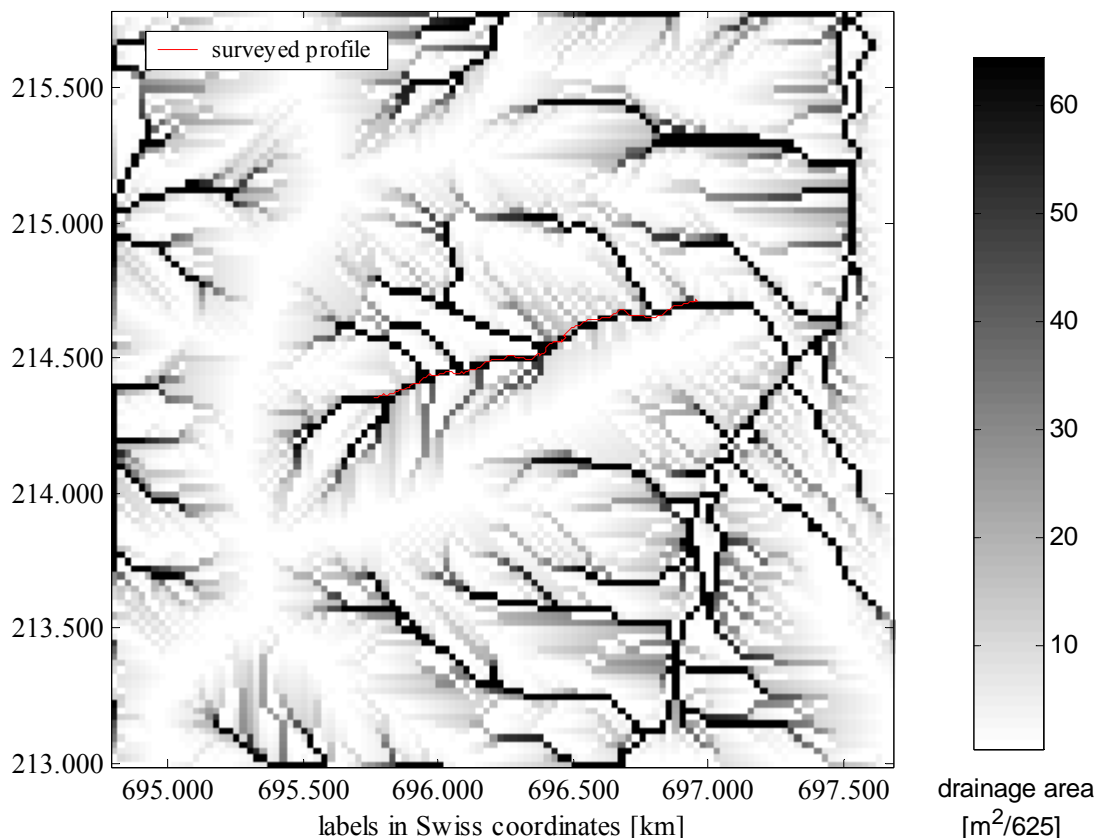


**Figure 5.6: Flow accumulation matrix of Vogelbach drainage area. Also shown is the surveyed profile in this study.**

The network structure of the Vogelbach is quite regular. Two major tributaries enter the main stream but they do not change the downstream flow conditions significantly. The increase of drainage area with longitudinal distance (Figure 5.7) shows the positions of those two tributaries between cross sections 4 and 5 and further upstream between 13 and 14. Big tributaries compromise the assumption of a stream regularly evolving with distance and slope.

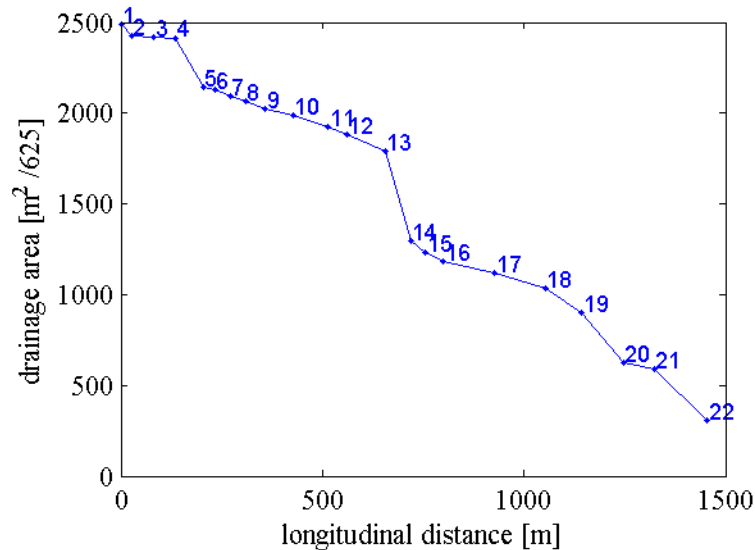


Figure 5.7: Drainage area computed for each cross section position and plotted against longitudinal distance.

## 5.4 Particle-size distribution

### 5.4.1 $D_m$

Collecting totals of 60, 80 and 100 particles allows examining if the sample size for a sampling location was large enough. If the calculated median diameter  $D_m$  remains close for the different sample sizes, the sample size can be estimated as sufficient.

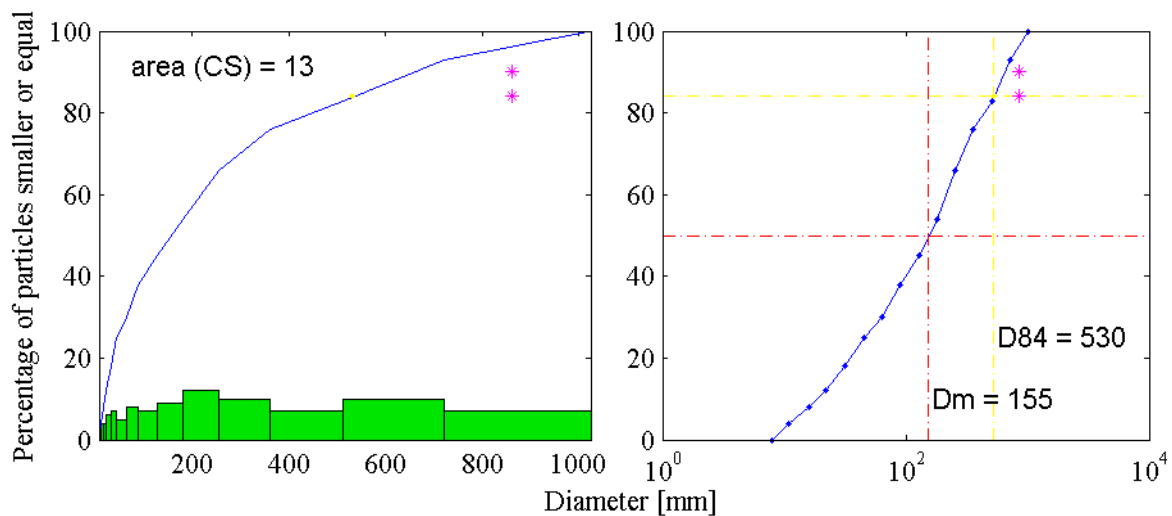
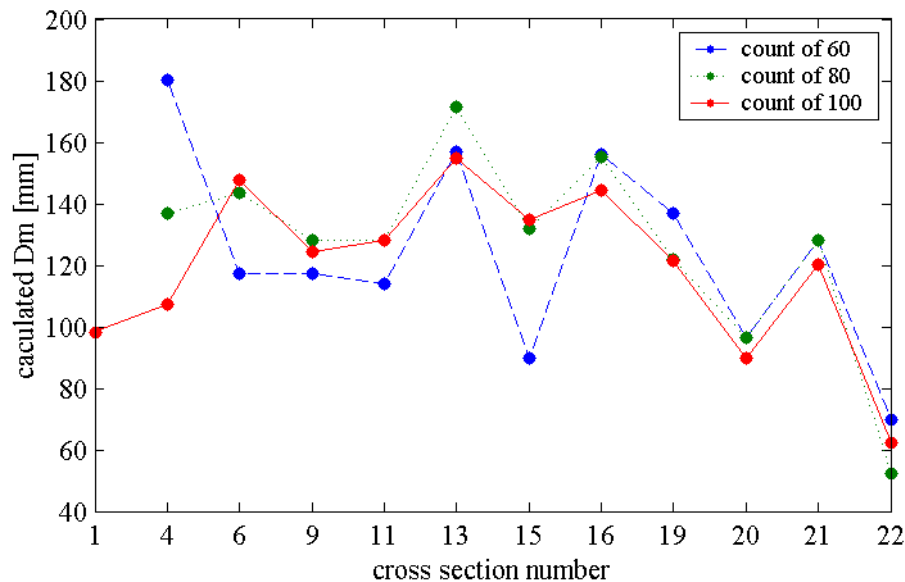


Figure 5.8: Cumulative density function of particle diameters at cross section 13. Calculated  $D_m$  and  $D_{84-SC}$  ( $D_{84}$  in the figure) are shown in right figure with logarithmic x-axis. The mean of the five largest boulders ( $D_{84-boulders}$ ) is shown as magenta stars at a percentage of 84 and of 90.

The cumulative density function (cdf) of b-axis larger or equal than the classes defined in 4.4 were plotted for all cross sections. Visually, the differences between cross sections are very small. As example, Figure 5.8 shows the cdf for cross section 13.  $D_m$  was calculated as the diameter with 50 % of stones smaller. As this percentage does not necessarily fall on a class limit, a logarithmic interpolation between the two classes is used (Table 5.1).



**Figure 5.9: Median diameters determined at different cross sections with counts of 60, 80 and 100 particles.**

$D_m$  calculated with only 60 particles differs much from the two other ones. The differences between  $D_m$  calculated with 80 particles and with 100 particles are generally less than the differences between sampling cross sections (Figure 5.9). Therefore  $D_m$  out of 100 sampled particles can be considered as a meaningful value.

Typically one would expect a coarsening of sediments going upstream. In the Vogelbach, sediment size seems to be more influenced by the steepness of hillslopes, their sediment supply and by the stream sections themselves. The most upper section of the studied part of the stream is characterised by a decrease in slope and by a large amount of woody debris. This debris retains a lot of small sediments creating little basins with flow conditions and even vegetation untypical for mountain streams. These conditions apply to cross sections 20 to 22, where small medium diameters were found (Figure 5.9, Table 5.1).

#### 5.4.2 $D_{84}$

The average of the five largest boulders ( $D_{84\text{-boulders}}$ ) does not correspond to the  $D_{84\text{-SC}}$  gained through the cumulative density function of the sediment count. It is more between a  $D_{90}$  and  $D_{95}$ . The difference probably results from errors in both techniques. Five boulders are too few to produce a meaningful average. The count of 100 particles is good for the estimation of the median diameter but again, not many particles larger than  $D_{84\text{-sc}}$  are recorded, and the class limits (Chapter 4.4) may not be appropriate. An additional source of error is that some of the really large boulders are not part of the sediment load of the stream. They were placed randomly during hillslides and are likely too large to be moved during floods. Perhaps those boulders which increase  $D_{84\text{-boulders}}$  a lot should not be counted. Practically it is often difficult to decide if a boulder should be counted or not.

Besides this shift of  $D_{84\text{-boulders}}$  to higher values some correlation between slope and  $D_{84\text{-boulders}}$  exists (Figure 5.10). At higher slopes, because of higher flow velocities the stream develops higher shear stresses accentuating erosion and incision and allowing to move larger blocks. From steeper hillslopes larger calibre sediment supply is likely.

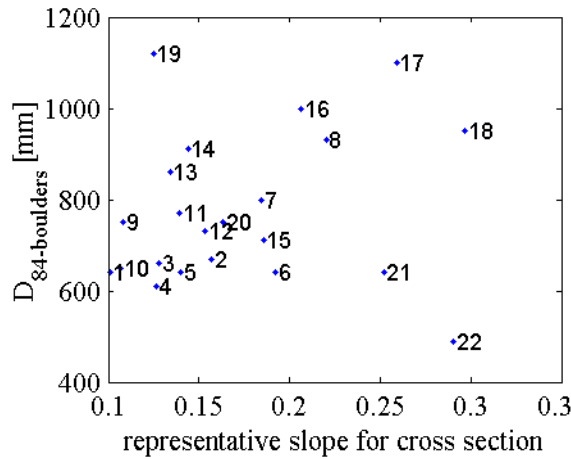


Figure 5.10: Relation between  $D_{84\text{-boulders}}$  and the representative slope at cross sections.

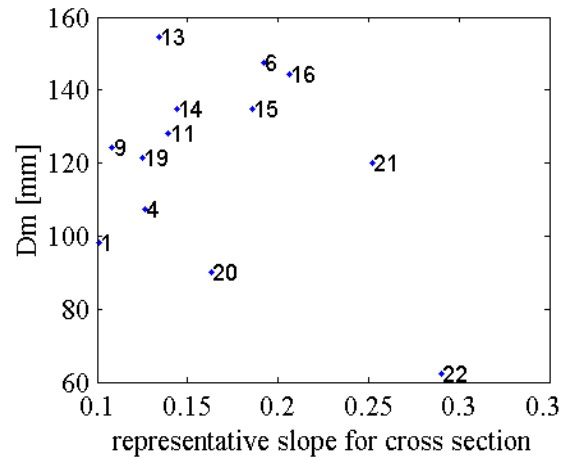


Figure 5.11: Relation between  $D_m$  and representative slope at cross sections where sediment count was done.

A correlation between  $D_m$  and slope appears for the same reasons (Figure 5.11). In both of these plots, the point for cross section 22 is apart from the others. Cross sections 20 and 21 also plot out of the trend in at least one of the plots. This is, especially for cross section 22, due to the larger amount of woody debris in the most upper part of the surveyed section where small sediment is retained because of logs forming steps, and  $D_m$  is lower.

Table 5.1: Median diameter ( $D_m$ ) and diameter with 84% of particles smaller ( $D_{84\text{-SC}}$ ) computed with the 100 particle count at 12 of the 22 cross sections. Average diameter of the five largest boulders ( $D_{5\text{ lar. boulders}}$ ) in each cross section zone.

CS	$D_m$ [mm]	$D_{84\text{-Sed. count}}$ [mm]	$D_{5\text{ lar. boulders}}$ [mm]	CS	$D_m$ [mm]	$D_{84\text{-Sed. count}}$ [mm]	$D_{5\text{ lar. boulders}}$ [mm]
1	98	386	640	12	---	---	730
2	---	---	670	13	155	530	860
3	---	---	660	14	135	---	910
4	107	429	610	15	135	468	710
5	---	---	640	16	144	474	1000
6	148	405	640	17	---	---	1100
7	---	---	800	18	---	---	950
8	---	---	930	19	121	453	1120
9	124	333	750	20	90	382	750
10	---	---	650	21	120	388	640
11	128	421	770	22	62	328	490

## 6 Analysis of step-pool parameters

In the following, the evolution of the step dimensions (their height and length) along the stream is studied. Particular focus is on the evolution of step dimensions with changing drainage area, discharge and slope. A second important aspect is the interaction between the step dimensions themselves.

### 6.1 Influence of slope and discharge

The drainage area contributing to a stream is related to the river network and structure. The more regular the channel network, the stronger will be this relation, and the more regular will be the increase of drainage area and therefore discharge going downstream. In general, mean channel slope increases upstream. The evolution of step parameters along a stream can thus be subscribed to either the change in slope or the change in discharge. Chin (1998) attributes the changes in step length along her study streams to discharge, whereas Whittaker (1987) relates step length to slope by an inverse power law (Chapter 2).

In the Vogelbach, slope is not increasing regularly in the upstream direction. The steep section in the middle of the stream breaks the uniform relation between slope and drainage area. It should therefore be easier to discern the influence of both factors on changes of step parameters along the stream.

#### 6.1.1 Step height and length against longitudinal distance

No correlation between longitudinal distance from the study reach outlet upstream (closely related to drainage area) and the step dimensions can be detected in scatter plots showing each individual step (Figure 6.1 and Figure 6.2).

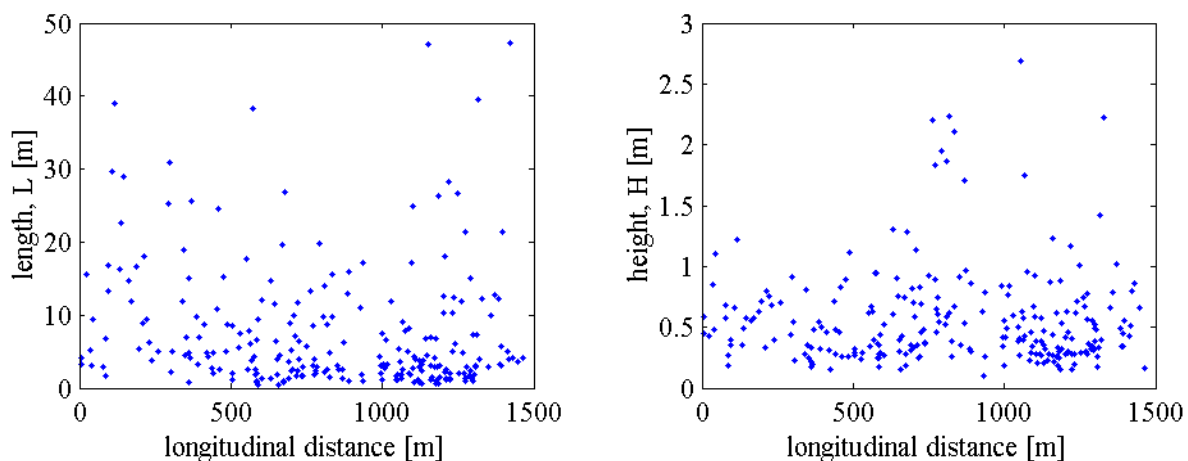


**Figure 6.1: Step length (lenght3) along the stream. Figure 6.2: Step height along the stream. Position 0 corresponds to survey starting at downstream gauge.**

An increase in step height and a decrease in step length can already be seen in the central steeper section around 1000 m upstream of the starting point of the survey. This suggests that step parameters may be related to channel slope.

#### 6.1.2 Step height and length against slope

When step height or length are plotted against slope, the way in which slope is computed plays an important role. Slope should be taken over an area that is not too small but still in



hydraulic connection with the step. That means, a length up- and downstream on which the step has some influence. Using a small moving window for the calculation of the channel slope representative for a step induces an error as the slope will be influenced by the step height itself. In the extreme, the slope would be the slope from step base to step crest. The theoretical minimum of:

$$\text{slope} = \frac{H}{2 \cdot w} \quad (3)$$

(with  $H$  the step height and  $w$  half the moving window size) below which the slope can hardly be, becomes important for very small moving windows. This minimum corresponds to a horizontal topography with the step inducing all elevation loss. The few points on the left side of this limit (with slope  $< H/2w$ ) (Figure 6.3) are due to reverse slopes in deep pools above or/and under the step. The almost obligatory position of all points on the right side of this line could be misinterpreted as a trend in the data. This is especially the case for small moving windows where this line represents already steep slopes.

Changing from a small to a large moving window the slopes of large steps will decrease much more than the ones of small steps. For larger steps the elevation loss over the moving window due to the step itself is in proportion much larger than for smaller ones. The choice of  $w$  therefore changes the shape of the plot of height versus slope (Figure 6.3)

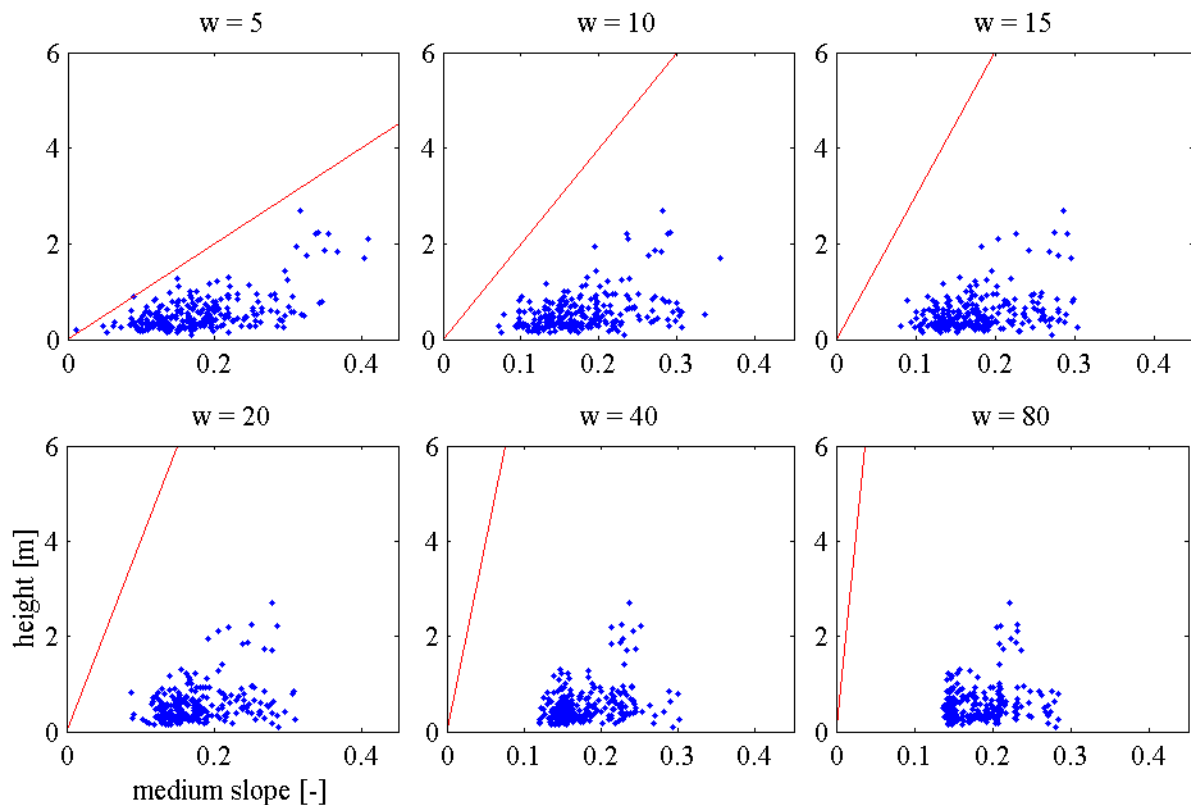


**Figure 6.3:** Step height versus representative slope at the step location for different moving window sizes during computation of slope,  $w$  is half the moving window in meters. The red line represents the theoretical minimum of  $S = H/2w$ .

The purpose here was to study variations of step dimensions with slope, so one would be tempted to use a very small moving window in order to gain variability in slope. Figure 6.3 shows that for large moving windows the slope range becomes very small and much less

interesting. So what is the smallest moving window that can be used? An assumption is to take it long enough so that at least one average step length (length3) of the largest category can be within the window. In chapter 7.1 (Table 7.1) an average length of 19.1 m is found for the fifth and largest category. Plots like the ones in Figure 6.3 show that when  $w$  is continuously increased, a rapid decrease in the slope of large steps occurs till about  $w = 10$ , giving support to this assumption. A moving window of 30 m ( $w = 15$ ) is chosen for further calculations in this study.

Besides the loss of variability in slope, too large a moving window induces error as the slope would no longer be representative anymore for the area on which the step has hydraulic influence. In Figure 6.3 the group of steps getting isolated on the side of steeper slopes for large moving windows is situated between two very steep bedrock reaches. A too important increase of  $w$  includes the bedrock reaches in the moving window and increases the slope.

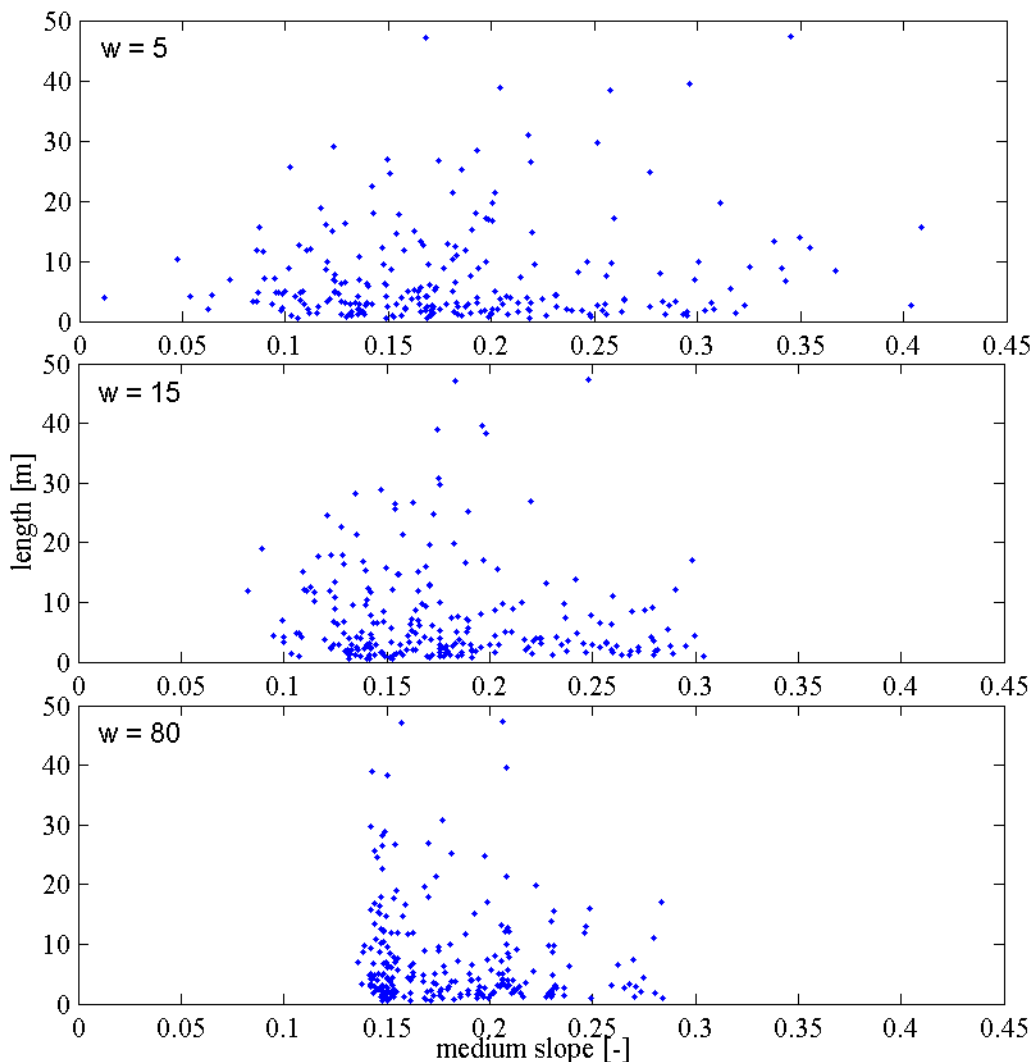


**Figure 6.4:** Step length (length3) versus slope for individual steps using different moving window sizes to calculate the slope.

As step height and length are correlated (chapter 6.2 and 7.3) the size of the moving window also has an influence when plotting step length against representative channel slope. If not mentioned otherwise, step length is always computed as length3. Step height and length are positively correlated, so for high steps the step length tends to have large values too. Now

using a too small moving window, the slope will be overestimated as explained above. This will move the long steps to higher slopes. Figure 6.4 illustrates this shift for moving windows of 10, 30 and 160 m. The 10 m window is too short and results in step length and channel slope being independent of each other. The 30 m window gives a plot in which long steps have already moved to lower slopes. With a very large moving window of 160 m, the tendency of step length increasing with slope on the gentle slope side of the plot as visible in the two previous plots is totally lost. Only a decrease of step length with slope is visible. This decrease means that at high slopes steps of all classes are more numerous and so closer to each other. One cannot distinguish a certain average step length for each slope but rather an approximate maximum spacing depending on slope. In the plot using  $w = 15$  in Figure 6.4, the maximum that still seems to be in the central slope range is made of only about 5 steps being all in the largest height class. When the step lengths are plotted against slope separately for the 5 categories (Figure 6.5), already with  $w = 15$  the trend of decreasing maximum step spacing with increasing slopes is evident in the 4 smallest categories. Only for the largest one, where the step length exceeds the moving window size, more scatter remains. For the following, if not mentioned otherwise, slope is always computed over a moving window of 30 m ( $w=15$ ).

The results are important, because many previous studies have suggested a negative non-linear relationship between average step length and channel slope (e.g. Chin 1999 and others). However, the results for the Vogelbach in Figure 6.4 and Figure 6.5 point to a weak relationship between step length and channel slope.

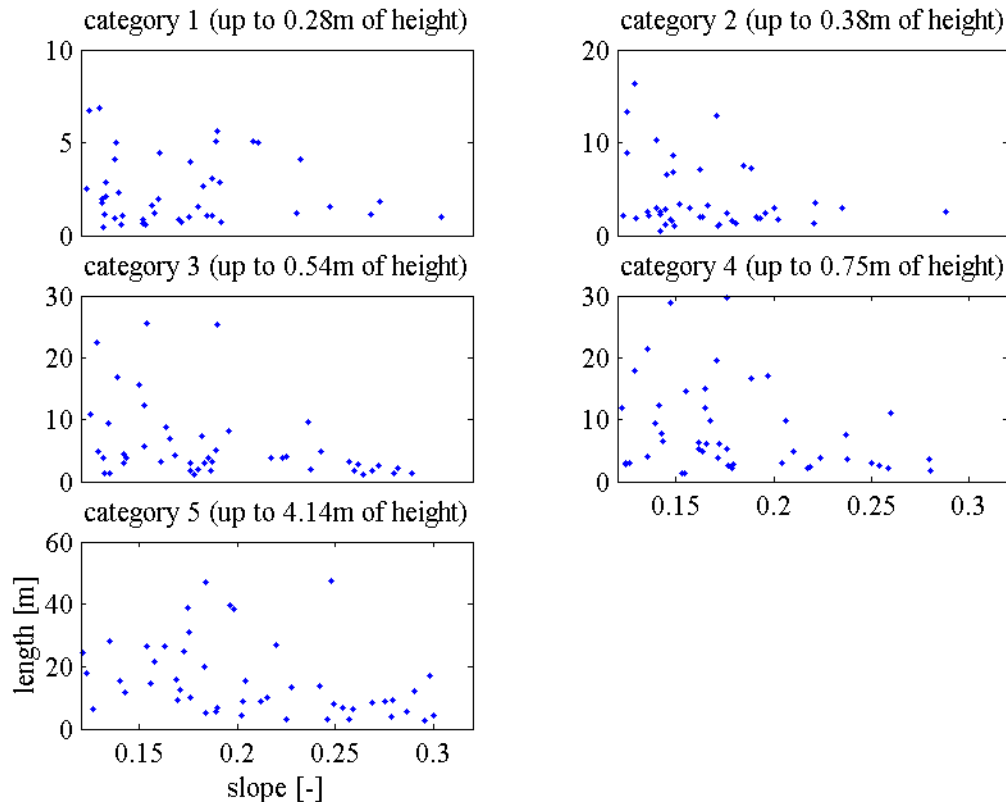


**Figure 6.5 : Individual step length (length3) versus representative slope ( $w = 15m$ ) for the five categories of height. N.B. The scale of the length axis varies from plot to plot.**

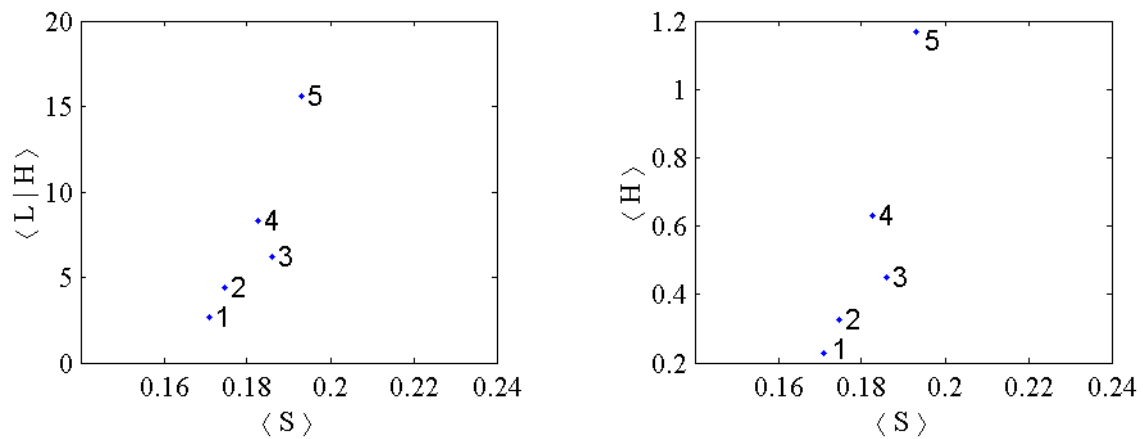


**Figure 6.6: Height-category averaged length (length3) versus slope. Category 5 is the highest slope category.**

When the values of step height, length and slope are averaged over the five categories of step height a clearer plot is obtained which needs however to be interpreted carefully. Figure 6.7 shows that the larger categories have generally a mean step height placed at higher slopes. But as can be seen in the plots of individual height against slope (Figure 6.3) the variability is very high. One standard deviation for the slope average of the different classes easily exceeds the differences between the classes (Table 7.1). For the mean lengths of the steps in those 5 height categories, a very similar trend is observed (Figure 6.6). The categories containing the higher steps plot at higher length values. That means higher steps are on the average longer. This is not in contradiction with many previous studies finding a negative relation between slope and length because Figure 6.6 states only that the longer and higher steps are preferentially placed at steeper slopes, but that does not mean that there are no small ones between them. It is neither in contradiction with the above results for individual step dimensions, which also show a decrease of step length with slope.

The important difference to previous studies resides in the definition of step length. When step length is taken to the next downstream step irrespective of its size a comparison with the here found relation of length to slope is difficult. The very striking similarity in shape between the relations of step height and length with slope could indicate a good relation between step height and step length. This is analysed in the following chapter.

## 6.2 Variation of step length with step height

The lengths of individual steps compared to their heights show a large funnel of ratios (Figure 6.8). A trend can be guessed but the variance of individual measures stays very high.

When the mean is taken for step heights and lengths of the categories, a strong linear correlation is obtained between the category means  $\langle H \rangle_i$  and  $\langle L \rangle_i$  (Figure 6.9). Median, minimum, maximum and quartile values illustrate the shape of distribution within the categories. The number of categories is varied to make sure the correlation is not only a spurious characteristic found with a particular number of categories (Figure 6.10). The slope of the line fitted through the averages is dependent on the number of categories. With more categories the next downstream step to a given step is less probably of equal or higher category and therefore the lengths are longer. The linear nature of the fit is not influenced.

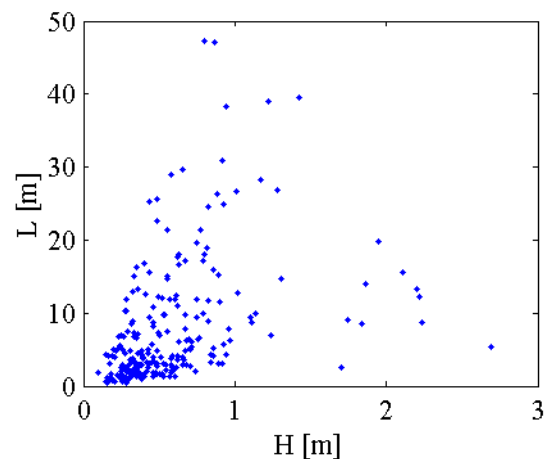


Figure 6.8: Step length (length3) versus height for individual steps.

When instead of the step length measured till the next step of equal or higher class (length3) as it is defined in this study, step length is measured till the next step irrespective of its size (length1) the linear relation between  $\langle H \rangle$  and  $\langle L \rangle$  is not clear (Figure 6.10). For the smallest category the way in which length is computed makes no difference. For all others the step lengths are shorter using length1 and tend toward a maximum between 5 and 10 m for the largest steps (Figure 6.10).

The linear relation coming out when lengths of large steps are not truncated by superposed small steps indicates a basic geometric similarity between steps of all sizes. The ratio of step height to step length ( $H/L$ ) tends to stay constant. However, as for the variations of step dimensions with slope the variance within the categories is very high (Chapter 7.1).

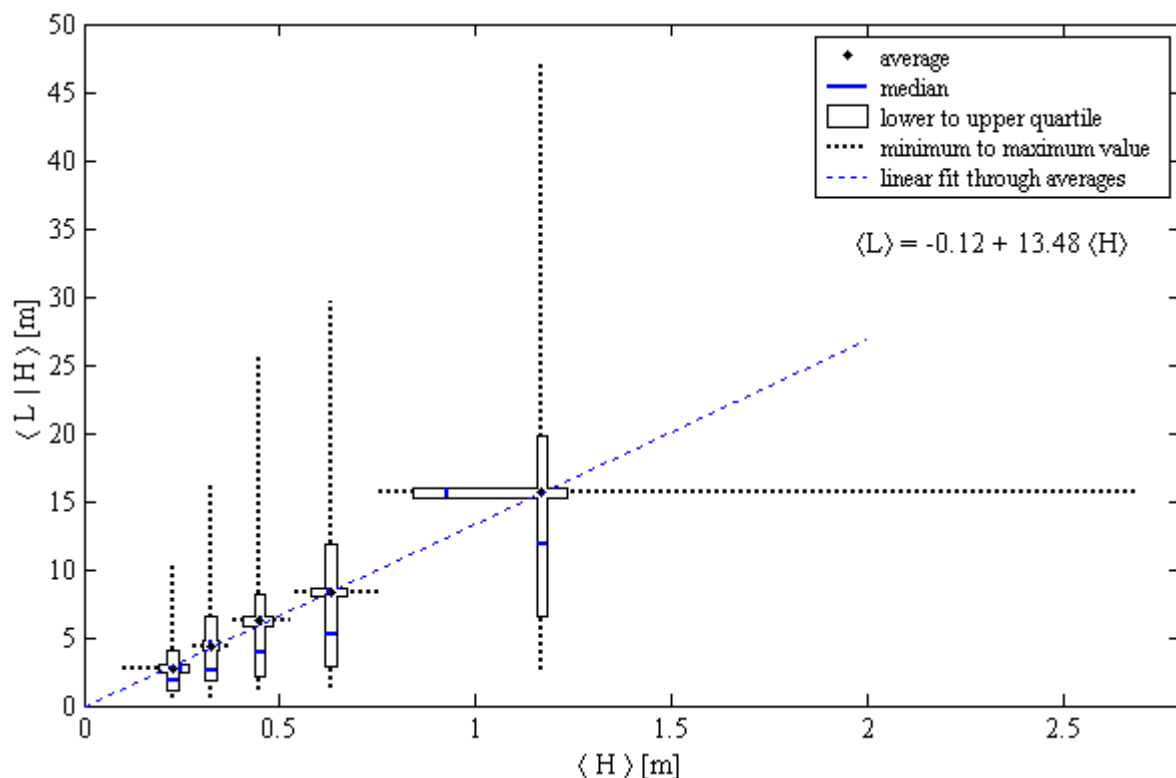


Figure 6.9:  $\langle H \rangle$  versus  $\langle L \rangle$  for steps divided into 5 categories. Median and quartiles of each category are also shown.

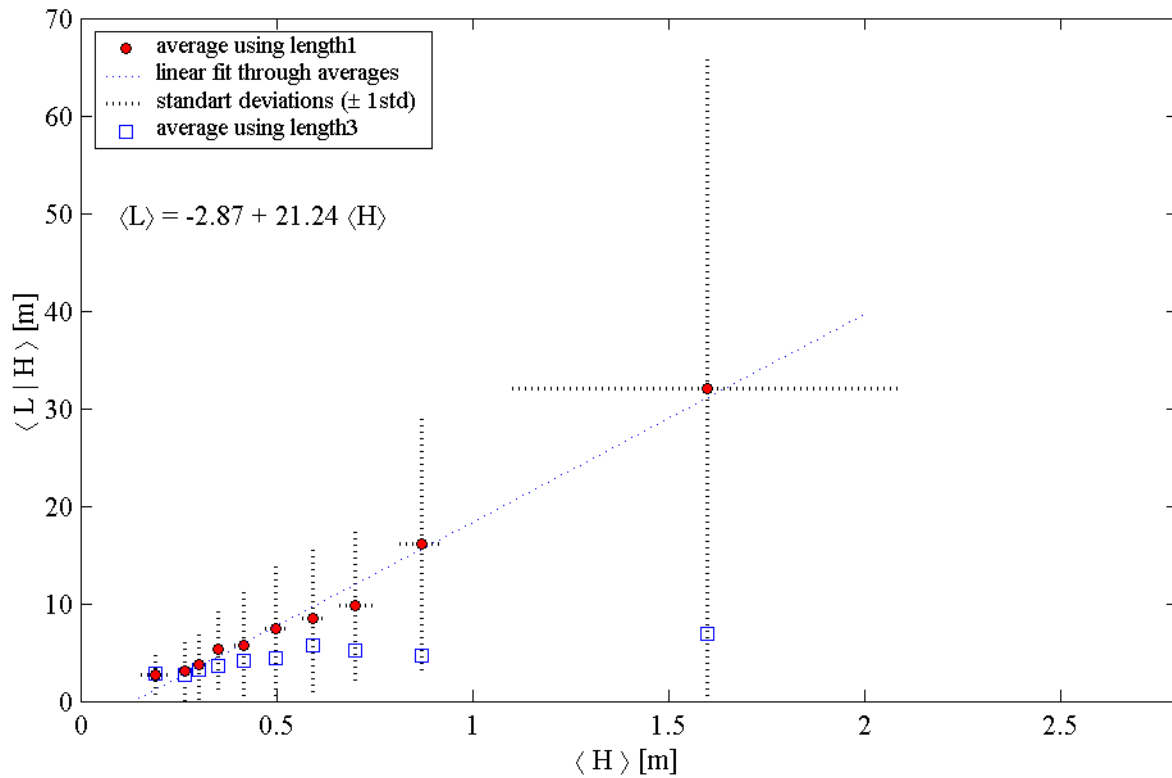


Figure 6.10:  $\langle H \rangle$  versus  $\langle L \rangle$  with steps divided into 10 categories. Length3 is the length as defined in this study. Length1 is the step length measured to the next downstream step irrespective of its size.

It is to note that  $\langle H \rangle_i$  and  $\langle L \rangle_i$  are not independent random variables. The length is averaged over categories that are themselves defined by the step height, the distribution of  $\langle L \rangle$  is conditional on  $H$  (Kottogoda and Rosso 1997, chapter 3.3 and 3.4). The mean of  $L$  knowing that  $H$  is in the range from  $h_{\min}$  to  $h_{\max}$  can be written as:

$$E [ L | H \in [h_{\min}, h_{\max}] ] = \sum_{\text{all } i} l_i \cdot p_{L|H} (l_i | h_{\min} < h < h_{\max}) \quad (4)$$

### 6.3 Steepness ( $H/L$ )

Abrahams, Li and Atkinson (1995) hypothesise that steps adjust to maximize flow resistance. They make the statement that to achieve this, the steepness ( $H/L$ ) of steps exceeds the slope of the channel. They give a range of  $(H/L)/S$  between 1 and 2 in which their field and flume data lie (Figure 6.12). If the steepness equals the slope this means that all elevation loss is due to steps. Larger values of steepness are found if deep pools create reverse slopes so that the sum of step heights over a reach exceeds the elevation difference.

Abrahams et al. (1995) concentrate their field investigations on reaches with well preserved step-pool architecture. This is not the purpose of this study where the intention is to analyse a stream which has the necessary conditions for step-pools to develop as one evolving element over its entire length. This makes comparisons difficult because the Vogelbach is not composed only of well developed steps and especially pools what will automatically result in lower values of steepness divided by slope.

If step length is calculated as in Abrahams et al. (1995), and most other studies, simply as the distance between following steps, a relation is indeed found between steepness and slope. The

category averages plot on the lower limit of the range defined by Abrahams et al. with  $\langle H/L \rangle$  very close to  $\langle S \rangle$ . Figure 6.11 shows a representation for a comparison with Abrahams' data. The Vogelbach data plot in a narrow slope range. Note that with an average slope of about 0.2 m/m the Vogelbach is a very steep mountain stream. In fact there are very few datasets of step-pool morphologies in streams this steep reported in the literature. It has been observed however, that as mean channel slope increases  $(H/L)/S$  tends towards 1, that is reverse slopes in pools become increasingly uncommon in steep streams (Zimmermann and Church 2001).

Figure 6.13 shows the same points in more detail. Although there is little variation in slope, the higher steps tend to be in the higher slopes. Steepness is not correlated with the height classes if length is calculated as defined in this study (length3). That  $H/L$  is almost constant was already shown in chapter 6.2. Increasing the number of classes to 10 gives more variation in the steepness values (Figure 6.14). But it is only scatter; using length3 there is no trend between  $\langle H/L \rangle$  and  $\langle s \rangle$  in the direction Abrahams et al. (1995) find.

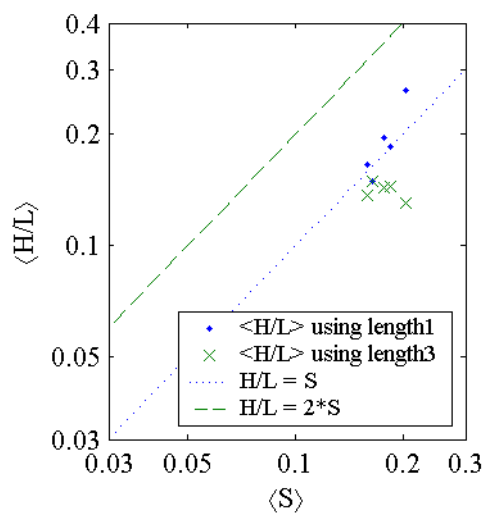


Figure 6.11: Category averages of steepness versus slope. Length 3 is the length as defined in this study. Length 1 is step the length measured to the next downstream step no matter its size.

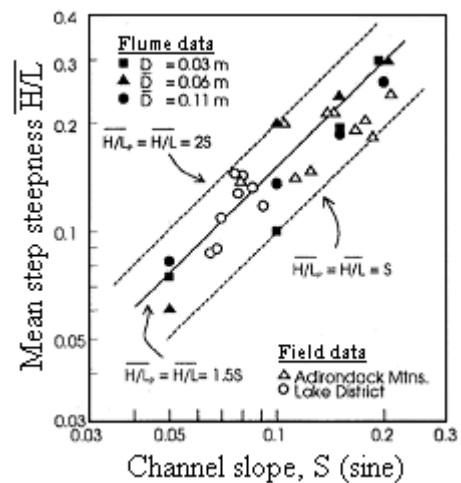


Figure 6.12: Abrahams, Li and Atkinson (1995) graph of mean steepness against channel slope for natural step pools and flume experiments with step dimensions providing maximal flow resistance.

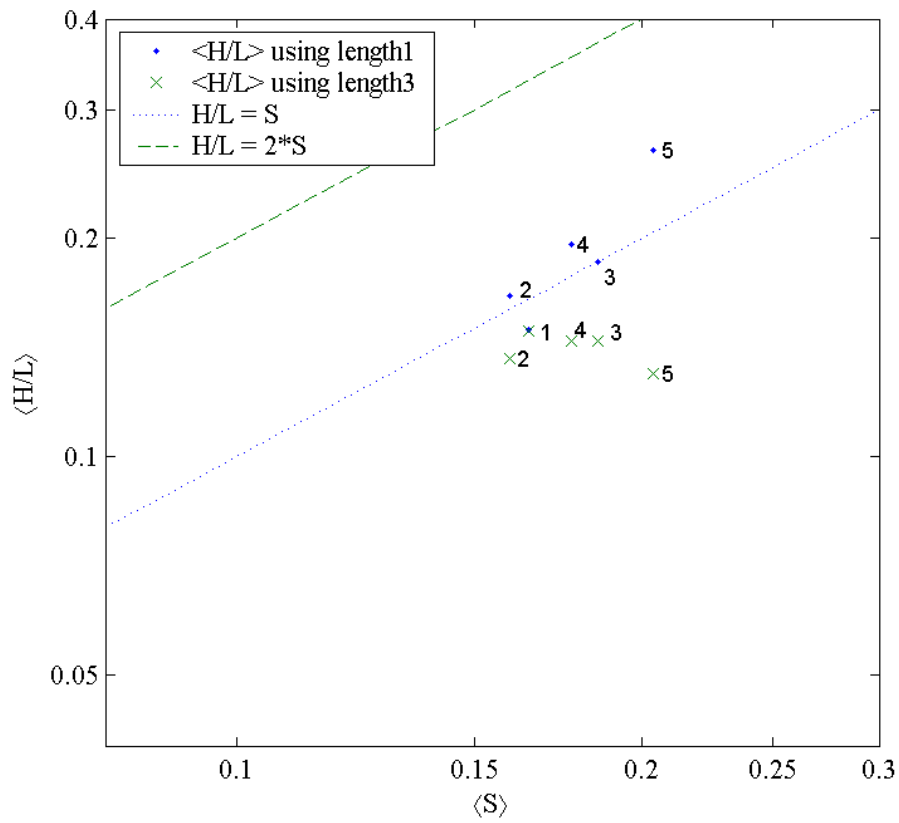


Figure 6.13: Steepness category averages versus slope category averages with steps divided into 5 categories.

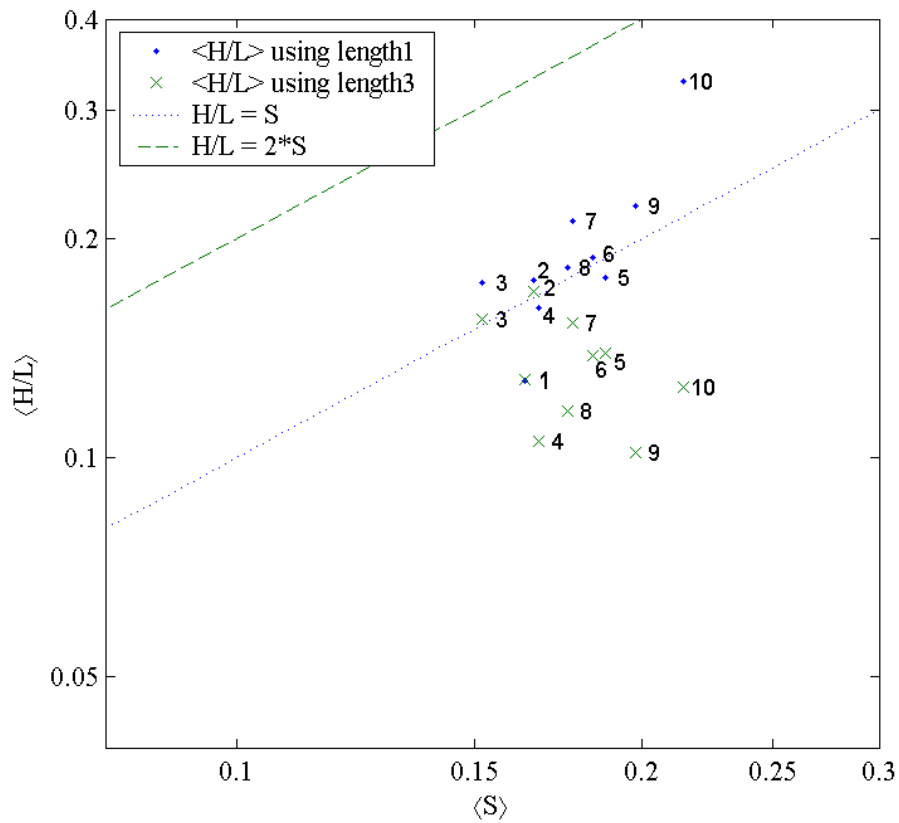


Figure 6.14: Steepness category averages versus slope category averages with steps divided into 10 categories.



Steepness is defined as step height divided by its step length. It was already noted that because of scouring of the pools, reverse slopes are created and the steepness of a step can exceed the average slope of a reach. When the stream is divided into reaches or the steps in categories, it becomes useful to calculate averages of the steepness. One has to calculate the steepness of each step first and then establish the average of those. Some preceding studies have found no significant difference when dividing the average height of all steps by the average length of all steps (e.g. Abrahams et al. 1995 and others). This is surprising as the mean of a general function is only equal to the function of the means as a first order approximation.

First order approximation: 
$$\overline{\left(\frac{H}{L}\right)} \approx \frac{\overline{H}}{\overline{L}} \quad (5)$$

This approximation can be used only if H and L are independent, and the variances of H and L are small, which in case of step lengths and heights are not good assumptions.

An exact (analytical) solution could be found with the Reynolds decomposition. H and L can be written as a mean part and a fluctuation part:

$$L = \overline{L} + L' \quad , \quad H = \overline{H} + H' \quad (6)$$

Defining l as the inverse of L:

$$l = \frac{1}{L} \quad , \quad l = \overline{l} + l' \quad (7)$$

The mean of the steepness becomes:

$$\overline{\left(\frac{H}{L}\right)} = \overline{(H \cdot L^{-1})} = \overline{(\overline{H} + H') \cdot (\overline{l} + l')} = \overline{\overline{H} \cdot \overline{l}} + \overline{\overline{H} \cdot l'} + \overline{H' \cdot \overline{l}} + \overline{H' \cdot l'} \quad (8)$$

The mean of a sum is the sum of the means of the individual terms. The mean of a fluctuation part multiplied by a constant is zero so the two middle terms can be suppressed and it results:

$$\overline{\left(\frac{H}{L}\right)} = \overline{\overline{H} \cdot \overline{l}} + \overline{H' \cdot l'} \quad (9)$$

As the mean of H and the mean of l are constants:

$$\overline{\left(\frac{H}{L}\right)} = \overline{H} \cdot \overline{l} + \overline{H' \cdot l'} = \overline{H} \cdot \overline{L}^{-1} + \overline{H' \cdot l'} \quad (10)$$

The second term is the covariance term between step height and the inverse of step length (  $\text{cov}(H, L^{-1})$  ). In this study it is found that the correlation between H and L is important and

thus  $\text{cov}(H, L^{-1})$  cannot be neglected. Unfortunately the first term cannot be transformed into a term containing only H and L. An exact analytical solution is therefore not available.

Using a Taylor series expansion about the mean values of random variables H and L, a second order approximation expression for a function of two random variables like equation (11) can be obtained.

$$z = \frac{H}{L}, \quad z = f(H, L) \quad (11)$$

Second order approximation:

$$\bar{z} \approx f(\bar{H}, \bar{L}) + \frac{1}{2} \cdot \left( \left( \frac{\delta^2 z}{\delta H^2} \right) \cdot \text{var}(H) + \left( \frac{\delta^2 z}{\delta L^2} \right) \cdot \text{var}(L) \right) \quad (12)$$

It shows an extra term in comparison with the first order approximation which is important to assess the exactitude of the first order approximation. For a more detailed development of these formulas, refer to Browne (2000), chapter 2.

An approximate formula for the mean value of  $z = H/L$  can now be derived in terms of the means and variances of H and L.

$$\bar{z} = \overline{\left( \frac{H}{L} \right)} \approx \frac{\bar{H}}{\bar{L}} \cdot (1 + \hat{L}^2) \quad (13)$$

where  $\hat{L}$  , is the coefficient of variation: 
$$\hat{L} = \frac{\sqrt{\text{var}(L)}}{\bar{L}} \quad (14)$$

The variance of L is high even within one step category. Calculating the fraction of the means is thus not a proper method to get a mean steepness. The value found this way would always be too small, the largest error occurring at largest variances of L. So:

$$\overline{\left( \frac{H}{L} \right)} \geq \frac{\bar{H}}{\bar{L}} \quad (15)$$

The method of taking the mean of all steepness has the weakness that it is an average of slopes computed over different lengths. By dividing the steps in height categories this problem is mostly eliminated.

Figure 6.15 shows the ratio of category averaged height to category averaged length,  $\langle H \rangle / \langle L \rangle$ , versus average slope  $\langle S \rangle$ . In comparison to Figure 6.13 the points plot much lower thus illustrating that the first order approximation of equation (5) is not precise in the case of step pool dimensions.

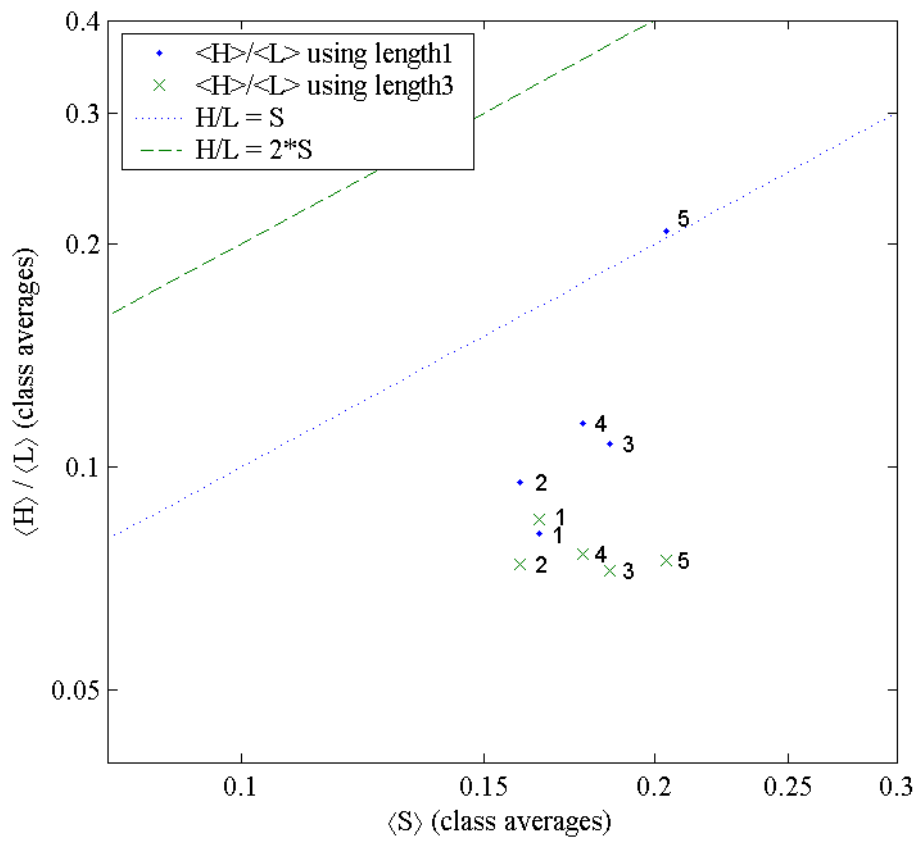


Figure 6.15: Category averages of step height divided by category averages of step length versus slope category averages with steps divided into 5 categories.

## 7 Statistical analysis of step-pool geometry

### 7.1 Statistical moments

When the step-pool morphology is treated as a system of superposed step-pool sequences and steps are divided into categories based on their height, interesting relations are found between the step parameters. However the individual values present large variance within the categories (Table 7.1), the standard deviations are close to the mean values. Zimmermann and Church (1999) see these high variances as indication for a random positioning of the steps. Whittaker (1987) in his discussion chapter replies to T. E. Lisle that “(he) agrees that boulder steps appear to be randomly arranged but randomness does not rule out statistical order.”

**Table 7.1 : Statistical moments for the parameters of steps classified by height categories.**

Category		1	2	3	4	5	all categories
Maximum step height in category [m]		0.28	0.38	0.54	0.75	4.14	
Height	mean [m]	0.23	0.32	0.45	0.63	1.17	0.56
	variance [m <sup>2</sup> ]	0.002	0.001	0.002	0.004	0.239	0.162
	standard deviation [m]	0.046	0.028	0.046	0.061	0.489	0.403
	maximum [m]	0.28	0.38	0.53	0.75	2.69	2.69
	minimum [m]	0.10	0.28	0.38	0.54	0.75	0.10
	25% quantile [m]	0.19	0.30	0.41	0.58	0.84	0.19
	75% quantile [m]	0.27	0.35	0.49	0.67	1.24	0.27
median [m]	0.25	0.33	0.45	0.62	0.93	0.25	
Length	mean [m]	2.68	4.39	6.20	8.29	15.61	7.46
	variance [m <sup>2</sup> ]	4.69	16.00	37.48	49.53	137.49	69.06
	standard deviation [m]	2.17	4.00	6.12	7.04	11.73	8.31
	maximum [m]	10.22	16.31	25.64	29.63	47.33	47.33
	minimum [m]	0.47	0.48	1.04	1.25	2.60	0.47
	25% quantile [m]	1.04	1.82	2.08	2.90	6.60	1.00
	75% quantile [m]	4.11	6.56	8.13	11.86	19.76	1.54
median [m]	1.79	2.60	3.89	5.29	11.79	1.20	
Slope (sine)	mean [m]	0.165	0.160	0.186	0.177	0.204	0.178
	variance [m <sup>2</sup> ]	0.002	0.001	0.003	0.002	0.003	0.003
	standard deviation [m]	0.046	0.038	0.053	0.046	0.055	0.050
Step steepness (sine)	mean [m]	0.149	0.136	0.145	0.144	0.130	0.141
	variance [m <sup>2</sup> ]	0.011	0.010	0.012	0.012	0.014	0.012
	standard deviation [m]	0.104	0.102	0.108	0.108	0.120	0.108

### 7.2 Distribution type

The distribution of step lengths and heights is very heavily tailed. This can be shown in various ways. Simple histograms (Figure 7.1 and Figure 7.2) already reveal this feature. Another useful representation type are plots of cumulative density functions (cdf). The linear trend observable in the central section of the double logarithmic representation of the cdf for step heights (Figure 7.4) is typical for heavy tailed distributions. The cdf for step lengths does not show this feature (Figure 7.3).

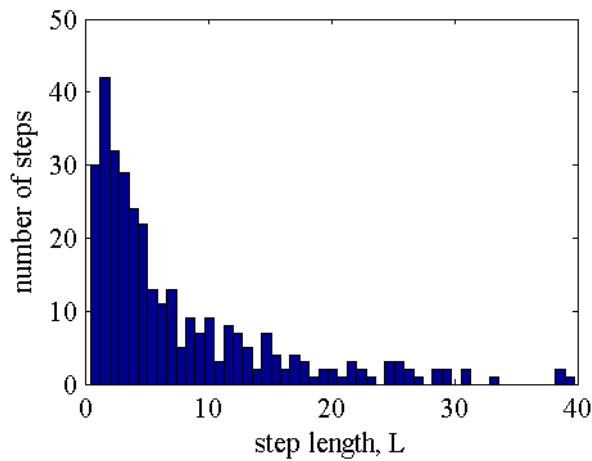


Figure 7.1: Histogram of step lengths. The four steps with lengths exceeding 40m are not shown.

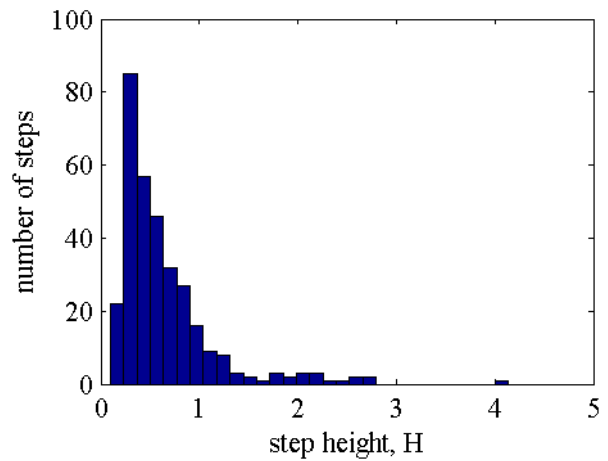


Figure 7.2: Histogram of step heights

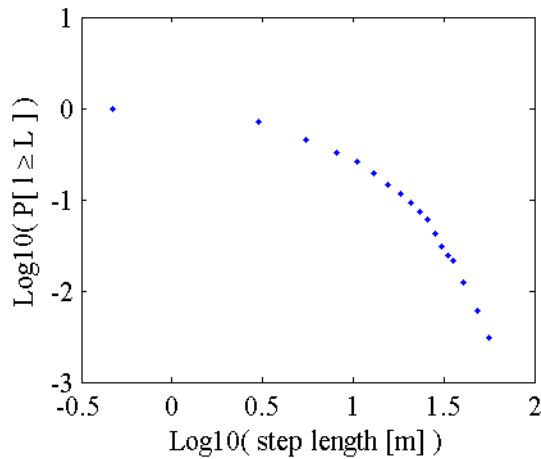


Figure 7.3: cdf of step lengths.

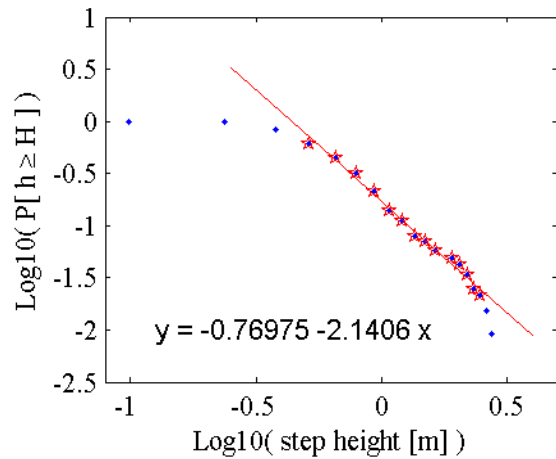


Figure 7.4: cdf of step heights. With line fitted through the points marked as stars.

For a quantitative measure of the heavy tail property, the coefficient of skewness can be computed. It measures the asymmetry of a data set about its mean:

$$\hat{\gamma} = \frac{\sum_{i=1}^n (x_i - \bar{x})^3}{n \cdot s^3} \quad (16)$$

Where  $s$  is the standard deviation and  $n$  the sample size. Distributions are said to be positively skewed when they have a positive and large  $\hat{\gamma}$ . Values of the skewness coefficient for both step height and length are very high.

$$\hat{\gamma}_{(\text{height})} = 2.3746$$

$$\hat{\gamma}_{(\text{length})} = 3.5719$$

For normal distributions  $\hat{\gamma}$  is asymptotically normal distributed with mean zero and variance  $6/N$  (Salas et al. (1980), p. 93). The  $(1-\alpha)$  probability limits, with  $\alpha$  the significance level, may be defined as:

$$\pm u_{1-\alpha/2} \cdot \sqrt{\frac{6}{N}} \quad (17)$$

Where  $u_{1-\alpha/2}$  is the  $1-\alpha/2$  quantile of the normal distribution and  $N$  the sample size. Taking significance level of 1%, the 0.995-quantile of the normal distribution is 2.576. With a sample size of 246 steps the probability limits are  $\pm 0.4023$ . The hypothesis of normality is clearly rejected for both, the distribution of step heights and step lengths with 99% confidence.

### 7.3 Correlation coefficients

Correlations seem to exist between the step dimensions (height and length) and the slope of the stream (chapter 6.1.2 and 6.2). However the correlations found in this study are too weak to justify a fitting of the points. The correlation coefficients,  $r$  reflect this weakness but still are a solid argument for the sign of linear dependences (negative or positive correlation).

$$r = \frac{C(x,y)}{\sqrt{C(x,x) \cdot C(y,y)}} \quad (18)$$

$r = 1$  for a perfect correlation.  $C$  is the covariance respectively the variance if  $x = y$ :

$$C(x,y) = \frac{1}{n} \cdot \sum_{i=1}^n (x_{(i)} - \bar{x}) \cdot (y_{(i)} - \bar{y}) \quad (19)$$

The correlation coefficients between step height, step length (computed in three different ways) and representative slope for each step computed with a moving window of 30 m ( $w = 15$ ) are calculated and listed in Table 7.2.

The third technique to compute step length (length3) is from a hydraulic point of view more correct because the used sine slope is the loss of head (nearly equalling water surface elevation) per unit channel length. This measure is proportional to the energy dissipation due to resistance to flow and is used in preceding studies too. Because of the reasons explained in chapter 5.2.4 it is however more difficult to compute exactly (generally it is computed too short) than the horizontal projection of length (that is length2). As the diminution of length2 due to projection is small, length2 often exceeds length3 and gives even stronger correlation between step height and length. But the difference is very small, thus not contradicting the hypothesis of a correlation between step length and height and justifying to keep length3 as standard computation technique.

Some positive correlation is found between step height and length as well as between slope and step height (Table 7.2). No correlation is found between slope and step length. This being coherent with the theory (Chin 1998) that step length is linked to slope only via step height which is itself largely dependent on sediment size.

**Table 7.2: Correlation coefficients between different step parameters.**

	height	length2	slope15		height	length3	slope15
height	1.000	0.387	0.347	height	1.000	0.390	0.347
length2		1.000	-0.082	length3		1.000	-0.074
slope15			1.000	slope15			1.000

## 7.4 Auto-covariances

Auto-covariance can be used to check for periodicity in the sequence of steps of different sizes along the stream. As a first approximation only the order in which the steps are located along the stream together with their height is considered. If major steps would tend to develop every given distance counted in separations of minor steps, it would be detectable in the plot of an auto-correlation function.

The auto-covariance  $c_k$  is the covariance of a vector with itself lagged by  $k$ . The denominator, being the auto-covariance at lag 0 (corresponding to the variance), normalizes the sequence so the auto-covariance at zero lag always equals 1:

$$\mathbf{r}(\mathbf{x},k) = \frac{\frac{1}{n} \cdot \sum_{i=1}^{n-k} (\mathbf{x}_{(i)} - \bar{\mathbf{x}}) \cdot (\mathbf{x}_{(i+k)} - \bar{\mathbf{x}})}{\frac{1}{n} \cdot \sum_{i=1}^n (\mathbf{x}_{(i)} - \bar{\mathbf{x}})^2} \quad (20)$$

For a serially independent series,  $C_k$  (the term in the nominator) is approximately zero for  $k > 0$ . Here we consider up to  $k = 30$  (out of 246 steps).

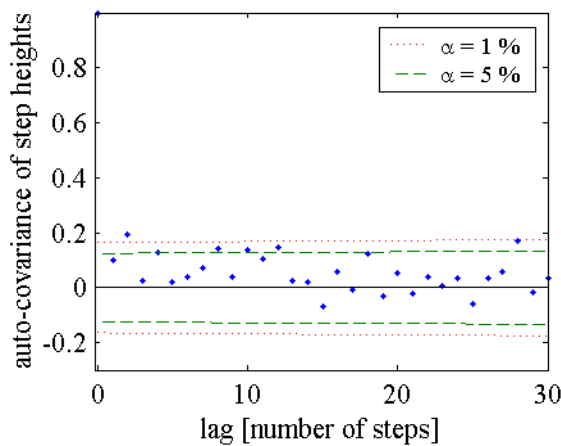


Figure 7.5: Auto-correlation of step heights vector.

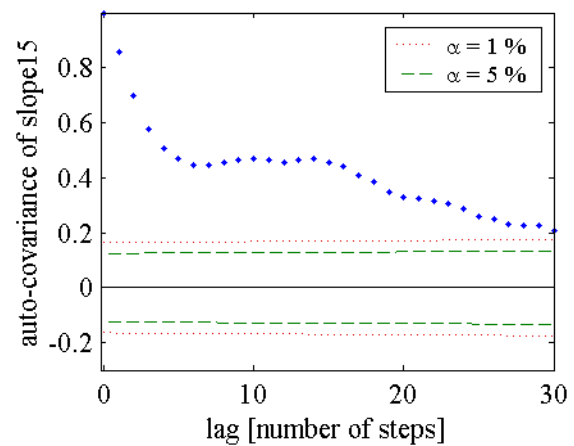


Figure 7.6: Auto-correlation for the vector of representative slopes for each step.

The 95 % and 99 % confidence intervals,  $r_\alpha$  are shown according to Salas (1980), p.91:

$$\mathbf{r}_\alpha = \frac{\pm \mathbf{u}_{1-\alpha/2}}{\sqrt{N}} \quad (21)$$

With  $N$  the sample size,  $\alpha$  the significance level (0.05 and 0.01 in this case) and  $u_{1-\alpha/2}$  the  $1-\alpha/2$  quantile of the standard normal distribution (1.960 and 2.576 respectively). The sample size varies with the lag as it corresponds to the number of steps minus the lag.

A point outside of the confidence interval means significant correlation at the significance level  $\alpha$  exists. Whereas a point within the interval states that no statistically significant correlation is found.

For a lag of zero, the correlation is perfect and the auto-covariance equals one. For the step heights (Figure 7.5) no positive or negative correlation exists between adjacent steps or steps separated by a certain number of steps. No periodicities are detected by the auto-correlation function. The auto-correlation drops directly to a value close to zero. There is one point plotting outside the confidence interval.

As an example the auto-covariance function for the representative slope for each step is shown in Figure 7.6. There is obviously dependence between slopes at successive steps.

It is to note that the steps are not situated at regular intervals. For a proper analysis this would have to be taken in account. The results have to be taken cautiously. Another problem is that the step heights along the stream cannot be considered as totally independent. They depend on slope and sediment supply conditions which vary along the stream. So it is only an approximation to use all step heights sorted by their position along the stream as one vector.



## 8 Flood frequency analysis

Many steps have a height comparable with the size of the largest boulders they are composed of. This is observed in field investigations for channels not as steep as the Vogelbach (e.g. Rosport and Dittrich, 1995; Cin, 1999) but is partially applicable to the Vogelbach too. Further, the incipient motion of boulders of a certain size can be correlated with discharge of the stream. So the recurrence intervals for floods can be used to estimate the frequency of formation of steps of a certain size.

Another application is that using the shape of the measured cross sections, stream width may be computed for different discharges and compared with the measured widths. The best fit of computed to measured width was found for a discharge of about  $13 \text{ m}^3/\text{s}$  (see chapter 9, Figure 9.3). With a flood frequency analysis a return period can be assigned to that particular discharge considered as bed forming.

The discharge data measured by the WSL at the Vogelbach gauge are an hourly record from 1969 to 1984 and a 10 min record from 1985 to 2002. The hourly data consists of points manually digitised from a registration paper. The peaks in this first period seem to be lower than in the more detailed second one. It is clear that an hourly record is not detailed enough to get a proper registration of flood peaks in the Vogelbach. The data from 1969 to 2002 are gained from automatic discrete measurements of water level at the gauge. Due to the small drainage area and steepness, floods are of short duration and may easily come and go within one to a few hours (Figure 8.1). For this reason only the 10 min record from 1985 to 2002 is used for the flood analysis. An annual peak and a peak over threshold method are applied to estimate flood frequencies and the results are compared.

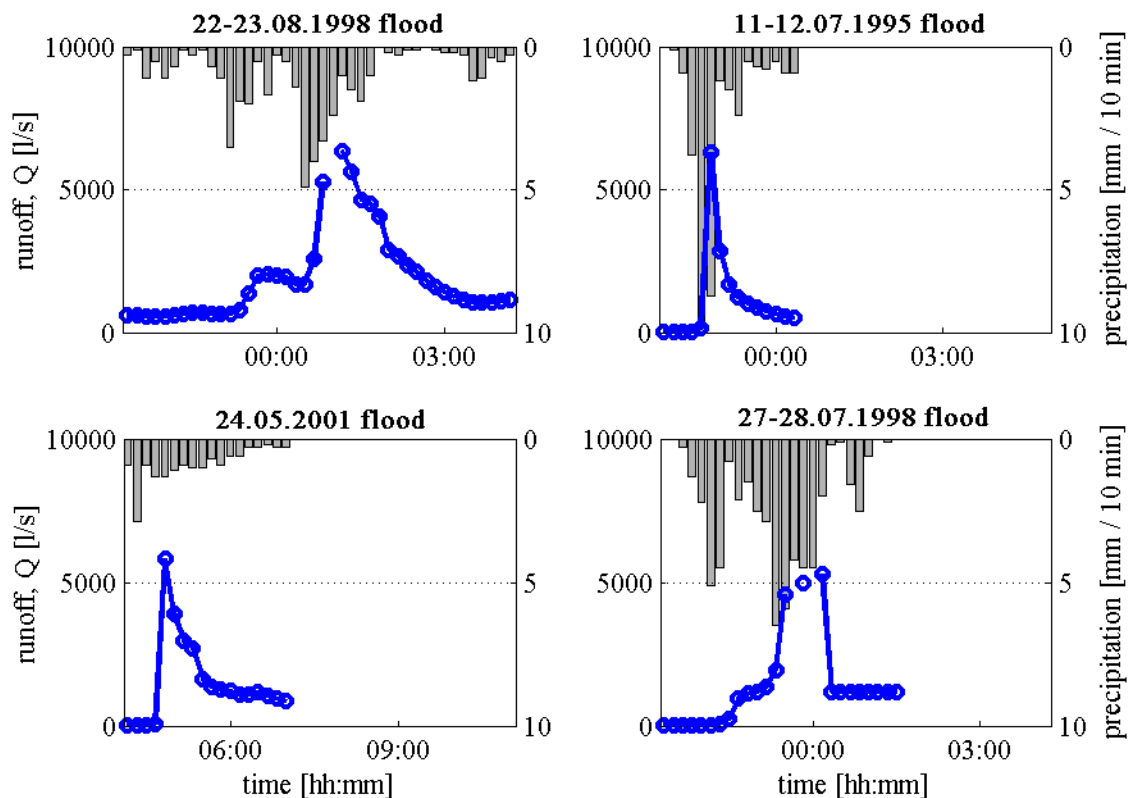


Figure 8.1: Four largest flood events during the 1985 - 2002 period. The measurement interval for discharge is 10 minutes. Discontinuous data indicate periods of missing records.

Figure 8.1 shows representations of the four largest recorded floods in the period 1985-2002. Enormous changes in discharge occur from one 10 minute record to the next. Even this high sampling rate seems to be insufficient to register the shortest peaks properly. For better data the sampling frequency would have to be raised. To keep the amount of data reasonable, one could imagine discharges between the 10 minutes records recorded only when discharge exceeds a defined threshold. On the other hand this would lead to an unequally spaced time series.

For the two events in 1998 the actual peak could have been missed. There are missing records just beside the maximums recorded. All floods of 1998 and the 20 highest overall were checked and these two are the only ones with missing values. A problem of the recording mechanism must be assumed because of very high discharge. Looking at the plots of Figure 8.1 even if the actual maxima cannot be estimated it appears that discharge was higher than measured. The truncation of two very large events is an important source of error for the statistical analysis.

Parallel to a statistical analysis of measured events, it is possible to estimate flood intensities without any previous discharge measurements. Using only an estimated heavy precipitation event and information on the soil cover and topography of the area a good estimation is possible (Chapter 8.3).

Lenzi (2001) pointed out the importance of considering not individual flood events but cycles of decreasing events during which the stream will continuously adjust morphological features on smaller scales. The hypothesis of superposed step-pool sequences in this study is based on the same idea. To test the hypothesis, some time should have passed since the last extraordinary large flood. Figure 8.2 shows all floods in the period 1998 - 2002 exceeding a 1800 l/s threshold. Since the large flood event in spring 2001 numerous smaller ones occurred possibly allowing the formation of step sequences of smaller magnitude.

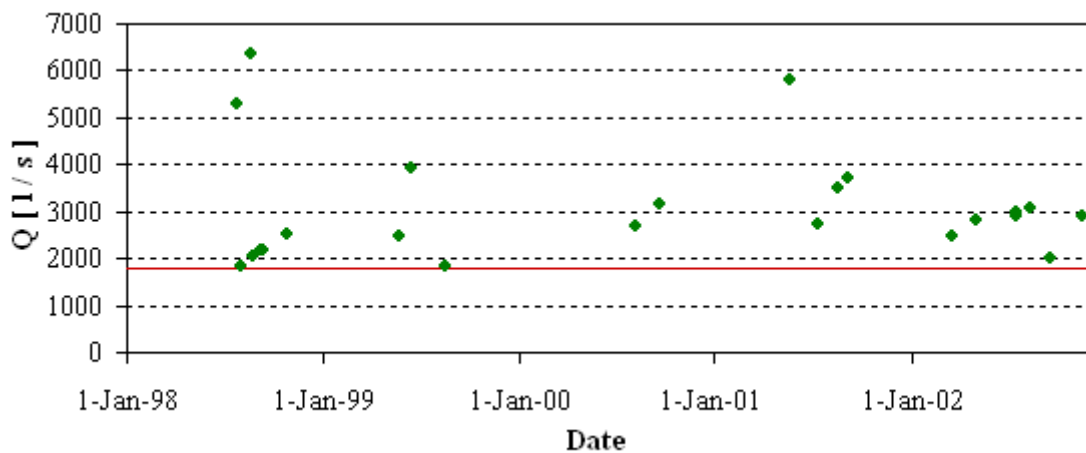


Figure 8.2: Flood events in the Vogelbach since 1998 exceeding 1800 l/s threshold.

### 8.1 Annual peak method

Analysis is conducted on the 18 annual discharge maxima from 1985 till 2002. The peaks are plotted using the Weibull plotting position. That means the probability of nonexceedance,  $F_X(x)$  assigned to a particular event is:

$$F_X(x) = P(X \leq x) = \frac{i}{n+1} \quad (22)$$

Where  $X$  is a random variable and  $x$  a possible value for  $X$ , in particular  $x$  takes the values of the recorded peaks. The  $n$  annual peaks are sorted in descending order so that  $x_{(1)} \geq \dots \geq x_{(i)} \geq \dots \geq x_{(n)}$ .

As the sampling interval is annual, the inverse of the probability of exceedance is equal to the recurrence interval  $T_a$  in years:

$$T_a = \frac{1}{1 - F_X(x)} \quad [a] \quad (23)$$

The highest recurrence interval corresponding to the highest flood event in a  $n = 18$  years data set is therefore:

$$T_{a \max(n=18)} = \frac{1}{1 - \frac{18}{18+1}} = 19 [a] \quad (24)$$

All floods for higher recurrence intervals lay in the extrapolation range.

A Gumbel distribution is used to fit the data and several methods are used to estimate the parameters. The cumulative distribution function and the used parameter estimators for the Gumbel distribution are the following:

$$F_X(x) = P(X \leq x) = e^{-e^{-\frac{x-\xi}{\alpha}}} \quad (25)$$

Method-of-moments estimators:

$$\alpha = \frac{\sigma \cdot \sqrt{6}}{\pi} = 1060.4 \quad , \quad \xi = \bar{x} - 0.5772 \cdot \alpha = 3370.2 \quad (26) \text{ and } (27)$$

Gumbel estimators:

$$\alpha = \frac{\sigma}{\sigma_n} = 1279.7 \quad , \quad \xi = \bar{x} - \bar{y}_n \cdot \alpha = 3312.2 \quad (28) \text{ and } (29)$$

L-moment estimators:

$$\alpha = \frac{\lambda_2}{\ln(2)} = 986.6 \quad , \quad \xi = \bar{x} - 0.5772 \cdot \alpha = 3412.8 \quad (30) \text{ and } (31)$$

With  $\alpha$  and  $\xi$  being the scale and location estimators,  $\bar{x}$  the mean of annual peaks, 0.5772 the Euler constant,  $\sigma$  the standard deviation,  $\lambda_2$  the second L-moment,  $\bar{y}_n$  and  $\sigma_n$  constants depending only on sampling size.  $\bar{y}_n$  and  $\sigma_n$  are taken from Dyck and Peschke (1995), table 23.3. The second L-moment is:

$$\lambda_2 = 2 \cdot \left( \frac{1}{n} \cdot \sum_{i=1}^n X_{(i)} \cdot \left( 1 - \frac{i - 0.35}{n} \right) \right) - \bar{x} = 683.9 \quad (32)$$

For detailed information on methods see Dyck and Peschke (1995), chapter 23.5.2 (for method of moments and Gumbel method) and Stedinger et al. (1993) (for L-moments and also method of moments estimators).

Method-of-moment and L-moment estimators give very similar results. The Gumbel estimators lead to lower recurrence intervals (Figure 8.3). The recurrence intervals are very high in comparison with the results of the stream width analysis (chapter 9). A discharge of about 13 m<sup>3</sup>/s is found to best fit the observed widths and so being channel forming discharge. The annual peak analysis shows a recurrence interval of already 200 years for a 10 m<sup>3</sup>/s flood according to the lowest estimates with the Gumbel method. This could be due to a lack in high floods in the relatively short interval of 18 years, or due to recording problems discussed above. It is in any case a strong motivation for a partial duration analysis.

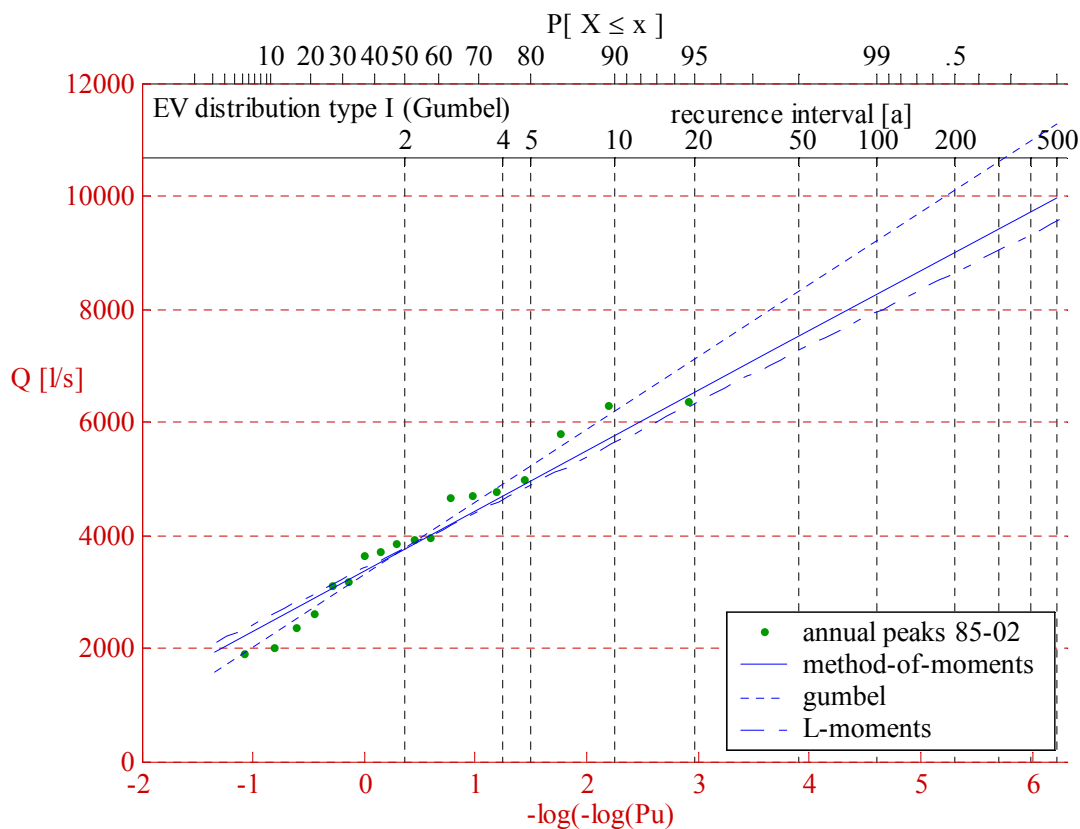


Figure 8.3: Annual flood frequency analysis for the Vogelbach using the Gumbel distribution and three parameter estimation methods.

In the nearby Erlenbach stream with a comparable drainage area of 0.74 km<sup>2</sup>, the highest recorded flood in July 1984 was 12 m<sup>3</sup>/s with a return period estimated to be 30-35 years (Rickenmann and Hegg, 2000).

## 8.2 Partial duration method

The annual peak method is more suitable for large basins with a strong seasonal regime, where the biggest floods are more regular in time. For a small catchment, variability from year to year is much higher and the second biggest flood in one year can very well be more important than the biggest one of other years. If one had an almost unlimited long data set this would not be a problem, but with a short series of 18 years the loss in information is very high.

For the partial duration or peak over threshold (POT) method all peaks of independent events higher than a defined threshold are analysed. This threshold should be chosen low enough to get at least one flood value per year. The second problem is to select only independent events and not two peaks resulting from the same storm. This was done automatically here using a FORTRAN routine, but also checked manually. In the routine only the highest peaks in a continuous series of records all over the threshold is taken. Two high peaks of the same event can be interpreted as two floods if the threshold lies over the intermediary low but below both peaks. A secondary peak is not expected to be of the same magnitude as the primary one, especially for little catchments as the Vogelbach where no superposition of hydrographs coming from tributaries differently influenced by a precipitation event and having different flow times is likely. This is why the threshold should be kept high in order to minimize this double picking effect. For the Vogelbach,  $1.8 \text{ m}^3/\text{s}$  is found to be the lowest value for which at least one peak occurs each year. A total of 74 independent peaks exceed this value for the 18 analysed years.

The independency condition is not a problem for the annual peak method as a flood on new-year resulting in a maximum for one year with the primary peak and in the other with a secondary peak is not likely.

Following Stedinger et al. (1993), chapter 18, the partial duration method consists of two steps. First the arrival rate of events larger than a threshold is modelled. Then the distribution of the magnitude of these events is modelled. For the first step if  $\lambda$  is the arrival rate, equal to the average number per year of events larger than the threshold and  $G(x)$  is the probability that events when they occur are smaller than  $x$  ( $x \geq \text{threshold}$ ), then  $\lambda^*$  is the arrival rate for events of the level  $x$ :

$$\lambda^* = \lambda \cdot [1 - G(x)] \quad [\text{events/a}] \quad (33)$$

As the events are independent, the probability of no exceedances of  $x$  for one year can be calculated with the Poisson distribution:

$$F_a(x) = e^{-\lambda^*} = e^{-\lambda \cdot [1 - G(x)]} \quad (34)$$

For the distribution  $G(x)$  a general Pareto distribution can be used:

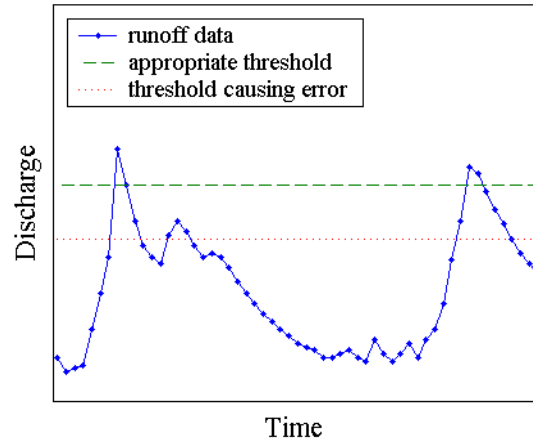


Figure 8.4: Illustration of possible error caused by low threshold. Two peaks are recorded during the same flood event.

$$G(x) = 1 - \left( 1 - \kappa \cdot \frac{x - x_0}{\alpha} \right)^{1/\kappa} \quad (35)$$

where  $x_0$  is the threshold,  $\kappa$  the shape parameter and  $\alpha$  the scale parameter:

$$\kappa = \frac{\bar{x} - x_0}{\lambda_2}, \quad \alpha = (\bar{x} - x_0) \cdot (1 + \kappa) \quad (36) \text{ and } (37)$$

With the simple relation between probability of no exceedances and return period  $T_a$ :

$$T_a = \frac{1}{1 - F_a(x)} \quad (38)$$

The return period can now be determined for any event/discharge  $x$  (Figure 8.5).

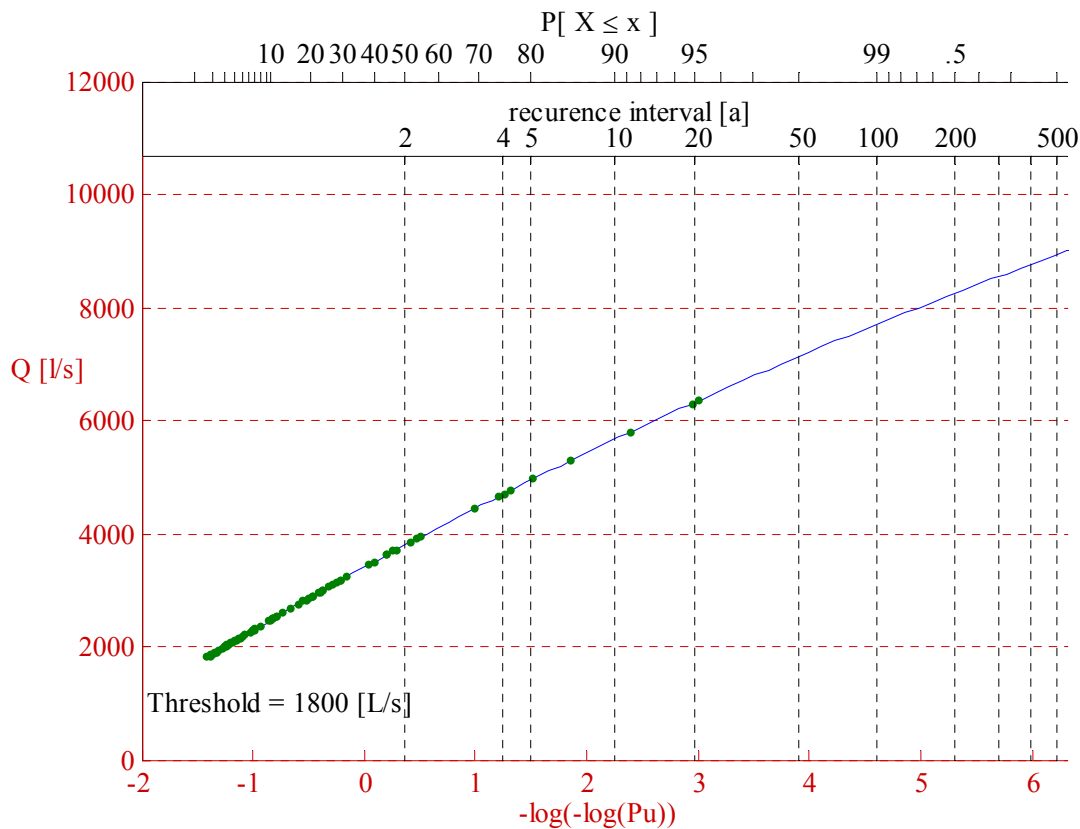


Figure 8.5: Partial duration frequency analysis for the Vogelbach with a threshold of 1800 l/s.

With the peak over threshold method a higher number of events could be considered than with the annual peak method. The method seems to confirm the lower values of around  $8 \text{ m}^3/\text{s}$  for a  $HQ_{100}$  and not the values found using the Gumbel estimators from the analysis of annual peaks.

### 8.3 Flood estimation without flow measurements

Information on topography, soil, geology, vegetation and landuse together with rainfall intensities can be used to gain estimations of the magnitude of floods, this without any flow measurement. The Swiss Federal Institute for Water and Geology (BWG) defined three size

categories for catchment areas. With 1.55 km<sup>2</sup>, the Vogelbach typically belongs to the smallest basins. The Vogelbach was used by Forster and Hegg (2002) to test and compare several methods in their study on estimation of flood peak discharges in small torrential catchments.

The main difference between flood estimations for medium size and small (< 10 km<sup>2</sup>) basins lies in the availability of high resolution surface information. Small scale variability is present in small as well as in medium size basins but in the latter effects on the runoff tend to compensate due to the presence of several subbasins. Easily available information sources (topographic map of Switzerland 1:25'000, map of Landuse 1:200'000, geologic atlas of Switzerland 1:25'000 and others) are not sufficient to reveal small scale variability.

The large scale information sources are however a good base to gain a first impression of the order of magnitude and repartition of parameters and can be summarized to a structure hypothesis. *Where could consolidated soils be located? Where are wetlands likely to be found?*

The infiltration conditions on the surface and the capability of water absorption of soil layers are decisive for runoff generation. The hydrological behaviour of the soil can be classified with the following criteria:

- **Wetlands.** Wetlands have the property of high natural water saturation and are indicators for low permeable soils. They can therefore be considered as highly runoff generating. Typical plants, so called moisture indicators, as for instance pestilence wort can be used for the delimitation of wetland zones. The shallow, clay rich soil conditions as they predominate in the Vogelbach due to the Flysch bedrock are particularly favouring wetlands (or simply saturated soil conditions).
- **Consolidation.** A strong mechanical impact (intensive use as pasture, heavy machinery, ski runs) reduces the permeability. This is not the case for the Vogelbach as the surfaces free of forest are barely used as pastures.
- **Macropores.** Macropores created by bioturbation increase infiltration and percolation into deeper layers. Before a field investigation the presence of macropores is difficult to guess.
- **Humus layer.** A thick humus layer on top of a saturated layer has a positive influence on water absorption. As for the macropores, the humus thickness is difficult to predict without field descriptions.
- **Soil skeleton.** A high percentage of soil skeleton increases permeability.
- **Soil structure.** Shallow lying (<40 cm) water storing layers have negative consequences on the absorption capacity.

A short field investigation is essential to verify and if necessary correct the delimited hydrological response units (HRU) in the structure hypothesis and to measure a few representative soil profiles. A runoff coefficient can then be estimated for each zone with the schema developed by Rickli and Forster (1997) (Figure 8.6). Figure 8.7 shows the delimited zones for the Vogelbach.

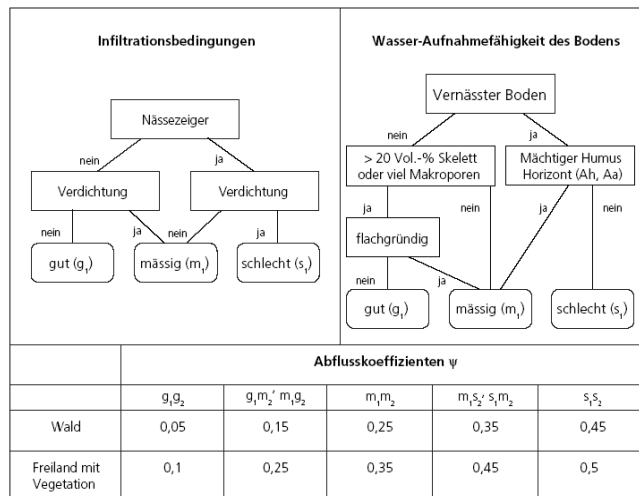


**Figure 8.6: Schema for the estimation of runoff coefficients for the different soil types.**

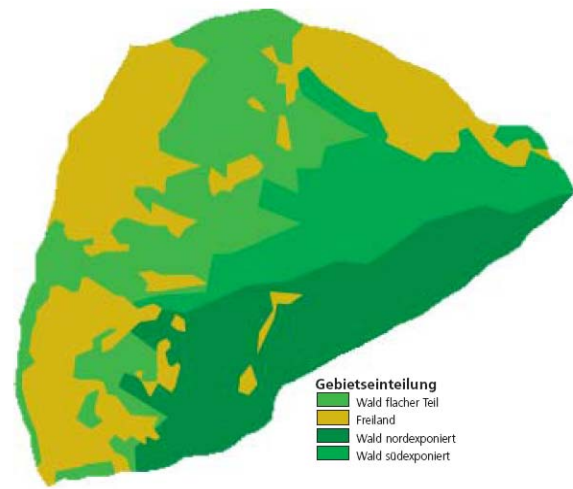


**Figure 8.7: Delineated HRUs for the Vogelbach (Rickli and Forster 1997).**

Forster and Hegg (2002), verified several methods to obtain runoff coefficients from the information cited above on seven small catchment areas in Switzerland and compared the results. They developed a procedure to obtain reliable runoff coefficients for a HQ100 using the different methods. Their results are presented in Spreafico, Weingartner, Barben and Ryser (2003). The rainfall intensities which are an important input in four of the five estimation methods are taken either from the Hydrological Atlas of Switzerland or from other long term measurements if available.

The method developed by Müller in the early 40's determines the highest expected flood and not a HQ100. Its only input parameters are the drainage area and the runoff coefficient. In most of the catchments this method gives values well above the statistically determined HQ100 and thus is used as the upper bound. Exceptions are small, but high runoff generating basins (like the Vogelbach). The method by Taubmann gives systematically the smallest values. It was therefore used as lower bound. Together with three other methods (modified flow time method, Kölla, Clark-WSL) they consider the strongest rainfall event for a length equal to the concentration time of a basin. Computation of concentration time and formulas for the final HQ100 value vary from one method to another. For a complete description and formulas the reader is referred to Forster and Hegg (2002).

None of the tested single methods for small catchment areas was found to give good results in all cases. The spectrum of particularities that can occur in streams is much too large to allow one method to cover all cases. All methods have their strengths and weaknesses. Out of the set of five methods, Forster and Hegg (2002) present a guideline to end up with a HQ100 value and information on its reliability. Two methods are defined as giving maximum and minimum results respectively. An average of the three other methods, but differently weighted depending on their relative position to the maximum and minimum values, gives the final HQ100. Upper and lower limits are given by the overall maximum and minimum which sometimes are not found with the methods by Müller and by Taubmann. Figure 8.8 shows the results for the Vogelbach.



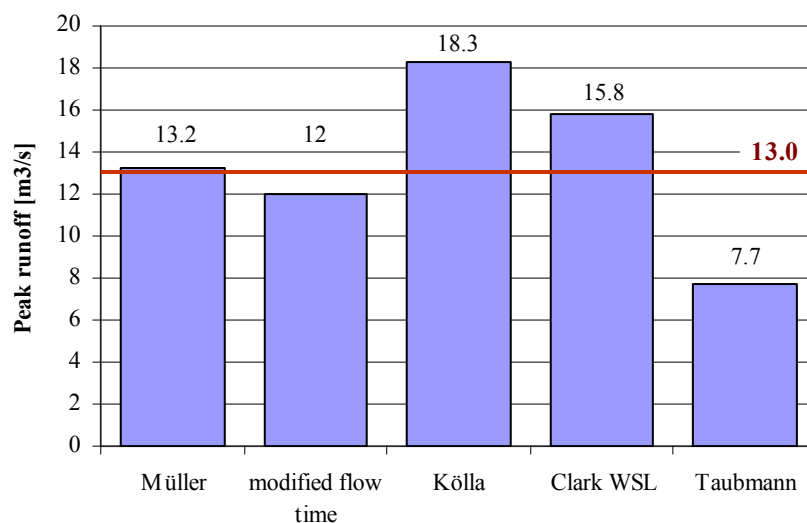


**Figure 8.8: HQ100 using different techniques. Müller and Taubmann give upper and lower bounds. Considering the channel capacity, a HQ100 of 13.0 m<sup>3</sup>/s is suggested. (Forster and Hegg, 2002).**

The fact that the upper bound defined by the Müller method (13.2 m<sup>3</sup>/s) is exceeded by two methods is a sign that flood estimation for the Vogelbach by empirical methods is delicate. As also the method of modified flow time gives a result close to the upper bound, a proposition for a HQ100 of 13 m<sup>3</sup>/s is made.

To check the plausibility of the results, a comparison with the channel capacity is strongly suggested. For the Vogelbach, Forster and Hegg (2002) measured a cross section channel area for estimated bankfull water level at a location close to the measurement station of 5 m<sup>2</sup> and estimated the flow velocity to be 2 m/s. The resulting 10 m<sup>3</sup>/s are less than the value found by analysing the catchment characteristics. Considering this, HQ100 is set to 11.5 m<sup>3</sup>/s, with a variation range from 10 m<sup>3</sup>/s to 18 m<sup>3</sup>/s. The lower limit results from the channel capacity.

## 8.4 Comparisons

A statistical analysis of peak runoff on the Vogelbach was first done by Forster and Hegg (2002), who found a HQ100 of about 7 m<sup>3</sup>/s. They used data from a time period of 16 years with hourly data and partially reconstructed flow peaks additionally to 16 years with 10 min data. In this study, using only 18 years of 10 min data HQ100 is found to be around 8 m<sup>3</sup>/s. The hourly data was not used because of the flashiness of the floods as explained earlier. In the flow routing chapter (chapter 9) the discharge corresponding best to the active channel width is approximately 13 m<sup>3</sup>/s.

The values found evaluating only the characteristics of the basin by Forster and Hegg (13 m<sup>3</sup>/s) correspond to the flow routing ones of this study. The measure of the area of a single cross section and estimation of flow velocity seems questionable in comparison with the other methods and should be considered only as a check for the order of magnitude. The two statistical evaluations probably suffer from the inappropriate sampling interval and missing peaks. In conclusion the higher values seem more reliable.

## 9 Channel width simulation

Parallel to this diploma thesis a semester project was conducted by Sebastiano Pollock on flow routing of extreme events in two mountain streams, one of which was the Vogelbach. One of his main themes was a better understanding of the impact of roughness in mountain streams. His flow routing simulations with HEC-RAS were used in this study. The basic idea is to simulate the passage of a flood wave with a given return period through the Vogelbach main stream, and to examine the magnitude of the flood that would be required to fill the active channel. The active channel width was defined by exposed alluvial bed sediment and measured in the field.

The Manning's roughness coefficient ( $n$ ) is a very sensitive coefficient in a flow simulation. It has a large impact on flow velocity and therefore on water depth and channel width. A first simulation is conducted with a constant  $n = 0.07$  and repeated for different discharges. This value was chosen after consulting previous studies and especially the WebPages of the United States Geological Survey (USGS) page providing pictures of streams and the corresponding  $n$  values. Input for the simulation are the 22 measured cross sections, different bed parameters like the roughness coefficient  $n$  and different discharges for each cross section accounting for the fact that the runoff is a function of drainage area, and may be less in upper cross sections than in lower ones for a same event using:

$$Q_i = Q_1 \cdot \left( \frac{\text{Drainage area at cross section } i}{\text{Drainage area at cross section 1}} \right)^\beta \quad (39)$$

Where  $Q_i$  is the discharge at cross section  $i$ , the coefficient  $\beta$  is variable ( $0 < \beta < 1$ ) and the drainage areas are as computed in chapter 5.3. A steady state analysis was conducted with  $Q_i$  as cross sectional inputs. It was assumed that the steady state profile would approximate well the water depth during the passage of the flood peak.

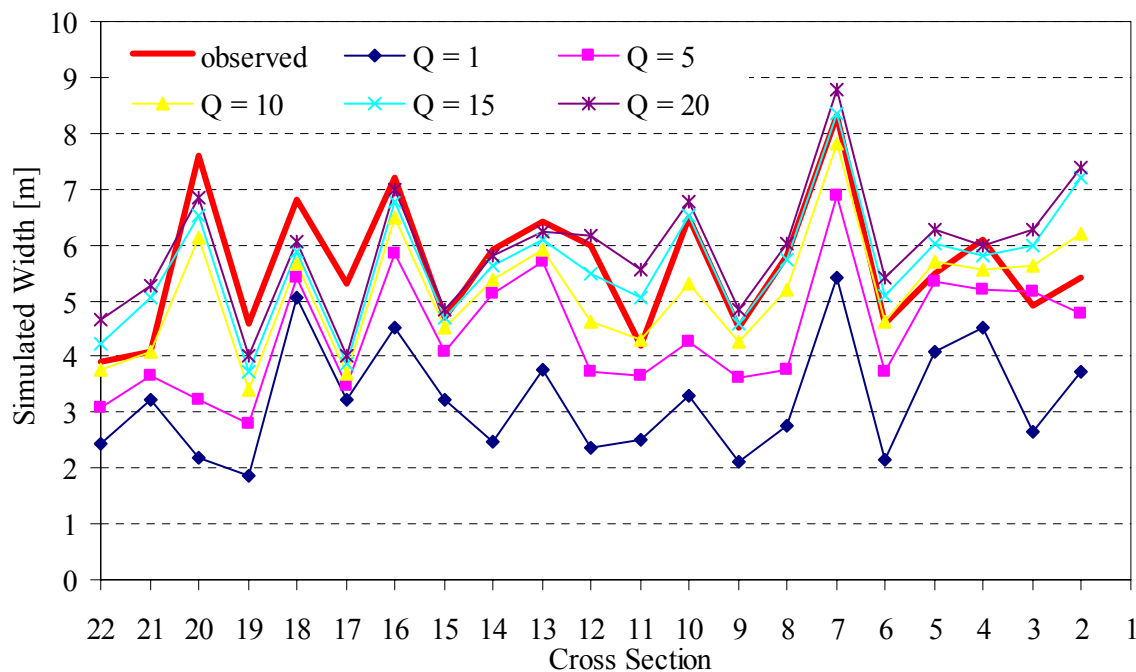


Figure 9.1 : Simulated widths at cross sections 2 to 22 for different discharges with  $n = 0.07$  and  $\beta = 0.5$ .

The HEC-RAS output file contains values of flow depth, velocity, Froude number, critical flow depth, flow area and top width at each cross section. The simulated top widths are compared with the measured ones (chapter 4.3) at each cross section. For a discharge of 15 m<sup>3</sup>/s the widths correspond best but differences between measures and simulation are not always in the same direction (Figure 9.1). This could indicate a significant variation of  $n$  from cross section to cross section. Cross section 1 is not shown because it was measured on the concrete gauge.

Manning's coefficient can be estimated more precisely using different formulas. All of these formulas contain the hydraulic radius which in turn, in the case of a simulated rare event in the Vogelbach, can only be taken from simulation. An iterative process is necessary. For the purposes of this study a two step manual iteration was sufficient. (a) First the simulation was run with a constant  $n$  and a discharge was chosen for which widths correspond best. As the cross sections consist of approximately 10 points their profiles are not precise enough to calculate the wetted perimeter necessary for the hydraulic radius. The hydraulic radius is therefore approximated by the average flow depth.

$$\text{hydraulic radius, } R = \frac{\text{flow area}}{\text{wetted parameter}} \quad (40)$$

$$\text{average depth, } d = \frac{\text{flow area}}{\text{stream width}} \quad (41)$$

and **average depth**  $\geq$  **hydraulic radius** as **stream width**  $\leq$  **wetted perimeter**

(b) With the average depth for the hydraulic radius and other measured parameters new values for  $n$  are calculated for each cross section. These values are used in a second run to get better estimates of flow depth.

For the estimation of  $n$  the standard formula by Limerinos (1970) (taken in Jarrett, 1985) is:

$$n = \frac{0.1129 \cdot R^{1/6}}{1.16 + 2.0 \log \cdot \left( \frac{R}{D_{84}} \right)} \quad (42)$$

In which  $R$  is the hydraulic radius in meters and  $D_{84}$  the length, in meters, that equals or exceeds 84% of the particle intermediate diameters.  $D_{84}$  is taken from the counts of 100 samples similarly to  $D_m$  and not as the average of the five largest boulders. As the sediment count was not done at every cross section missing values are interpolated.

Another approach is made by Jarrett (1985). As particle size information is difficult to get they studied the relation between particle-size and slope. The result is a formula specially developed for high-gradient streams ( $>0.002$ ) without need of particle-size information:

$$n = 0.32 \cdot S^{0.38} \cdot R^{-0.16} \quad (43)$$

In which  $R$  is the hydraulic radius in meters and  $S$  the friction slope.

Figure 9.2 shows the obtained values for  $n$  at the cross sections using both formulas. Although Jarrett's expression is written for steep channels it gives unrealistically high values. The relation between slope and channel size which it is based on does not seem to be extrapolatable to the extreme slope range of the Vogelbach. Using average flow depth  $d$

instead of hydraulic radius  $R$  is not exaggerating  $n$  as  $d$  always equals or exceeds  $R$  and the exponent is negative. Considering this, Limerinos gives a better approximation for  $n$ .

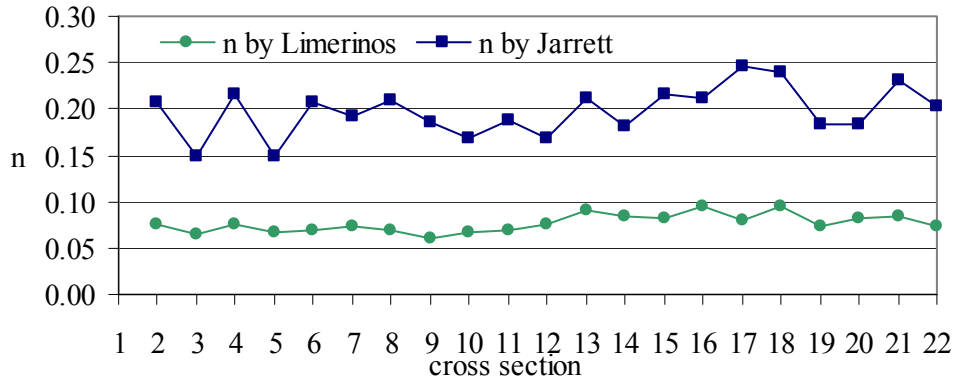


Figure 9.2: Computed  $n$  values. Blue squares: using Jarrett, green dots: using Limerinos.

Flow values of 10 to 15  $\text{m}^3/\text{s}$  at cross section 1 are simulated with HEC-RAS in the second run using the values for  $n$  found with Limerinos. The simulated widths are again compared with the observed ones (Figure 9.3). There is a slight increase in the fit.

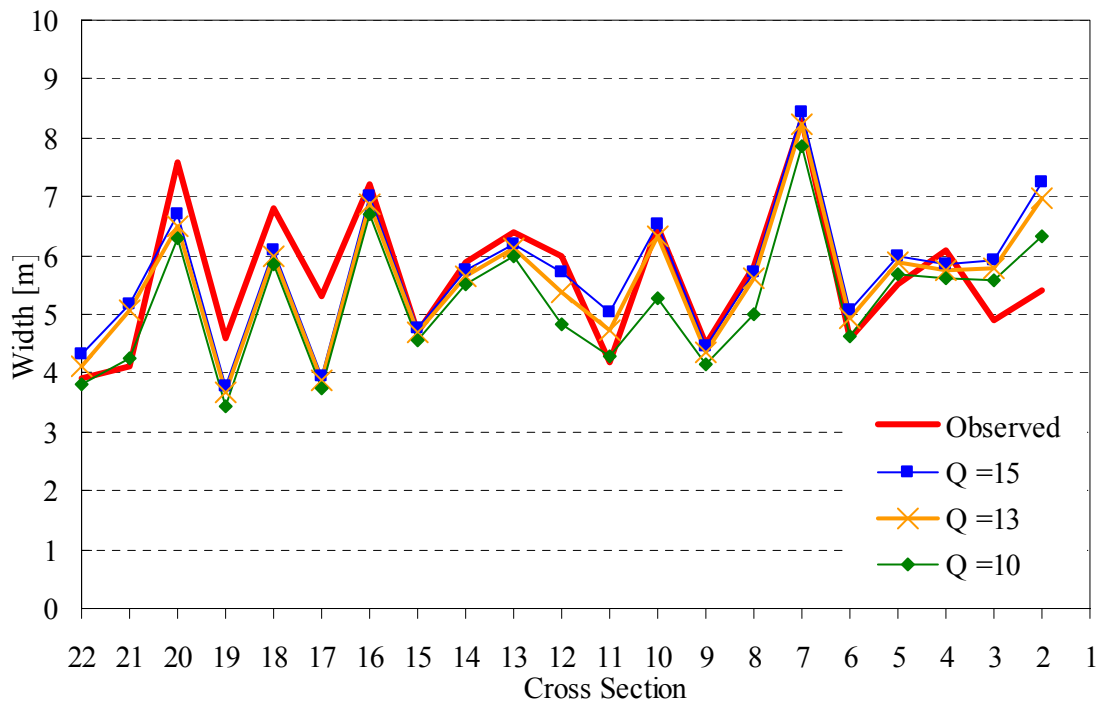
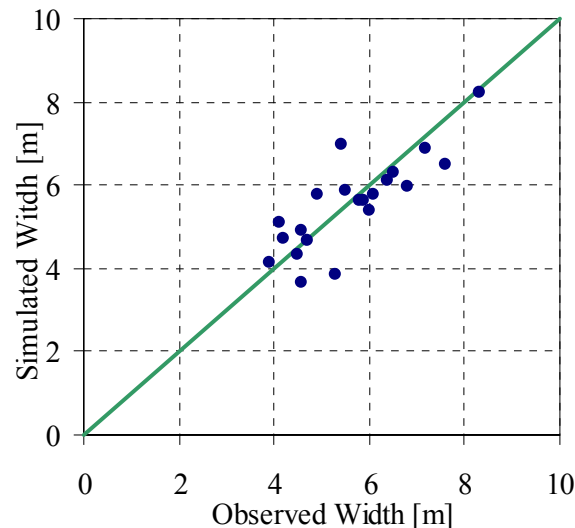


Figure 9.3: Simulated widths with  $n$  computed with Limerinos at cross sections 2 to 22 and  $\beta = 0.5$ .

**Table 9.1: Sum of squares of the differences between measured and observed widths at each cross section.**

	Q [m <sup>3</sup> /s]								
	1	5	10	11	12	13	14	15	20
<b>n = 0.07</b>	142.92	51.48	14.02					12.14	14.62
<b>n using Limerinos</b>			12.55	10.86	10.55	<u>10.46</u>	10.77	10.99	

**Figure 9.4: Simulated versus observed widths at cross section locations for a discharge of 13 m<sup>3</sup>/s.**

For a quantitative judgment of the results the sum of squares of the differences between measured and observed widths at each cross section are calculated (Table 9.1); this for constant  $n$  values of 0.07 and for  $n$  values computed with the Limerinos formula. The best fit is obtained with a discharge of 13 m<sup>3</sup>/s at cross section 1. Figure 9.4 shows the simulated versus the observed widths for this discharge. The points lay close to the unit slope line confirming again the good fit.

Especially the simulated width of cross section 2 is still much larger than the observed one. It is important to remember that the measurement of active channel top width was quite subjective. When measuring the width an important part is visual judgment. It is most of the time not obvious to decide what the bankfull channel width is. This large difference in observed and simulated width for cross section 2 could be due to a wrong estimation in the field. Also for time reasons the particle-size distribution curve was not determined at each cross section. Cross section 2 for instance was not measured but interpolated between cross section 1 and 4. For the lower reaches this should not be a source of error as the particles are visually very similar in close cross sections. For the cross sections in the steep reaches where the particle tracking could not be done due to the steepness, the interpolation is not a good but the only solution. The interpolated values are probably too small for the steep reaches. Visually an important increase of  $D_m$  was for instance noticed from cross section 19 (particle-size curve determined) to cross section 18 (too steep for investigations). Larger values of  $D_{84}$  would increase the roughness and increase the simulated widths. This would give better simulations for cross sections 17 and 18 that were too steep for detailed investigations. At cross sections 19 to 22 the particle-size curve could be determined in the field; errors must be due to something else.

## 10 Comparison with check dams in nearby streams

Check dams are retention structures on streams built perpendicular to the flow direction (Figure 10.1). They are mostly made of concrete for the resulting resistance to abrasivity, but wood or a combination of natural rocks and mortar can also be used for esthetical or biotope reasons. The purpose of check dams is to add flow resistance (reduce channel slope) to a stream in order to stabilize the channel bed and to serve as small sediment storage dams. This is particularly so during high discharge events when the flow is able to move natural steps creating a smoother transport surface for all particle sizes what will again increase flow velocity and transport capacity. In extreme cases for floods of high magnitudes in steep streams ( $>25$  degrees, Chatwin et al., 1994) the movement of bed material will transform the flow into a debris flow.

In upper, very steep channel sections, check dams reduce the incidence of failure by reducing the channel gradient. In lower sections they store debris flow sediments. All over the channel check dams reduce the volume of channel-stored material by preventing downcutting of the channel and resulting destabilization of sidewalls.

Check dams can be seen as the anthropogenic equivalent to step-pool sequences. A good comprehension of natural step-pool systems will therefore be useful to improve check dam functionality.

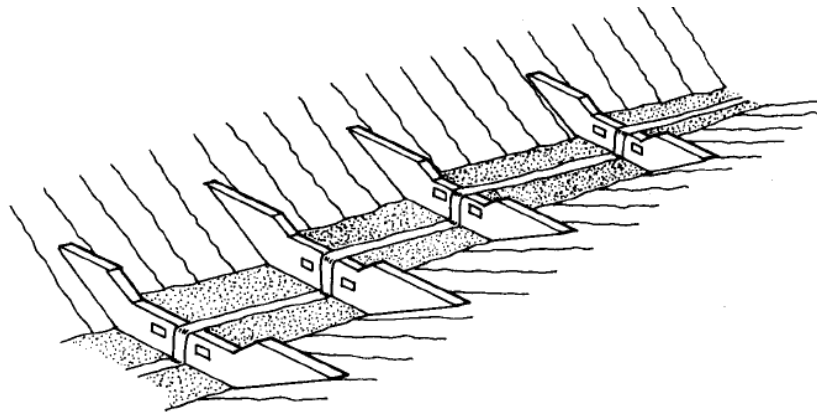


**Figure 10.1:** Sketch of check dams after Eisbacher and Clague (1984).

Natural organization of steps is thought to approach one with maximum flow resistance (Abrahams et al., 1995). This is exactly the aim of check dams and therefore their design height and separation should be close to natural steps. Of course from an economic point of view it may be more advantageous to construct few high check dams than many small ones. On the other hand, too large check dams will accumulate sediments for a long time creating a lack in downstream networks. This presents a danger during extraordinary high floods: in case of dam failure (which is improbable in the case of concrete dams) the available amount of sediments for transportation will be even larger than without check dams at all. Sometimes special basins with easier access are arranged between two check dams from where material can be removed to prevent too large an accumulation of sediments.

Lenzi and Comiti (2003) analyse scouring downstream of check dams which were designed to simulate the geometry of natural step-pools. They separate the pools between the steps into scour holes and runs and analyse the dimensions of the scour holes. They found that for long-spaced check dams scour holes are well-defined and depositional dynamics are prevalent downstream of the holes, raising the bed level and forming gentler runs. For short spaced dams the erosive processes are prevailing, no runs can form. Scour hole depth may increase if

it was not already in equilibrium with check dam geometry. Scour depth is generally found not to exceed a certain relative value given by the finding that the elevation difference from crest to scour hole bottom,  $H$  does generally not exceed twice the value of the elevation difference between crest and next downstream crest,  $Z$ . This gives support to Abrahams' et al. (1995) theory that step steepness,  $\langle H/L \rangle$  does not exceed twice the channel slope,  $S$ . The two relations are identical as:

$$c = \frac{H/L}{S} = \frac{H/L}{Z/L} = \frac{H}{Z} \quad (44)$$

Besides this upper limit, the geometry of scour holes is also found to be approximately invariant. The ratio between normalized scour depth,  $H/Z$  and normalized scour length,  $l_s/L$  stays in a close range;  $L$  being the step length and  $l_s$  the scour hole length (Figure 10.2).

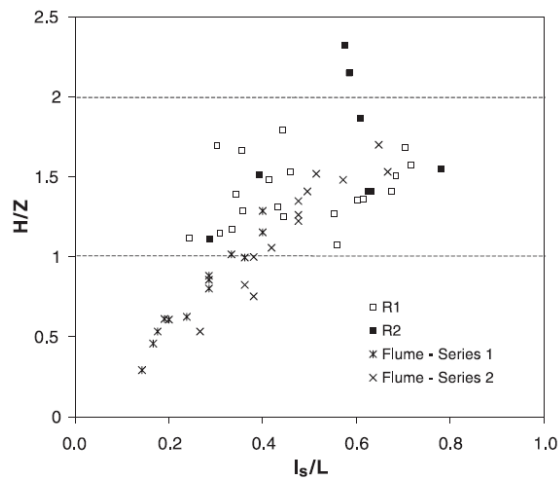


**Figure 10.2: Steepness factor  $c = H/Z$  versus normalized scour hole length by Lenzi and Comiti (2003).  $H$  is the elevation difference from crest to scour hole bottom and  $Z$  the elevation difference between crest and next downstream crest.  $L$  is the step length and  $l_s$  the scour hole length.**

Check dams have been installed widely in tributaries of the Alp river. The lowest part of the Vogelbach counts about 20 of them. In the following discussion, check dams built in the Butzibach just opposite of the Vogelbach and in the Gämschtobel joining the Alp 500 m downstream of the Vogelbach will be discussed. Their use there is much more intensive and the slopes are closer to the slopes of the investigated section of the Vogelbach.

In the Gämschtobel, a first series of check dams was built in 1983 about 500 m above the junction with the Alp. These structures were partially damaged during the 25 July 1984 flood and reconstructed in 1985. In 1990 and 1991 two other check dam series are constructed downstream of the existing one, filling the entire channel length to the Alp. Before building the check dams, an initial longitudinal profile was measured in order to set up the plans for the realization. The dam spacing and crest elevation are precisely recorded on plans. Because no longitudinal profile has been measured after the construction, no information exists on the exact height that those dam-steps developed once a new equilibrium was reached by scouring or naturally backfilling the pools. However the slopes between the dams are very gentle. In a first approximation in order to assess step height created by dams, these slopes are taken as horizontal.

Figure 10.3 shows the slopes from each check dam crest to the downstream crest and the slopes at the same locations before the correction for the Gämschtobel. The slopes have a more regular distribution after the correction; they are kept constant over finite sections but of

course adapted from section to section to follow the general topography of the channel. The highest slopes in the upper part are successfully removed. This more regular shape is not synonymous with smoother flow surface as each slope is actually composed of a vertical (dam) and a nearly horizontal (distance to next dam) element. Comparing the magnitudes of initial step height to the ones of the dam-steps would be interesting but the initially measured longitudinal profile is, due to its original purpose, not precise enough to show the presence and dimensions of natural steps.

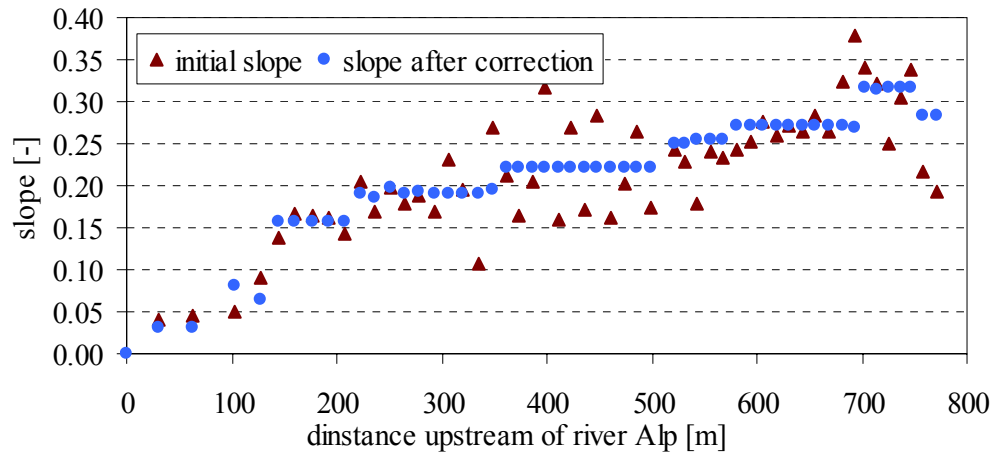


**Figure 10.3: Slopes before and after building check dams in the Gämstobel.**

Studies have been conducted on how to design check dams to obtain large increases in channel roughness but only little scouring causing damage to the structures themselves. Chatwin et al. (1994) proposes to calculate dam spacing  $L$ , given dam height  $H$ , the original channel slope  $\theta$  and the slope after backfilling the structures  $\gamma$  as follows:

$$L = \frac{H}{\tan(\theta - \gamma)} \quad (45)$$

VanDine (1996) approximates this formula for the calculation of a minimum spacing of check dams:

$$\text{minimum spacing} > 2 \cdot l > \frac{H}{\tan(\theta) - \tan(\gamma)} \quad (46)$$

With  $l$ , the length of potential downhill scour (Figure 10.4). As the gradients and especially  $\gamma$  are small values the approximation is fairly good. Both formulas simply stipulate that the backfilling starting at a certain crest should not come in contact with the base of the next upstream check dam. Otherwise a part of the added material will simply serve to raise the channel bed. Referring to Figure 10.4 the following inequality is required:

$$H + \tan(\gamma) \cdot L \stackrel{!}{\leq} \tan(\theta) \cdot L \quad (47)$$

From this, equation 46 can easily be derived.



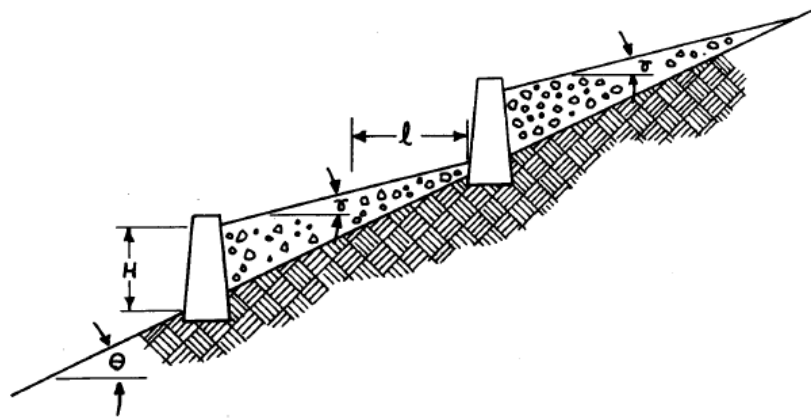


**Figure 10.4:** Factors that influence spacing of check dams and formula for spacing of check dams. Schema by VanDine (1996).

For the structures built on the tributaries of the Alp, the backfilled slopes are very small. In comparison to the original channel slope of about 20 % they can be neglected. The average step height of the check dams, again assuming that the created pools can be approximated horizontal, is 2.9 m. The average spacing is 14.3 m. If one considers the spaces between the steps to be horizontal, the ratio of step height to step length will be nothing else than the slope of the stream. This is thus not giving much new information. Qualitatively the dam-steps fall in the largest step category as defined in chapter 5.2.2 with an average height of 1.3 m (Table 7.1). The average length of that category is 19.1 m, which exceeds the spacing of the dams. However, the natural large steps contain series of small steps within them. This is not the case for dam-steps and thus justifies closer spacing of check dams. The spacing of the check dams in the studied tributaries of the Alp is close to the spacing of natural step-pools. Check dams are built for major floods where in natural streams only the largest steps have importance. But the variability in size of natural step-pools gives them more regularity in the sediment supply to the lower channel network because sediment transport is possible also during smaller flood events.

---

## 11 Conclusions

A continuous 1.5 km profile of a steep mountain stream was surveyed and dimensions of step-pool structures were computed from it. Considering the step-pool morphology as resulting from superposed sequences with the lengths of the larger steps, possibly including smaller more recent steps, seems to be an appropriate hypothesis. Results show a linear relation between sequence-averaged height and length of a step-pool sequence. High variability in the step dimensions is found even within the sequences and is ascribed to the variable nature of the mountain environment and sediment supply. The morphology and nature of hillslopes have a large impact on the stream and change over short distances. In steep streams regularity must be searched in statistical moments rather than in absolute values and temporal changes must be taken into account. After high magnitude low frequency floods, streams may adjust their morphology for several subsequent smaller floods.

To allow an objective analysis of the step-pool morphology, the Vogelbach was not divided into smaller reaches for which average properties were computed but treated as a continuous reach. A better consideration of the hillslope sediment supply could explain some of the high scatter remaining in the individual step steepness.

Slope and step length computed out of the longitudinal profile are found to be very sensitive to the way they are computed. To allow later comparisons, the definitions of step length and channel slope representative for a step therefore need to be precise and computations must be coherent with the definitions.

The individual correlations between step height, step length and slope are rather poor. It appears, however, that correlation is stronger between step length and height than between any of these parameters with slope.

The differences in discharges found for  $HQ_{100}$  in this and previous studies demonstrate the difficulty to determine a precise  $HQ_{100}$  value for very small mountainous drainage areas. For a statistical analysis very long runoff data series sampled with a high frequency are necessary. For the determination through hydrotopes the catchment needs to be precisely partitioned and the parameters leading to the runoff coefficients well known.

The comparison of step-pool morphology with check dam dimensions shows a general agreement in the height to length ratio but more precise measures of scouring downstream of check dams would be necessary for a complete analysis.

## 12 Acknowledgments

Different people contributed to the achievement of this study. The engagement of all of them made working on this diploma thesis interesting and enjoyable for me. Starting with the field measurements I would like to thank Dirk Schoerer for taking the challenge to measure through a steep channel during not always easy weather conditions. My supervisor, Peter Molnar took time for field investigations too and encouraged me to work independently while always staying available for help. Patrick Thee from the WSL in Birmensdorf taught me with enthusiasm how to use instruments for the topographic investigation and took time to process the measures with me. Brian McArdell, also from the WSL, let me benefit from his experience in sediment sampling. The channel widths simulation was largely improved by the roughness values found by Sebastiano Pollock in his flow routing study. Finally, appreciation is also expressed to the people from the engineering agency Birchler Pfyl & Partner AG in Einsiedeln for kindly making plans of sediment control structures available for me.

## 13 References

- Abrahams A. D., Li G., Atkinson J. F. 1995:** Step-pool streams: Adjustment to maximum flow resistance. *Water Resources Research* 31(10): 2593–2602.
- Browne J. M. 2000:** Probabilistic Design. Swinburne University of Technology, School of Engineering and Science. www.ses.swin.edu.au/homes/browne
- Burch H. 1994:** Ein Rückblick auf die hydrologische Forschung der WSL im Alptal. In: *Beiträge zur Hydrologie der Schweiz*, (Gedenkschrift zu Ehren von Hans M. Keller, Hrsg. WSL/SGHL), 35:18-33.
- Chartrand S. M., Whiting P. J. 2000:** Alluvial architecture in headwater streams with special emphasis on step-pool topography. *Earth Surf. Processes Landforms* 25, 583–600.
- Chatwin, S.C., D.E. Howes, J.W. Schwab, and D.N. Swanston. 1994:** A guide for management of landslide-prone terrain in the Pacific Northwest. 2nd ed. *B.C. Min. For., Victoria, B.C. Land Manage. Handb. 18. 220 p.*
- Chin A. 1989:** Step pools in stream channels. *Progress in Physical Geography* 13(3): 391–408.
- Chin A. 1997:** On the stability of step-pool mountain streams, *The Journal of Geology*, v.106, 59–69.
- Chin A. 1998:** The morphologic structure of step-pools in mountain streams. *Geomorphology* 27: 191–204.
- Chin A. 1999:** On the origin of step-pool sequences in mountain streams. *Geophysical research letters*, v. 26. no. 2, p. 231–234.
- Dyck S., Peschke G. 1995:** Grundlagen der Hydrologie. Verlag für Bauwesen, Berlin.
- Eisbacher, G.H. and J.J. Clague. 1984:** Destructive mass movements in high mountains: hazard and management. *Geol. Surv. Can., Pap. 84-16. 230 p.*
- Forster, F., Hegg Ch. 2002:** A suggestion for the estimation of flood peak discharge in small torrential catchments. *Proc. ICFE 2002. Bern*
- Grant G.E., Swanson E. F., Wolman M. G. 1990:** Pattern and origin of stepped-bed morphology in high-gradient streams, western Cascades, Oregon. *Geological Society of America Bulletin* 102: 340±352.
- Grant G. E., Mizuyama T. 1991:** Origin of step-pool sequences in high gradient streams: A flume experiment. In *Proceedings of the Japan-U.S. Workshop on Snow Avalanche, Landslide, and Debris Flow Prediction and Control*. National Research Institute for Earth Science and Disaster Prevention: Tsubuka, Japan.
- Jarrett R. D. 1984:** Hydraulics of high-gradient streams. *Journal of Hydraulic Engineering*, vol. 110, No. 11, Nov. 1984.
- Judd H, E. 1964:** A study of bed characteristics in relation to flow in rough, high-gradient natural channels: Ph.D. thesis, Logan, Utah, 182 p.
- Kennedy JF. 1961.** Stationary waves and antidunes in alluvial channels. *Rep. NKH-R-2, W.M. Keck Laboratory of Hydraulics and Water Resources, California Institute of Technology.*
- Kottegoda N. T., Rosso R. 1997:** Statistics, Probability and Reliability for civil and Environmental Engineers. The McGraw-Hill Companies, Inc..
- Limerinos J.T. 1970:** Determination of the Mannings coefficient from measured bed roughness in natural channels. *USGS Water-Supply paper 1898-B.*

- Lenzi M. A. 2001:** Step-pool evolution in the rio cordon, northeastern Italy. *Earth Surface Processes and Landforms* 26, p.991-1008(2001).
- Lenzi M. A., Comiti F. 2003:** Local scouring and morphological adjustments in steep channels with check-dam sequences. *Geomorphology* 55 (2003), p. 97-109.
- Montgomery D. R., Buffington J. M. 1997:** Channel reach morphology in mountain drainage basins. *Geological Society of America Bulletin* 109(5): p. 596–611.
- Pollock S. 2004:** Flow analysis with Hec-Ras, flow routing in a mountain stream (Vogelbach), Semester project IHW ETHZ, unpublished.
- Rickenmann D., Dupasquier P. 1995:** EROSLOPE project no. EV5V-0179: Final report WSL. *Swiss Federal Institute for Forest, Snow and Landscape Research: Birmensdorf, Switzerland.*
- Rickenmann D., Hegg C. 2000:** EROSLOPE II: Dynamics of sediments and water in alpine catchments – processes and prediction. *Swiss Federal Institute for Forest, Snow and Landscape Research: Birmensdorf, Switzerland.*
- Rickli C., Forster F. 1997:** Einfluss verschiedener Standortseigenschaften auf die Schätzung von Hochwasserabflüssen in kleinen Einzugsgebieten. *Schweiz. Zeitschr. Forstwesen*, 148 Jg., Nr. 5: 367–385
- Rosport M., Dittrich A. 1995:** Step pool formation and stability – a flume study. In: *Management of Sediment. Philosophy, Aims, and Techniques*. 6th Int. Symp. River Sedimentation Nov. 1995, New Delhi, India. Eds.: C. V. J. Varma et al. New Delhi: Oxford Publ. 1995, pp. 525 – 532.
- Salas J. D., Delleur J. W., Yevjevich V., Lane W.L. 1980:** Applied modelling of hydrologic time series, *Water resources publications*.
- Spreafico M., Weingartner R., Barben M., Ryser A. 2003:** Hochwasserabschätzung in schweizerischen Einzugsgebieten, Praxishilfe. *Berichte des BWG Bern, Serie Wasser Nr.4*
- Stammach M. 1988:** Rutschungen im hintern Alptal (Kt. Schwyz). Diplomarbeit Universität Zürich, unveröffentlicht, 96p.
- Stedinger J. R., Vogel R.M., Foufoula-Georgiou E. 1993:** Frequency analysis of extreme events. Chapter 18 of *Handbook of Hydrology*, ed. DR. Maidment, McGraw Hill.
- United States Geological Survey (USGS) WebPages,** Manning's roughness coefficients.  
[Thttp://wwwrcamnl.wr.usgs.gov/sws/fielmethods/Indirects/nvalues/index.htm](http://wwwrcamnl.wr.usgs.gov/sws/fielmethods/Indirects/nvalues/index.htm)T
- VanDine D.F., 1996:** Debris flow control structures for forest engineering. *British Columbia ministry of forests, research branch*
- Whittaker J. G. 1987:** Sediment transport in step-pool streams. In: *Sediment transport in Gravel-Bed Rivers*. Thorne CR, Bathurst JC, Hey RD (eds). Wiley: Chichester; 545–579.
- Whittaker J. G., Jaeggi M. N. R. 1982:** Origin of step-pool systems in mountain streams. *American Society of Civil Engineers, Journal of Hydraulic Division* 108: 758–773.
- Zimmermann A., Church M. 2001:** Channel morphology, gradient profiles and bed stress during flood in a step-pool channel. *Geomorphology* 40 (2001), p. 311-327.

## 14 Appendix

<b>A Matlab codes .....</b>	<b>Appendix 2</b>
<i>A.1 Step definition .....</i>	<i>Appendix 2</i>
<i>A.2 Step categories.....</i>	<i>Appendix 3</i>
<i>A.3 Step lengths.....</i>	<i>Appendix 4</i>
<i>A.4 Slope.....</i>	<i>Appendix 5</i>

## A Matlab codes

In the following a few extracts of Matlab codes specific to this study are shown as examples. The illustrated codes perform the step definition, the calculation of step height and length and assign a representative slope to each step. As these are the main parameters this study deals with, the few codes of the next subchapters represent the technical equivalent to the explanations of parameter computation techniques explained in the thesis.

### A.1 Step definition

This Matlab code is responsible for defining steps out of the measured longitudinal profile and for calculating their height. The slope between two points is used as the relevant parameter. A critical slope has to be defined for this purpose. If it is exceeded the upper point is considered as a step crest. If the slope between such a defined crest and the next upstream point exceeds again the critical slope, then the heights are merged to form one larger step, and so on till a slope is found that does not exceed anymore the critical slope. An exception is made to this rule if the directly following crests are not of the same type (normal sediments, bedrock, woody debris). In that case a new step is defined at each change in type. Input variables needed for the code are:

j	number of measured points (1145)
zl	elevation of point
L	Upstream distance along the profile computed as horizontal projection of line going through all points. $L = 0$ at gage.
critslope	slope over which a segment is considered as a step
numl	“point name” (number given by theodolithe)
sohlenum	point type (sediment, bedrock or woody debris)

```

for i=2:1:j % slope from point i to point downstream
    height(i) = zl(i)-zl(i-1);
    slope(i) = height(i) / ( L(i)-L(i-1) );
end

for k=1:1:15 % (necessary for the following while loop)
    slope(i+k)=0;
    L(j+k)=L(j)+k;
end

nbsteps=0;
jump=0;
for i=2:1:j
    if jump == 0

        if slope(i) >= critslope
            nbsteps=nbsteps+1;

            if slope(i+1) < critslope
                % considered as step
                step(nbsteps,:)= [nbsteps L(i) numl(i)-30000 height(i) slope(i) sohlenum(i)];
            end

            if slope(i+1) >= critslope & sohlenum(i) ~= sohlenum(i)
                % considered as step
                step(nbsteps,:)= [nbsteps L(i) numl(i)-30000 height(i) slope(i) sohlenum(i)];
            end
        end
    end
end

```

```

    if slope(i+1) >= critslope & sohlenum(i) == sohlenum(i)
        % merge steps
        k=1;
        while slope(i+k) >= critslope & sohlenum(i) == sohlenum(i)
            k=k+1;
        end
        k=k-1;
        heightcomb = zl(i+k) - zl(i-1);
        slopecomb = heightcomb / ( L(i+k) - L(i-1) );
        jump=k;
        step(nbsteps,:)= [nbsteps L(i+k) numl(i+k)-30000 heightcomb slopecomb sohlenum(i)];
    end

    end

    else jump =jump-1; % do not recomputed points as steps if they were already integrated in a step
        % starting below.
    end
end

```

## A.2 Step categories

This code classifies steps into height categories containing equal number of steps. The number of categories is defined by “nbclasses”. Input variables needed for the code are:

nbsteps	total number of steps (326)
sohlenum	point type (sediment, bedrock or woody debris)
height	step height

```

% separate sediment steps from all steps
%-----
nbNSsteps = 0;
for i=1:nbsteps
    if sohlenum(i) == 1 % NS step
        nbNSsteps = nbNSsteps + 1;
        NSheight(nbNSsteps) = height(i);
    end
end

% define the limits of the classes (equal number of NS steps per class)
%-----
nbclasses=5;

classsize=round(nbNSsteps/nbclasses);
sortNSheight=sort(NSheight);

class=1;
content=0;
for i=1:nbNSsteps
    if content < classsize
        sortNSheight(i);
        content=content+1;
    else
        content=1;
        topofclass(class)=sortNSheight(i);
        class=class+1;
    end
end
end

```



```
clear ('sortheight','class')

% assign each step to a category
%-----
class(1:nbsteps)=1;
for i=1:nbsteps
    for j=1:nbclasses-1
        if height(i) >= topofclass(j)
            class(i)=j+1;
        end
    end
end
end
```

### A.3 Step lengths

The code for the computation of step lengths directly follows the code for the definition of classes shown above. Step length is computed for steps of all types. Input variables needed for the code are:

nbsteps	total number of steps (326)
position	Upstream distance along the profile computed as horizontal projection of line going through all points. $L = 0$ at gage.
class	category to which step was assigned
x1	x-coordinate of point
y1	y-coordinate of point
z1	z-coordinate of point
pointnumber	number of point in the count of all 1145 measured points

```
% compute the different step length measures
%-----

% LENGTH 1 : step length without caring of classes
for i=nbsteps:-1:2 % from up to down, the lowest step has no length as there is no step underneath it
    length1(i)=position(i)-position(i-1);
end
length1(1)=position(1); %until concrete gage that is also a step

% LENGTH 2 : calculation of step length to next downstream step of higher or equal class
for i=nbsteps:-1:2 %from up to down, the lowest step has no length as there is no step underneath it
    skip=1;
    while class(i-skip) < class(i)
        skip=skip+1;
        if i-skip < 1
            break
        end
    end
    if i-skip==0 % larger steps just over step 1 are stopped at step 1. (Step 1 is already large).
        length2(i)=position(i)-position(1);
    else
        length2(i)=position(i)-position(i-skip);
    end
end
length2(1)=position(1); %until concrete gage that is also a step

% LENGTH 3 : claculation of step length using 3D distance from crest to crest to next downstream
% step of higher or equal class
for i=nbsteps:-1:2 %from up to down, the lowest step has no length as there is no step underneath it
```

```

skip=1;
while class(i-skip) < class(i)
    skip=skip+1;
    if i-skip < 1
        break
    end
end
if i-skip==0 % larger steps just over step 1 are stopped at step 1. Step 1 is already large)
    length3(i) = ( ( xl(pointnumber(i))-xl(pointnumber(1)) )^2 +...
    ( yl(pointnumber(i))-yl(pointnumber(1)) )^2 +...
    ( zl(pointnumber(i))-zl(pointnumber(1)) )^2 )^0.5;
else
    length3(i) = ( ( xl(pointnumber(i))-xl(pointnumber(i-skip)) )^2 +...
    ( yl(pointnumber(i))-yl(pointnumber(i-skip)) )^2 +...
    ( zl(pointnumber(i))-zl(pointnumber(i-skip)) )^2 )^0.5;
end
end
length3(1) = ( ( xl(pointnumber(1))-xl(1) )^2 +...
( yl(pointnumber(1))-yl(1) )^2 + ( zl(pointnumber(1))-zl(1) )^2 )^0.5;
%until concrete gage that is also a step

```

## A.4 Slope

Code calculating the mean channel slope for each point (of the longitudinal profile) with a moving window of 15 m. Variables needed for the code are:

j      number of measured points (1145)  
L      Upstream distance along the profile computed as horizontal projection of line going through all points. L = 0 at gage.  
zl      z-coordinate (elevation) of point

% Slope for each point i is calculated as the slope of a straight line fitted through all points measured  
% in a moving window of given size centered on point i.

% round each point on 5 cm  
for i=1:1:j  
    Lround(i)=round(L(i)\*20)/20;  
end

% interpolation along the Longitudinal profile every 5 cm (29403 points)  
xi=linspace(0,L(j),(L(j)/0.05)+1);  
zi = interp1(L,zl,xi);

interval =15 % moving window of 2 x 15 = 30 m

```

for i=1:1:j
    if Lround(i)*20+interval*20+1 > size(zi,2) % point closer than 15 m from upper end
        k=i-11;
        while Lround(k)*20+interval*20+1 > size(zi,2) % go back to find the point laying just
            k=k-1; % more than 15 m away from upper end...
        end
        % ... compute the slope for this point
        fitpolynom = polyfit(xi(Lround(k)*20-interval*20+1:Lround(k)*20+interval*20+1) , ...
        zi(Lround(k)*20-interval*20+1:Lround(k)*20+interval*20+1) , 1);
        mediumslope(i) = fitpolynom(1);
    elseif Lround(i)*20-interval*20+1 < 0 % point closer than 15 m from lower end
        k=i+1;
    end
end

```

---

```
while Lround(k)*20-interval*20+1 < 0           % go up to find the point laying just
    k=k+1;                                     % more than 15 m away from lower end...
end
% ... compute the slope for this point
fitpolynom = polyfit(xi(Lround(k)*20-interval*20+1:Lround(k)*20+interval*20+1) , ...
    zi(Lround(k)*20-interval*20+1:Lround(k)*20+interval*20+1) , 1);
mediumslope(i) = fitpolynom(1);
else
    % Points in the middle. Slope can be computed for each slope independently.
    fitpolynom = polyfit(xi(Lround(i)*20-interval*20+1:Lround(i)*20+interval*20+1) , ...
        zi(Lround(i)*20-interval*20+1:Lround(i)*20+interval*20+1) , 1);
    mediumslope(i) = fitpolynom(1);
end
end
```